Andreas KAISER, BSc

Hydraulic investigation of a tailrace tunnel for a pumped-storage power plant at the Danube

MASTER'S THESIS

to achieve the university degree of

Diplom-Ingenieur

Masters's degree programme: Civil Engineering Sciences, Geotechnics and Hydraulics

Graz University of Technology

Supervisor

Univ.-Prof. Dipl.-Ing. Dr.techn. Gerald ZENZ

Institute of Hydraulic Engineering and Water Resources Management

Graz, August 30, 2017

Abstract

The *Energiespeicher Sulzberg GmbH*, which is a subsidiary company of the *EVN AG*, is doing preliminary investigations for a pumped storage power plant in Lower Austria at the Danube.

The goal of this master thesis is to develop a hydraulic design for a tail-waterway with Scandinavian structure. The hydraulic simulation software WANDA 4.2 is used for this investigation. In order to get the necessary modelling accuracy three different surge tank inlets are examined. Furthermore this analysis includes flow rates with a range from 20 to 100 m³/s, four load cases and two different surge tank layouts. Load cases are defined by switching sequences between pump-mode and turbine-mode. Different surge tank layouts show the economical efficiency of the power plant design.

The findings for the decisive construction parts are compared and illustrated in graphs and tables.

Kurzfassung

Seit 2008 führt die *Energiespeicher Sulzberg GmbH*, welche eine Tochterfirma der *EVN AG* ist, Machbarkeitsstudien für ein Pumpspeicherkraftwerk an der Donau durch. Dieses soll sich in Niederösterreich nahe Ybbs befinden.

Mit der 1-D numerischen Berechnungssoftware WANDA 4.2 soll eine hydraulische Auslegung der einzelnen Bauteile erfolgen. Das Pumpspeicherkraftwerk soll in skandinavischer Bauweise errichtet werden. Um ein ausreichend naturnahes Modell erstellen zu können werden drei verschiedene Wasserschlosseinlässe untersucht. Des weiteren umfasst die Studie unterschiedliche Ausbauwassermengen von 20 bis 100 m³/s, vier verschiedene Lastfälle und zwei Alternativen für die Wasserschlossgestaltung. Die Lastfälle werden durch ein Umschalten zwischen Pumpen und Turbinieren erzeugt. Die unterschiedlichen Wasserschlosstypen werden auf deren Wirtschaftlichkeit überprüft.

Sämtliche Ergebnisse für die maßgebenden Bauteile werden in Graphen und Tabellen dargestellt.

Acknowledgement

This thesis was written during my time at the Institute of Hydraulic Engineering and Water Resources Management - Graz University of Technology. Without the guidance and encouragement of several people this thesis wouldn't exist:

First of all I want to thank my advisor Wolfgang Richter, who put a lot of time and effort in guiding, supporting and helping me with any questions or problems. Especially when I had already moved to Upper Austria, he never hesitated to assist me even on weekends. He was the person who introduced me to this topic and aroused my interest for it. I am very grateful for every aspect of his help and appreciate it a lot.

Furthermore I want to thank my family. My parents, Wolfgang and Sonja, have always been supportive and encouraged me during my studies. A heartfelt thank you goes to my brothers, Christoph and Mathias, who helped me with good advice and motivated me. Also I want to thank my grandparents, friends and other relatives who always had kind words for me in stressful times.

But the biggest thanks goes to my girlfriend Cornelia, who has been patient, understanding, encouraging and supportive during the whole time I was engaged in the writing of this thesis.

Affidavit

I declare that I have authored this thesis independently, that I have not used other than the declared sources / resources, and that I have explicitly marked all material which has been quoted either literally or by content from the used sources.

August 30, 2017
. . . . . .
Date

. . . . . .
Signature

Contents

Abstract iii

Kurzfassung v

Acknowledgement vii

Affidavit ix

Nomenclature xv

1 Introduction 1

2 Project description 3

2.1 Project development 3

2.2 Project location 4

2.3 Geological data 6

2.4 Effect on nature 7

2.4.1 Nature protection areas 7

2.4.2 Flood events 7

3 Pumped storage hydro-power 9

3.1 Construction parts 9

3.1.1 Power cavern 10

3.1.2 Pressure tunnel 10

3.1.3 Surge tank 11

3.1.4 Throttle 16

3.2 Hydraulic machinery 18

3.2.1 Hydraulic machine systems 18

3.2.2 Hydraulic machine types 18

4 WANDA 4 - Modelling and Analysis **21**

4.1 Program introduction 21

4.2 Analysis modes and properties 21

4.2.1 Calculation modes 21

4.2.2 Time properties 22

4.3 Basic components 22

4.3.1 Hydraulic nodes 22

4.3.2 Boundary condition 23

4.3.3 Pressurised pipe 23

4.3.4 Free surface flow conduit 24

4.3.5 Resistance 25

4.3.6 Shaft 25

4.3.7 Weir 26

5 Mechanical equipment **27**

5.1 Load case scenarios 27

5.1.1 Multiple load changes 27

5.1.2 Load shedding 28

5.2 Turbine 28

5.2.1 Pre-dimensioning 29

6 The two chamber surge tank **33**

6.1 Modelling and Analysis 33

6.1.1 Boundary conditions 33

6.1.2 Tailrace 33

6.1.3 Trifurcation 34

6.1.4 Surge shaft 34

6.1.5 Surge chambers 35

6.2 Type 1 - Surge tank without throttle 37

6.2.1 Type 1 - Turbine design flow rates 38

6.3 Type 2 - Surge tank with throttle 57

6.3.1 Type 2 - Turbine design flow rates . . . 58
6.4 Type 3 - Surge tank with aerated throttle . . . 76
6.4.1 Type 3 - Turbine design flow rates . . . 77
6.5 Comparison . . . 95

7 The three chamber surge tank **99**
7.1 Basic facts . . . 99
7.2 Modelling and Analysis . . . 100
7.2.1 The model . . . 100
7.2.2 Turbine design flow rates . . . 101
7.2.3 The tunnel chamber . . . 119
7.2.4 The pump chamber . . . 119
7.2.5 The overflow sill . . . 120
7.2.6 Load cases . . . 120

8 Comparison **123**
8.1 Surge tank size . . . 123
8.2 Inflow- and Outflow amplification . . . 125
8.3 Mass oscillation . . . 127
8.4 Conclusion and outlook . . . 128

Bibliography **i**

List of Figures **iii**

List of Tables **ix**

Nomenclature

Constants

ρ	Density of water	$\mathrm{kg/m^3}$
g	Gravitational acceleration	$\mathrm{m/s^2}$

Greek

α	Wave propagation velocity	$\mathrm{m/s}$
η	Total efficiency	-
γ_{Th}	Thoma factor	-
ξ	Resistance loss coefficient	-
ζ	Loss coefficient	-

Variables

A	Area	$\mathrm{m^2}$
A_{SVEE}	Svee Area	$\mathrm{m^2}$
A_{Th}	Thoma Area	$\mathrm{m^2}$
A_T	Headrace/Tailrace tunnel area	$\mathrm{m^2}$
$Amp+/-$	Outflow/Inflow amplification factor	-
B	Width of the weir	m
C	Chézy coefficient	$\mathrm{m^{1/2}/s}$
C_D	Discharge coefficient	-
C_v	Approach velocity coefficient	-
C_W	Weir loss coefficient	-
D_3	Impeller diameter	m
d_T	Tunnel diameter	m
f	Friction factor	-
f_u	Utility frequency	Hz
H	Head	m
H_0	Drop height	m
h_v	Headloss	m

k	Wall roughness	mm
$k_{u,F}$	Coefficient for Francis turbines	-
l_T	Headrace/Tailrace tunnel length	m
n	Rotational speed	$1/\mathrm{min}$
n_q	Specific rotational speed	$1/\mathrm{min}$
n_{syn}	Synchronous speed	$1/\mathrm{min}$
P	Power	W
p	Pressure	Pa
Q	Discharge	m^3/s
Q_M	Specific discharge	m^3/s
Re	Reynolds number	-
T_c	Device closure time	s
T_r	Reflection time	s
V	Volume	m^3
v	Velocity	m/s
z	Elevation	masl

1 Introduction

Fossil fuels are limited resources on this planet, therefore renewable and sustainable energies are gaining on importance. Not only to reduce CO2-emissions and therefore counteract the global warming, but also to ensure a long-term energy supply.
In Austria approximately 70 % of the provided electricity is from renewable sources. The biggest part of them is produced by means of hydropower. It can be separated in run-of-river (41 %) and pumped-storage power plants (21 %).

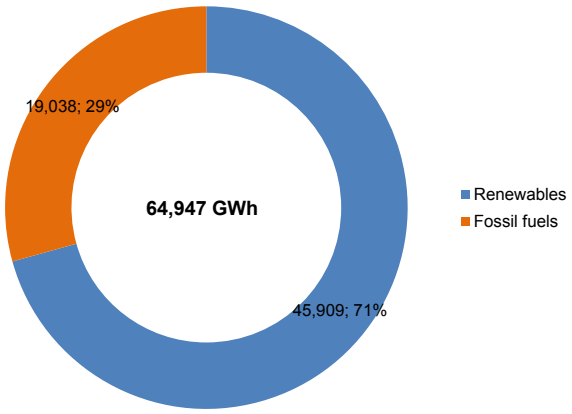

Figure 1.1: *Renewable and fossil fuel energy production in Austria (2015) [1]*

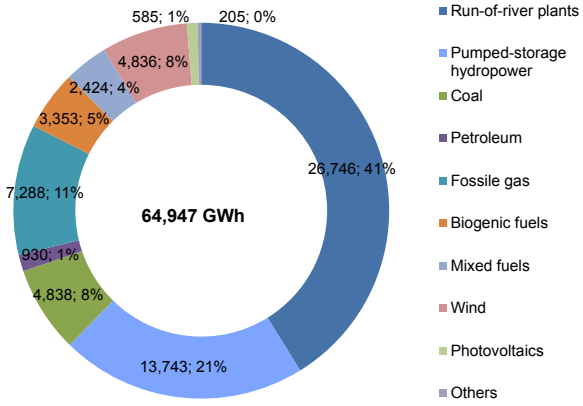

Figure 1.2: *Detailed energy production of Austria (2015) [1]*

The power demand in Austria is an ever changing parameter as seen in figure 1.3, therefore

particular attention has to be paid to load balancing systems, which store and provide energy on demand. For this purpose pumped storage hydro power plants are ideally suited. This type of power plant handles these large fluctuations in power demand by pumping water during low load periods from a lower to a higher located reservoir. In peak load periods the water is released through the turbines to generate electricity.

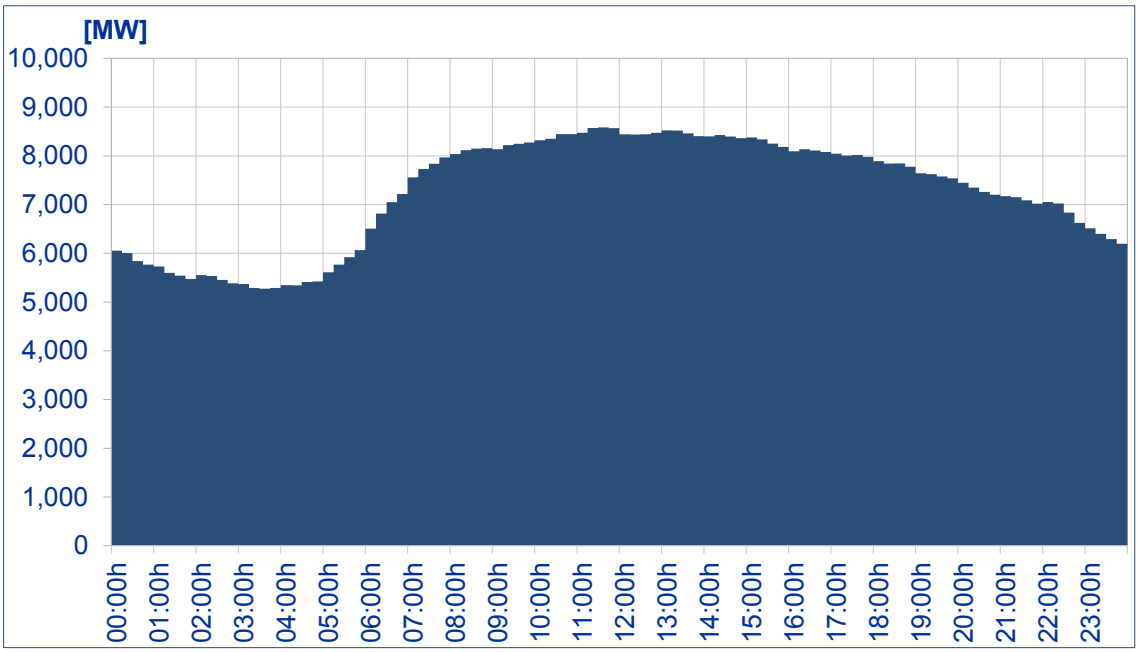

Figure 1.3: *Daily time-variation curve of the electricity demand in Austria (Wednesday, 21st of June 2017) [1]*

The main requirement for mechanical equipment as well as the hydraulic system is in response time. The pumped storage power plant is capable of these fast changes from pump- to turbine mode. These load modifications require a stable and fast reacting hydraulic system, therefore it is necessary to do proper planning in order to handle problems like the water-hammer effect, acceleration and deceleration of the water. The surge tank is designed conservatively, to ensure trouble-free operating modes.

The main objective of this thesis is to do a hydraulic investigation of a tailrace-tunnel for a pumped storage power plant with Scandinavian design. This means that the pressure shaft is directly connected to the upper reservoir. The power cavern is located in the mountain and connected with the lower reservoir with a long tailrace. To handle the water-hammer and mass oscillation a surge tank is located at the tailrace close to the power cavern. The calculations to do so are performed with WANDA 4.2, which is a software developed for hydraulic layouts.

2 Project description

2.1 Project development

Since 2008 the *Energiespeicher Sulzberg GmbH*, which is a subsidiary company of the *EVN AG*, has been doing preliminary investigation for a possible pumped storage hydro power-plant at the Sulzberg.
In the last years several different variants have been examined. Due to official requirements relating to nature protection some of them may not be possible to realise, as are others due to bad geological conditions. In order to perform simulations of the hydraulic behaviour within the tail-waterway, the most promising variant at the time being was picked for investigation.
According to the *Energiespeicher Sulzberg GmbH*, the system output should be between 340 and 700 MW. The power is calculated as seen in equation 2.1. To calculate the stored energy within the basin, equation 2.2 is used. In order to research different possibilities for this project, several flow rates within a range from 20 to 100 m³/s are investigated. Even though power drops below the desired range when flow rates are low (as seen in table 2.1), those values are important for the development of the tailwater design, especially for the design of the surge tank.

$$P = \eta_{tot} * \rho * g * Q * H_0 \qquad [W] \tag{2.1}$$

$$E = \rho * g * H_0 * V \qquad [Ws] \tag{2.2}$$

Table 2.1: *Performance and energy storage capability of the project*

Drop height	600 [m]
Storage volume	3,000,000 [m³]
Total efficiency	0.90 [-]
Energy Storage	4.41 [GWh]
Discharge	**Power**
[m³/s]	[MW]
20	105.9
30	158.9
40	211.9
50	264.9
60	317.8
70	370.8
80	423.8
90	476.8
100	529.7

2.2 Project location

The project area is located in the northwestern region of the state Lower Austria called ”Waldviertel” (Figure 2.1). The reservoir for the pumped storage hydro-power plant is located at the Sulzberg (852 m a.s.l.) at a height of approximately 815 m a.s.l. The Sulzberg belongs to the mountain range called Ostrong. The biggest summit of the Ostrong is called Grosser Peilstein (1061 m a.s.l.) and is located north of the Sulzberg.
The outlet structure leads in the Danube, that is at river kilometre 2052 on the orographically left side (Figure 2.2). The outlet is located between the barrages Ybbs-Persenbeug at river kilometre 2060.5 and Melk, which is situated at river kilometre 2038.1.Here the Danube has an elevation of 214.4 m a.s.l. This leads to the gross drop height of approximately 600 m.

Figure 2.1: *Overview of the Lower Austrian Danube - ortho-image [6]*

Figure 2.2: *Project area - ortho-image [6]*

2.3 Geological data

The ”Waldviertel” is the southernmost area of the Bohemian Massif, restricted to the south by the Danube. South of the Danube lies the Dunkelsteiner Forest, composed of other sediment types like flysch or limestone. The Bohemian Massif is the rest of a high mountain region which was levelled during the late Palaeozoic era. It contains mostly metamorphic rocks like granite, gneiss, mica schist, phyllite and the like.

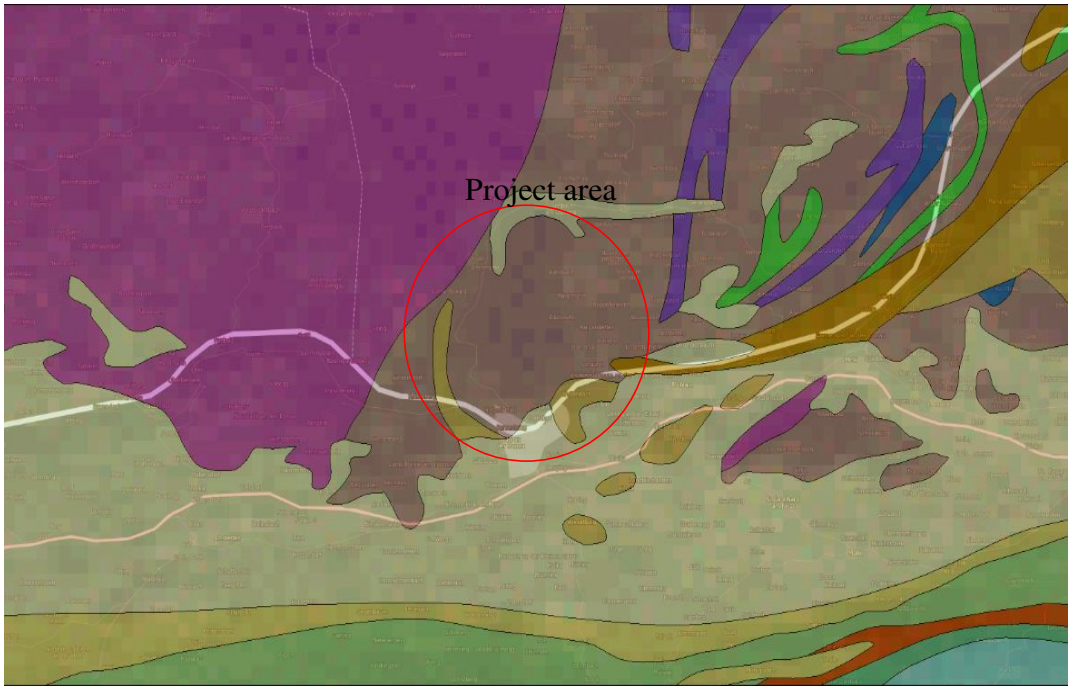

Figure 2.3: *Geological data of the project area [8]*

Figure 2.3 depicts the project area, located at the border to the Granite area (purple) of the Bohemian Massif. Within the project area mainly paragneiss, mica schist and phyllite (brown) can be found. The Bohemian Massif consists of very compact rock with very little fault zones, which was also confirmed by an exploration drilling with a depth of 655 m within the project area. Therefore the Scandinavian construction design of a high head power plant can be taken into consideration.

2.4 Effect on nature

2.4.1 Nature protection areas

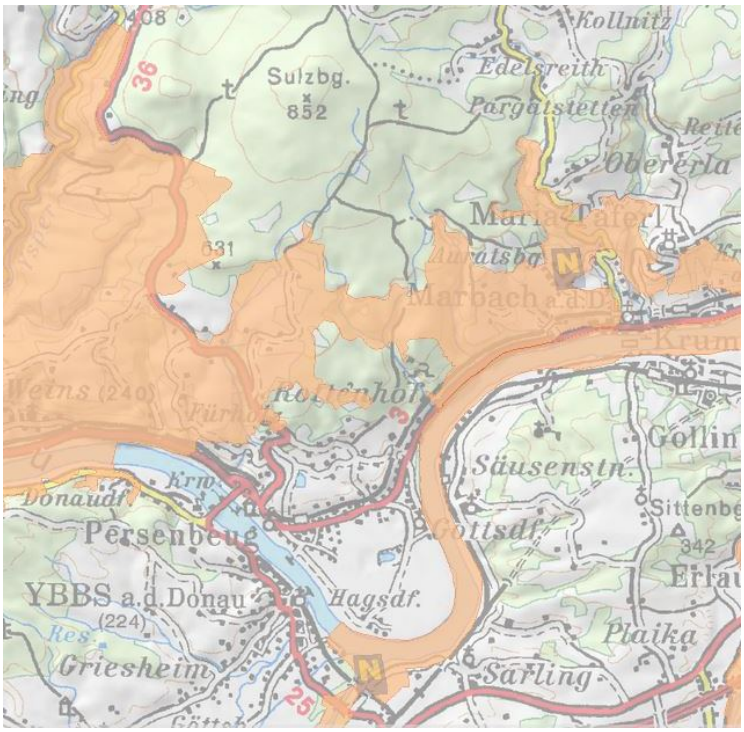

Figure 2.4: *Nature protection areas within the project region [14]*

Figure 2.4 shows that environmentally protected areas are located within the project region. This nature protection area is identified as a fauna-flora-habitat (FFH) of the European Union Natura 2000 project. The legal basis for Natura 2000 are both the Birds Directive and the FFH Directive.
The Natura-2000-network is the biggest nature protection project in the history of Europe. All member nations have to provide conservation plans and monitor the performance of these areas. Within Austria there are 219 protected areas belonging to the Natura 2000 project comprising an area of over 1,200,000 ha which is the approximate size of Upper Austria. [2]

The outlet structure is the only part of the power plant which intervenes with the protected area. Therefore, in order to successfully pass the approval procedures, the project has to include ecological compensatory measures.

2.4.2 Flood events

The influence of a pumped storage power plant on flood events depends on work regulations, but usually is non-existent. In case of a flood event, the turbines are usually stopped and therefore there is no increase in flow caused by the power plant.

3 Pumped storage hydro-power

3.1 Construction parts

In Scandinavia the mountains have a very solid, compact rock with hardly any vault zones. This makes it possible to build large power caverns within the mountain and construct the head-/tailrace without lining. Figure 3.1 shows a system sketch of a pumped storage power plant with Scandinavian design.
Characteristic for this scheme is a direct link between storage basin and power cavern with a pressure shaft. The power cavern is situated within the mountain and connected to the lower basin with a long tailrace, which is hydraulically isolated with a surge tank.

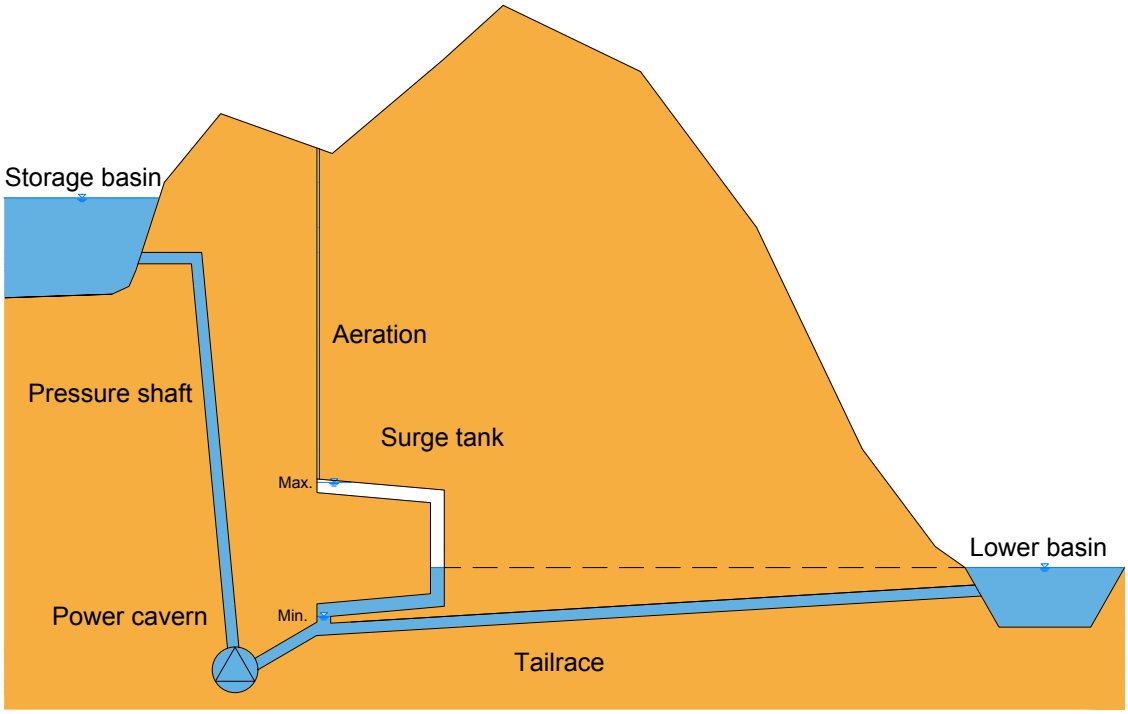

Figure 3.1: *System sketch of a power plant with Scandinavian design*

Figure 3.2 shows a scaled image of the observed tailwater part of a pumped storage hydro-power plant. The main parts are the power cavern, surge tank and the tailrace. The Danube is functioning as a lower situated reservoir. Diameters are not given since they correspond to the design flow rate of the turbines. Also the surge tank height and chamber length varies with every model and therefore can't be shown as a constant value.

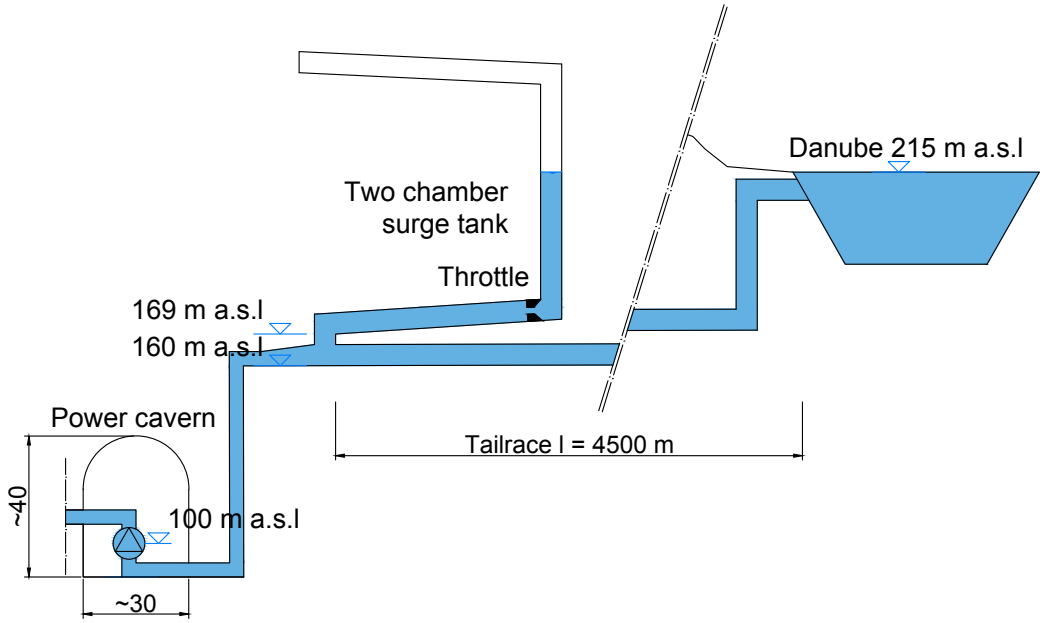

Figure 3.2: *Scaled image of the tailwater area*

3.1.1 Power cavern

The power cavern size is defined by the required space of the turbines, generators and transformers as well as the boundary conditions of the bedrock. The cavern shape and the location relative to each other and to the ground surface are also decisive factors for the stability of the design. The support system is defined by initial field stresses and discontinuity planes within the rock mass. [16]

3.1.2 Pressure tunnel

The pressure tunnel has the function of transferring the water from the reservoir to the turbines and vice versa with a low amount of hydraulic loss. Its diameter is defined by the cost of hydraulic losses and the construction costs. By adding up those two parameters the minimum costs can be determined (Figure 3.3).

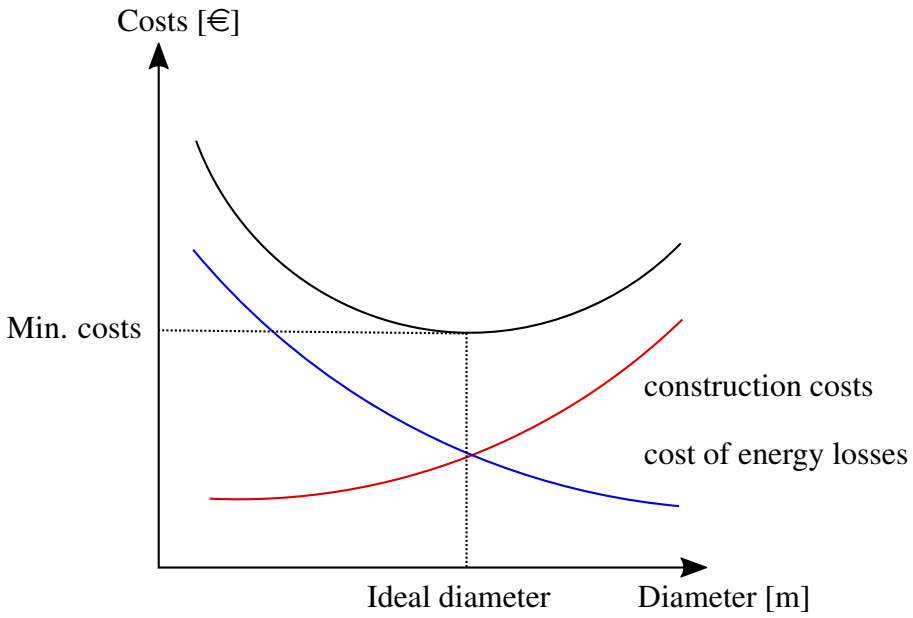

Figure 3.3: *Diameter determination scheme*

The lining of the waterway depends on the mountain water table, internal pressure and the overburden. With these boundary conditions the lining can be estimated using the so-called Seeber-diagrams. These diagrams take rock strength, lining strength, internal pressure, pressure due to grouting, shrinkage and other relevant characteristics into account, depending on which type of lining is examined. [17]

3.1.3 Surge tank

The surge tank is a significant structural element in pumped storage hydro-power. Its size is defined by the stability criteria and mass oscillation within the system. The surge tanks positioning and shape depend on the general power plant design. There are several different types of surge tank's based on the hydraulic mode of action.
The surge tank has to fulfil the following main tasks:

- Hydraulic isolation of the head-/tailrace

  This means a hydraulic uncoupling of the penstock from the head-/tailrace. In case a water hammer phenomenon occurs, the pressure rises in the stronger lined penstock, which is designed especially to withhold this pressure. As the head-/tailrace lining is usually not designed for high pressures like this, the surge tank isolates this part of the waterway. Thus it is possible to reduce construction costs significantly by choosing a thinner and cheaper lining.

- Dampening of the water hammer phenomenon

  When a sudden change in the flow conditions (valve closure) occurs, pressure waves develop within a hydraulic system, which then travel through the surges until they reach a free surface and get reflected. These pressure waves spread with speeds

up to over 1000 m/s (α). This phenomenon is called a water hammer. As mentioned before the surge tank functions as a hydraulic separation system for the head-/tailrace, but it also dampens this phenomenon. The reflection time (T_r) and therefore the length of the waterway until the pressure wave reaches a free water surface is an essential factor for the water hammer development as shown in the Joukovski-Equation below (Equation 3.1). Also the device closure time (T_c) is taken into account for this equation. With the closure time parameter the maximum water hammer can be controlled. With a longer closing time the water hammer gets smaller, but for the operation safety a fast closing device is more optimal. [9]

$$\Delta p = \rho * \alpha * \Delta v * \frac{T_r}{T_c} \qquad [Pa] \tag{3.1}$$

- Improvement of regulation

  By dampening the pressure waves a better stability within the control loop is reached. The reason for this is that the turbine controller adjusts the discharge on the basis of pressure changes and power demand of the electrical grid. [9]

- Compensation of water capacity

  Due to mass inertia of water it is necessary to compensate the water capacity in long flow paths. The consequences of missing water compensation would be the possibility of a water column separation within the hydraulic system, which might result in a huge water hammer. [9] [12]

3.1.3.1 Differential effect

The differential effect can be observed in the throttle and upper surge chamber of a surge tank.

- With a two-way throttle the water level deflection has a different intensity based on the loss coefficients of each direction.
- The upper surge chamber holds water back even when the head within the surge shaft has already sunk below the chamber edge. This phenomenon will be shown in more detail in the 1-D numerical computations.

3.1.3.2 Stability criteria

There are two different approaches for the stability criteria. The Thoma-equation (Equation 3.2) is based on the Bernoulli formula. It is commonly used for surge chambers at the headrace of a waterway.
The approach by Svee (Equation 3.3) is based on the general law of Newton $P = \frac{d(mv)}{dt}$. This formula is especially suited for tailrace surge chambers. However, under similar circumstances the profile limit of headrace and tailrace surge chambers are almost the same.

Both formulas differ the most when applied to a short waterway, since $\frac{h_v}{2g}$ and $\frac{1}{2g}$ have the same range, but when used for a longer waterway the two values start to converge. The only significant difference for the result is the γ_{Th} -factor. [13] [18]

$$A_{Th} = \frac{A_T * l_T}{2g * \frac{h_v}{2g} * (H_0 - h_v)} * \gamma_{Th} \qquad [m^2] \tag{3.2}$$

$$A_{SVEE} = \frac{A_T * l_T}{2g * (\frac{h_v}{v_0^2} + \frac{1}{2g}) * (H_0 - h_v - \frac{v_0^2}{2g}) - 2 * \frac{v_0^2}{2g}} \qquad [m^2] \tag{3.3}$$

3.1.3.3 Basin- and shaft type surge tank

Both basin and shaft surge tanks are basically composed of a straight shaft with a constant profile and an optional overflow structure. This shape allows unhindered water oscillation between shaft and headrace tunnel due to the wide entrance opening. This is also the reason for a total reflection of the pressure wave on the water surface.
Acceleration and delay processes show slower and smaller deflections of the water surface in basin type surge tanks. This allows for a low height shaft but also has a negative effect on the dampening of the mass oscillation. This means oscillation takes longer to come to an end. With a shaft type surge tank design and its smaller diameter this dampening effect can be increased, but this also leads to bigger deflection of the water surface and therefore the need for a higher surge shaft. [9]

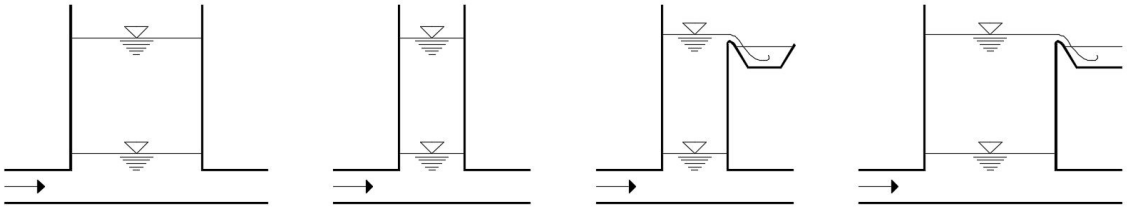

Figure 3.4: *Basin- and Shaft surge tanks [9]*

3.1.3.4 Chamber surge tank

This type of surge tank is most commonly used with two chambers. Usually the upper and lower chambers are placed above each other or in a shifted position and connected with a straight or inclined surge shaft.
The water level during a standstill of the power plant lies within surge shaft height. This results in fast rising pressure differences, which lead to fast acceleration and deceleration. The maximum hydro-peak defines the upper chamber's size. The upper surge chamber needs to be aerated and water level may not rise above the upper boundary.
The lower surge chamber has to ensure minimum pressure when the pump is active. Its

dimension depends on the tailrace head. The lower chamber must not run dry at any time. This would allow air to get into the system and could result in cavitation.
Compared to the shaft type, a chamber surge tank can be built with less height but higher construction effort. There are several different possibilities for chamber surge tank designs. Some examples are shown in figure 3.5. [9]

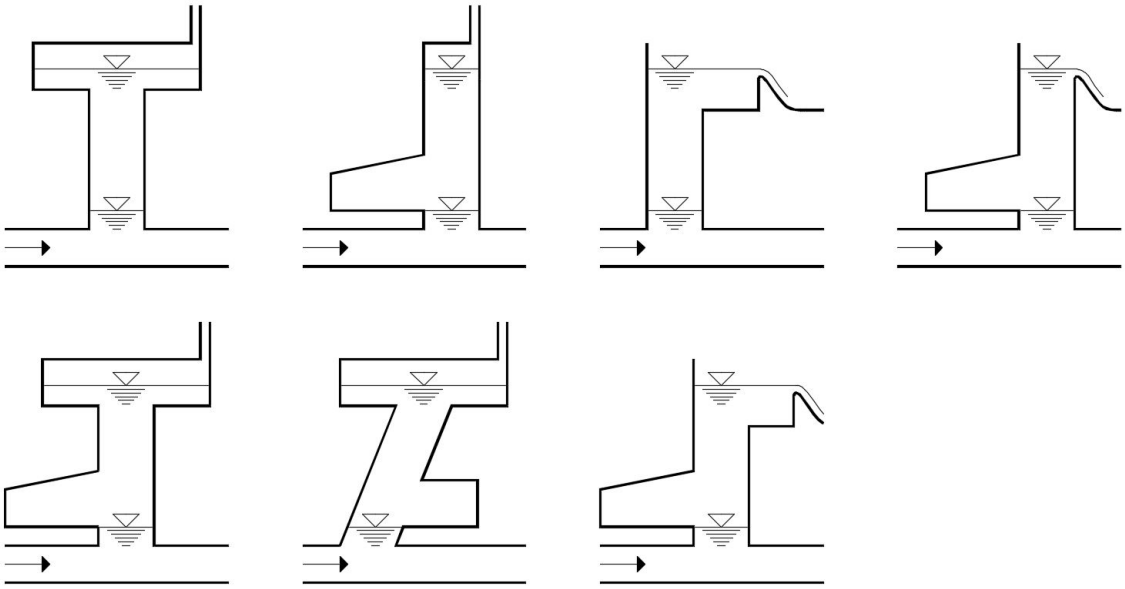

Figure 3.5: *Chamber surge tanks [9]*

3.1.3.5 Throttled surge tank

Shaft type and chamber surge tanks are weak dampening systems due to the fact that oscillation only gets curbed by friction and other hydraulic losses within the waterway. In order to produce a highly efficient pumped storage power plant, these losses have to be minimised. Using a throttled surge tank a stronger dampening effect can be achieved with regard to the stability criteria.
The sizing and special characteristics of a throttle are mentioned in chapter 3.1.4. [9]

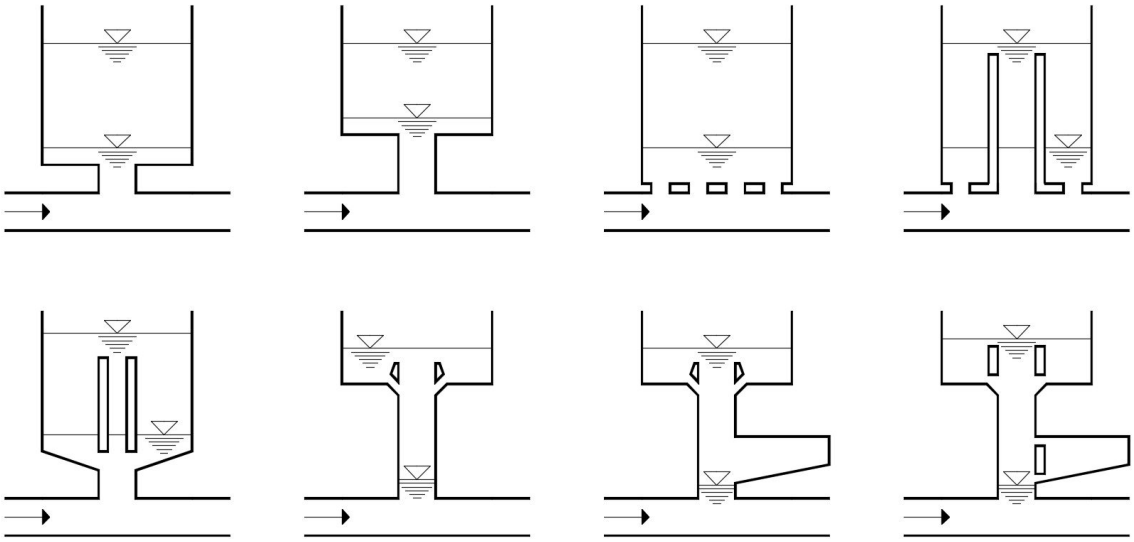

Figure 3.6: *Throttled surge tanks [9]*

3.1.3.6 Differential surge tank

A differential surge tank basically consists of two main chambers connected by a throttle. The first chamber, which is directly connected to the waterway, is called the riser duct. It has a smaller diameter than the main chamber and therefore compensates fast accelerations and delays with high deflections of the water level. Building an overflow structure at the riser duct's top, which leads to the bigger main surge chamber, prevents hydraulic losses. The dampening effect is enhanced by the back and forth flow into the main chamber through the throttle.
With an additional horizontal surge division the fast load changes of a pumped storage power plant can be handled. It is common for this type to have the throttle placed at the connection point between riser duct and lower surge chamber and/or main chamber. In this case the lower surge division needs an aeration shaft analogical to the riser duct. This shaft ends at the ridge of either the riser duct or the upper surge chamber. The addition of an upper surge division is optional but recommended. This structural arrangement implies a throttle with different loss coefficients in each direction. The resistance for a return flow has to be way bigger than for the inflow in order to prevent high overpressure. The so-called return-flow throttle provides these characteristics (Figure 3.7). [9] [10]

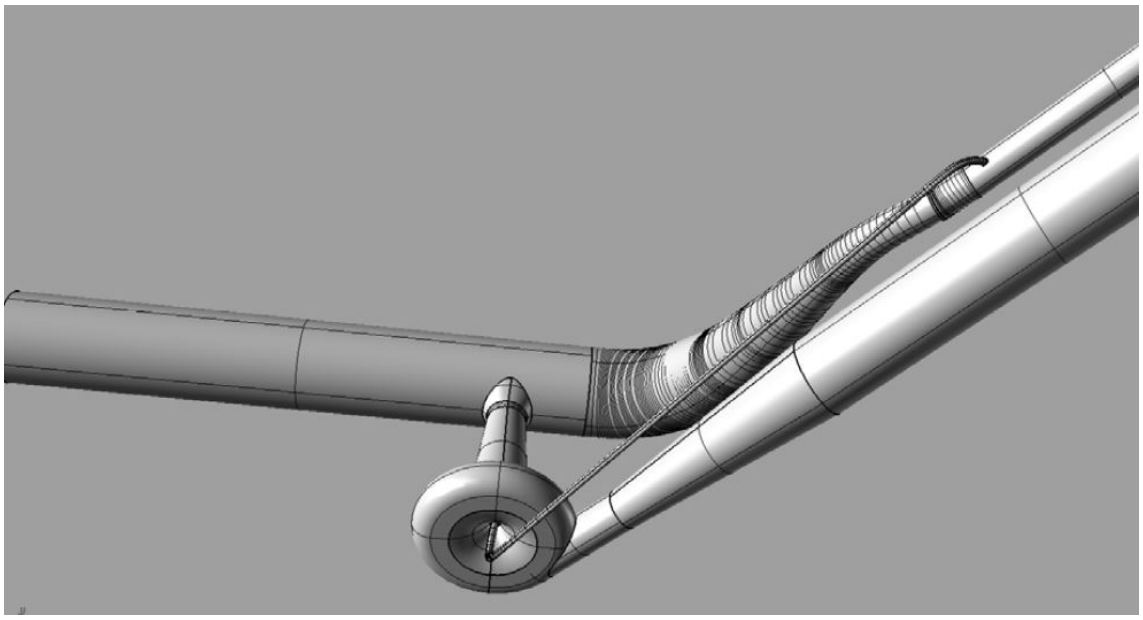

Figure 3.7: *Return-flow throttle pumped storage hydro-power Kaunertal [15]*

3.1.3.7 Pressurized surge tank

Even though a pressurized surge tank is mostly used in water supply facilities it can also be built for hydro-power plants. It is an airtight cavern most commonly built in solid rock with a low share of imperfections. This type of surge tank can also be built in less ideal conditions but it then gets more cost intensive.
Through water level deflections within the surge tank the air cushion gets compressed and provides counter-pressure. This pressure ensures smaller deflections and therefore a decrease in the volume required of the surge tank itself. [9]

3.1.4 Throttle

The throttle is needed to control the inflow and outflow of the surge tank. By ensuring a slower filling/emptying of the surge chamber either the diameter or height of the surge tank can be reduced.

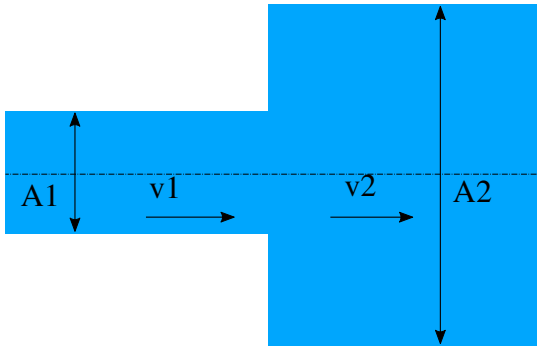

Figure 3.8: *Impact loss*

In order to calculate the loss coefficient the Borda-Carnot'sche loss formula (Equation 3.4) is used. This equation is related to a flow from the smaller to the bigger diameter. The computed loss coefficient is scaled with a factor of 1:3 for the reversed flow. [3]

$$\zeta = (1 - \frac{A_1}{A_2})^2 \qquad [-] \tag{3.4}$$

3.2 Hydraulic machinery

3.2.1 Hydraulic machine systems

Pumped-storage hydro power plants have to be very flexible in their operation, which means that the right choice of machinery is essential for the power plant. Each power plant has its own characteristics, therefore the pumps and turbines have to be adjusted to every single case. The decisive parameters can be: fast load changes, as well as size or efficiency of the machines. To fulfil those requirements, two different types of machines have been developed, the two-block and the three-block-system.

3.2.1.1 Two-block-system

The two-block-system is also known as pump-turbine. In this system, the pump and turbine are one combined block, and the generator, which is also operating as the electric motor for the pump-turbine, is the second one. By combining the turbine with the pump, up to 30% of the cost can be reduced compared to the three-block-system. This large cost reduction is based on the fact that less space is required. Furthermore half of the distribution lines and closing devices can be done without.
For a load change from turbine to pump mode the pump-turbine first has to be stopped completely. Then the electric motor drives the shaft connected to the pump-turbine in the other direction and therefore starts to pump water to the upper reservoir. Two-block-systems can be built with either reversible Kaplan- or Francis turbines.
The pump-turbine has to be designed for both turbine and pump mode, which is why the two-block-system has a lower overall efficiency. In general, turbine efficiencies can reach up to 93-95% and pump efficiencies up to 75-85%. By putting the main focus on one operating mode quite a good degree of efficiency can be reached. [7] [9]

3.2.1.2 Three-block-system

Three-block-system or ternary unit means that the generator, pump and turbine are separate machines connected by a shaft. The advantage of the ternary unit is that the pump and the turbine can be decoupled. This ensures faster load change and minimizes losses. With this tandem set a higher efficiency can be obtained due to the fact that the pump as well as the turbine can be designed autonomously. However, more space is needed for this type of machinery, which leads to higher construction costs. The ternary unit can be built with a Francis- or Pelton turbine, depending on the relative drop height. [7]

3.2.2 Hydraulic machine types

As already mentioned in chapters 3.2.1.1 and 3.2.1.2 different design types of hydraulic machines are possible for each system. The different machine types have their own area of application since they are only suitable for certain heights and discharge values, as shown in figure 3.9.

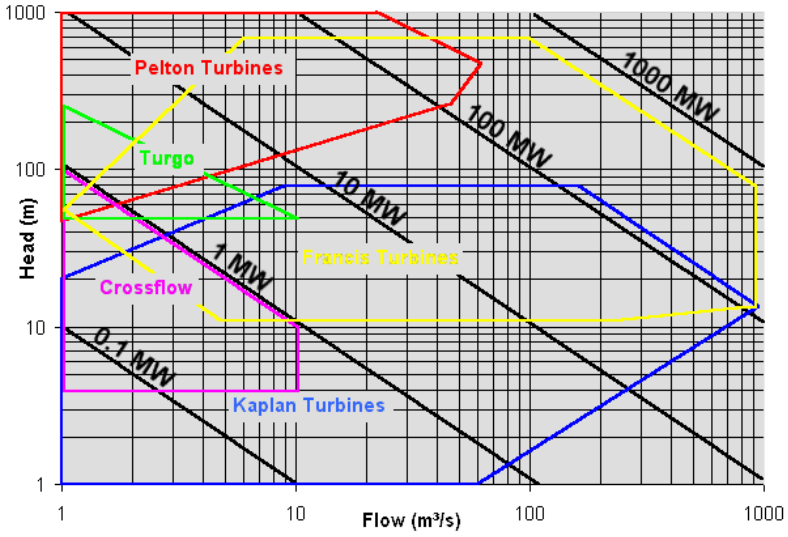

Figure 3.9: *Turbine application chart [11]*

3.2.2.1 Kaplan turbine

The Kaplan turbine is designed for low to medium head applications with rather high discharge values. This turbine type usually has its area of application at run-of-river plants, since they have constant discharge values. Consistent flow conditions are recommendable for the Kaplan turbine, due to the fact that efficiency depends on admission flow. [9]

3.2.2.2 Francis turbine

The Francis turbine is designed for medium head applications with constant admission flow. With drop heights from 5 m up to 750 m its area of application overlaps with both the Kaplan as well as the Pelton turbine. The advantage compared to the open-jet turbine is that the specific rotational speed is higher. This leads to smaller dimensions of the turbine itself.
A Francis turbine can be built in with a horizontal or vertical shaft. For medium- and high-head power plants the shaft is usually constructed vertically. The reason for this is to achieve uniform pressure distribution at the impeller, and therefore reduce risk for cavitation. [9]

3.2.2.3 Pelton turbine

The Pelton turbine is an open-jet turbine, which has its field of application at small or medium discharge rates with big drop heights. This height can reach up to 2000 m. This machine type is most commonly used for pumped-storage hydro power due to its adjustability and therefore the capability of covering peak demands.
At drop heights between 200-800 m, both the Francis as well as the Pelton turbine can be used. The application criterion for the turbines, apart from the constructive factors, is turbine efficiency. The Francis machine can reach up to 2 % higher efficiency with a

constant admission flow. Anyhow, the Pelton turbine has its advantages if admission flow undergoes a lot of changes. This leads back to the efficiency curve of this turbine type, which is flatter than that of a Francis turbine. [9]

4 WANDA 4 - Modelling and Analysis

4.1 Program introduction

WANDA 4.2 is a 1-D numerical program for hydraulic design and optimization of pipeline systems developed by the Dutch company Deltares (formerly: WL — Delft Hydraulics). This software is used for the analysis of steady and unsteady flow conditions in any desired pipeline network. *WANDA* is capable of modelling liquid, heat and gas flows. Cavitation and variable fluid properties can also be computed. Therefore it is possible to calculate a big variety of pipeline networks like fire fighting systems, sewage systems, water distribution networks, industrial plants, oil pipelines, water cooling systems, hydro-power plants and transportations systems for chemical products. [4] [5]

4.2 Analysis modes and properties

Due to the fact that *WANDA 4.2* has a big variety of applications it is necessary to define certain physical parameters in order to calculate the hydraulic system. These parameters are, among others, density, viscosity, fluid type (newtonian or non-newtonian fluid) and so on.

4.2.1 Calculation modes

WANDA 4.2 operates with two different types of calculation modes, the Engineering mode and the Transient mode. These different modes should enhance computation time and therefore speed up the modelling.

4.2.1.1 Engineering mode

In engineering mode the hydraulic model is designed with the help of a wide variety of predefined components. After the basic modelling, properties have to be assigned for each element.
While being in this mode, only steady state analysis is possible. This ensures short computation times which are beneficial for the first dimensioning of the hydraulic system.

4.2.1.2 Transient mode

While being in transient mode, WANDA is capable of simulating unsteady flow conditions. Phenomena like extended time simulations, waterhammer events and cavitation can be computed. For these calculations the components need adjusted settings depending on the time.

- Extended time simulation (quasi-steady)

An extended time simulation is basically a number of independent steady state calculations put in sequence, yet the computations are independent from earlier solutions. With this simulation the pipe friction is calculated for the new time step.

- Waterhammer

  Pressure waves develop within a hydraulic system when a sudden change in the flow conditions (valve closure) occurs. The waves then travel through the surges until they reach a free surface and get reflected. These pressure waves spread with speeds up to over 1000 m/s. Therefore this phenomenon has to be calculated over time.

- Cavitation

  Once the pressure within a hydraulic system drops below fluid vapour pressure, cavitation can occur. Pressure waves and abrupt changes in the pipe profile can result in these kinds of pressure variations.
  By recalculating the flow conditions at each time step depending on the pressure and fluid properties, which makes this kind of calculation CPU-intensive, the effect of cavitation is included.
  [4]

4.2.2 Time properties

The time parameters are: time steps, simulation time and output increment. These properties are applicable in transient mode only. A well-thought-out selection of time parameters is recommended, since they are responsible for computation time, accuracy and data file size.
The time step defines the precision of the calculation and computation time means the overall duration of the simulation. With the output increment the time steps shown in a time series are specified, but it has no influence on the simulation accuracy. [4]

4.3 Basic components

WANDA 4.2 provides a variety of components for hydraulic modelling and analysis. The used elements for this representational hydraulic design are described in the following chapters.

4.3.1 Hydraulic nodes

Using the *H-node* hydraulic components get connected with each other. When there are more than two components connected, the *H-node* becomes a master and slave system. This means when the only input parameter, that is elevation, is changed at one node (master) automatically all other connected nodes (slaves) change too.
The *H-node's* main variable is the head. Based on the type of node used it is possible to predefine the head. Furthermore the *H-node* pressure is calculated with the Bernoulli theorem (equation 4.1). In order to calculate those variables the *H-node* needs to be part

of a fully connected hydraulic system with at least one boundary condition for the head. [4]

$$H = z + \frac{p}{\rho g} + \frac{v^2}{2g} \tag{4.1}$$

4.3.2 Boundary condition

Basically there are two different types of boundary conditions, the pressure head *(boundH)* and the discharge (or flow) boundary condition *(boundQ)*.

4.3.2.1 Pressure head boundary condition

The *boundH* condition prescribes the head in a certain point of the system. With this boundary condition reservoirs can be modelled. The prescribed head is a total energy head, due to zero velocity within the reservoir. By employing the element *boundH* steady and unsteady state calculations are possible. The mathematical model for the computation is simply a function dependent on time (equation 4.2), which is added by the user with an action table.
To achieve a specified head the *boundH* component has to supply or consume fluid to or from the system. The continuity equation determines the discharge of the *boundH* element. By installing this boundary condition between two pipes it decouples the system with a total reflection of the waterhammer wave. [4]

$$H = f_{(t)} \tag{4.2}$$

4.3.2.2 Discharge (or flow) boundary condition

The component *boundQ* prescribes discharge in a certain point of the system. With this tool pumps and turbines can be modelled. Even though there is a certain element for pumps, the *boundQ* component is more simple. The boundary condition has a constant value during steady state computation. For the unsteady state computation the *boundQ* element is bound to a function dependent on time (equation 4.3), which is added by the user with a table. [4]

$$Q = f_{(t)} \tag{4.3}$$

4.3.3 Pressurised pipe

The element *pipe* is defined by the geometric profile, the friction model and the longitudinal geometric input. The geometry profile can either be a circle or a rectangle.

WANDA 4.2 supports several different friction models for Newtonian and non-Newtonian fluids. In this master thesis all pipes have been computed with the theoretical friction model of Darcy-Weisbach (Equation 4.4). The friction factor f is dependent of wall roughness k. These k-values subject to the material and age of the pipe and usually are within a range from 0.1 - 10 mm. The friction factor f is calculated by using the Colebrook-White equation (Equation 4.5). Local losses can also be added to the *pipe* by building in a *resist* element or combining it in the *pipe* model.

$$H_2 - H_1 = \frac{f l_T}{d_T} * \frac{Q|Q|}{2gA_f^2} \tag{4.4}$$

$$\frac{1}{\sqrt{f}} = -2log(\frac{k}{3.7d_T} + \frac{2.51}{Re\sqrt{f}}) \tag{4.5}$$

The longitudinal geometric input is done with a scalar value for length, length-height profile or with isometric layout specified absolute/differential XYZ-coordinates. The input is translated to a longitudinal profile (X-H profile). The input node elevation is the height of the centreline of the pipe.
Furthermore the element *pipe* has a lot of different parameters like wall thickness, wave speed mode, Young's modulus and so on. Those are used in order to calculate the occurring waterhammer in the hydraulic system. [4]

4.3.4 Free surface flow conduit

In order to simulate a slow filling or draining of a pipe, the element *free surface flow conduit* is used. It is capable of simulating the behaviour of free surface phenomena.
The geometry profile and the friction models for this element are the same as those mentioned in chapter 4.3.3. The only difference in geometry referred to the *pipe* is node elevation, which is at the bottom of the *conduit*.
The dynamic behaviour of this component is defined by the continuity and momentum equation. Those equations for free-surface flows are limited to slopes of 1:7.
The applied numerical algorithms to solve the free surface behaviour are described by equation 4.6 and 4.7. With those equations the sub-critical, super-critical and transitions between both flow types are described.

$$\frac{\partial A(\zeta)}{\partial t} + \frac{\partial}{\partial t}(VA(\zeta)) = 0 \tag{4.6}$$

$$\frac{\partial}{\partial t}(AV) + \frac{\partial}{\partial x}(AV^2) + gA\frac{\partial H}{\partial x} + g\frac{AV|V|}{C^2R} = 0 \tag{4.7}$$

It has to be assumed that the air within the *conduit* can enter or leave freely without causing pressure surges. [4]

4.3.5 Resistance

The *resist* class is used to simulate hydraulic losses in the system. Although the class includes several elements, the mathematical model stays the same. It is given in equation 4.8.

$$H_2 - H_1 = \frac{\xi Q_1 |Q_1|}{2gA_r^2} \tag{4.8}$$

With the specific *resist 2-way quadr.xi* component, head losses in both flow directions can be simulated. What is special is that the loss coefficient for the flow directions may be chosen differently, therefore it is suitable for throttle modelling. [4]

4.3.6 Shaft

The *shaft* element models a steep pipe with height-dependent area. It has an inflow at the top, which is an input parameter, and one at the shaft bottom. The bottom inflow height has to correspond with the node elevation. Within this component friction is neglected, therefore *resist* elements are commonly used with the *shaft*.

$$Q_1 - Q_2 = A\frac{dH_2}{d_t} \tag{4.9}$$

There are three different initial states of the *shaft*, which define how the element is operated during steady state calculations. However, equation 4.9 describes all initial states, and with equations 4.10 to 4.12 the boundary conditions of each state are described.

- Partially filled: The initial shaft level is lower than the top edge height. The upstream head equals or is higher than the edge level. The shaft level is determined by the downstream system.

$$H_1 = z_{edge}; H_2 < z_{edge} \tag{4.10}$$

- Submerged: The shaft is pressurised if the shaft level exceeds the top edge

$$H_1 = H_2 > z_{edge} \tag{4.11}$$

- Drained top: The shaft level is determined by the downstream system (upstream head is lower or equal to the top edge level)

$$Q_1 = 0; H_1, H_2 < z_{edge} \tag{4.12}$$

During the transient calculation the shaft behaves like a surge tower with height-dependent storage area, although without any friction considered. [4]

4.3.7 Weir

The element *weir* can have a discharge in both flow directions. With a higher head on the upstream side (H_1) than on the downstream side (H_2), it has a positive flow direction. As long as the flow over the edge is in a critical state (Figure 4.1) the mathematical model is based on the short crested weir formula according to Poleni (Equation 4.13). The loss coefficient C_W (Equation 4.15) is a product of individual loss coefficients. C_v is a correction factor for the upstream velocity of the weir. The energy losses that occur at the weir are corrected with C_D.
Flush flow occurs when no change of flow can be observed at the back of the weir. This means the downstream head gets big enough to influence the upstream flow (Figure 4.2). When this happens equation 4.13 is no longer valid and is replaced by equation 4.14 instead.
Once H_2 gets bigger than H_1 the flow direction of the weir changes from positive to negative and the equations adapt to this. Basically the same equations are valid for this case but with switched up indices. [3] [4]

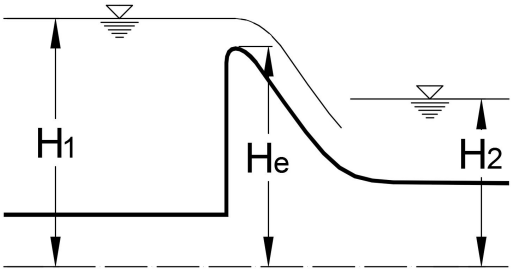

Figure 4.1: *Critical flow over weir*

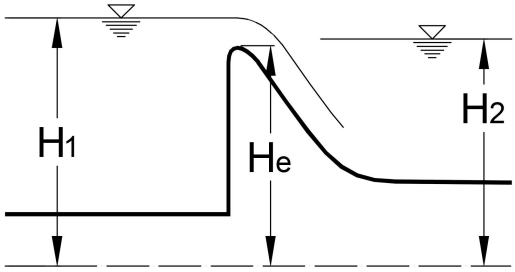

Figure 4.2: *Flush flow over weir*

$$Q = \frac{2}{3} * \sqrt{2g} * C_W * B * (H_1 - H_e)^{3/2} \tag{4.13}$$

$$Q = BC_W(H_2 - H_e)\sqrt{2g(H_1 - H_2)} \tag{4.14}$$

$$C_W = C_v * C_D \tag{4.15}$$

5 Mechanical equipment

5.1 Load case scenarios

Each pumped storage hydro-power plant is unique and has its own system performance, and therefore all possible load cases have to be taken into account. In general there would be four load case scenarios as seen in Table 5.1. Since the *Multiple load changes* and the *Load shedding* scenarios include the others, only these two are examined in detail. In civil engineering usually safety factors are used in order to ensure the stability of a structure. Safety factors can't be added to these simulations, therefore multiple load changes are observed. It is very unlikely that this load case ever occurs during operation, but it has established itself as a kind of safety loading case in hydraulic engineering.
These two load scenarios correlate with each other. This means that first the load cases are investigated in order to determine the minimum size of the surge tank. Then the specific model type is loaded with each load case scenario separately to analyse the maximum discharge of the system.

Table 5.1: *Load case scenarios*

Scenario:	Description:
Start/Stop	Starting and stopping of the turbines and pumps
Simple load change	A one time transition from turbine- to pump mode at peak flow
Multiple load changes	A triple transition form turbine- to pump mode at peak flow
Load shedding	A very fast stop during turbine mode

5.1.1 Multiple load changes

In order to perform a maximum possible load case, multiple load changes have to be simulated. In general three total load changes are performed to see if the system gets into an eigenfrequency. If that is not the case, the hydraulic system is stable and the computation can be carried on.
The ternary units start closed in this simulation. Within 30 seconds the discharge rises to its maximum. Once a peak flow (Q_{max}) occurs, the simulation is stopped and the time is noted for the next simulation. In the next computation a load change is initiated at this very time step. This means the turbine shuts down from 100 % to 0 % within 30 seconds and the pump starts, with a turbine to pump ratio of 1.35, again within 30 seconds. These steps have to be repeated vice versa three times.
This shows that the simulation of various operating modes in WANDA is an iterative procedure.

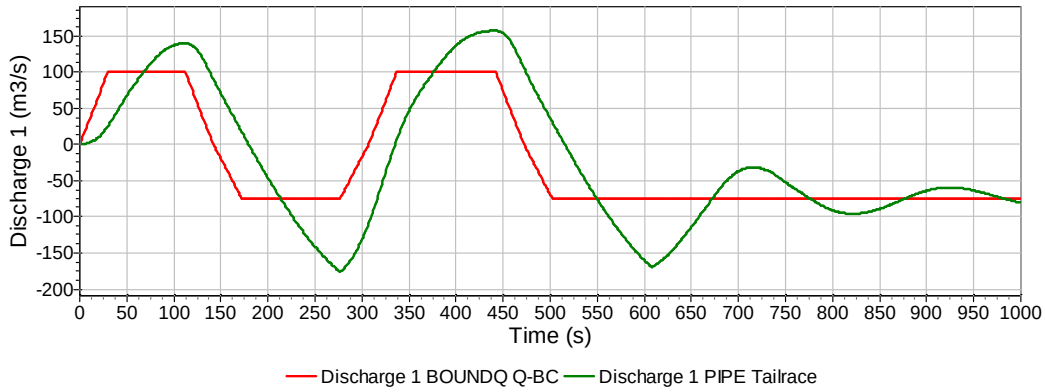

Figure 5.1: *Pump and Tailrace discharge for a load change scenario*

5.1.2 Load shedding

The load shedding differs from the load changes only at the very last load change. Instead of changing from positive to negative discharge (turbine mode to pump mode), the turbine comes to an abrupt stop within five seconds. This leads to a big mass compensation for the surge tank, which can be the defining load case for surge tank size, especially with higher design flow rates.

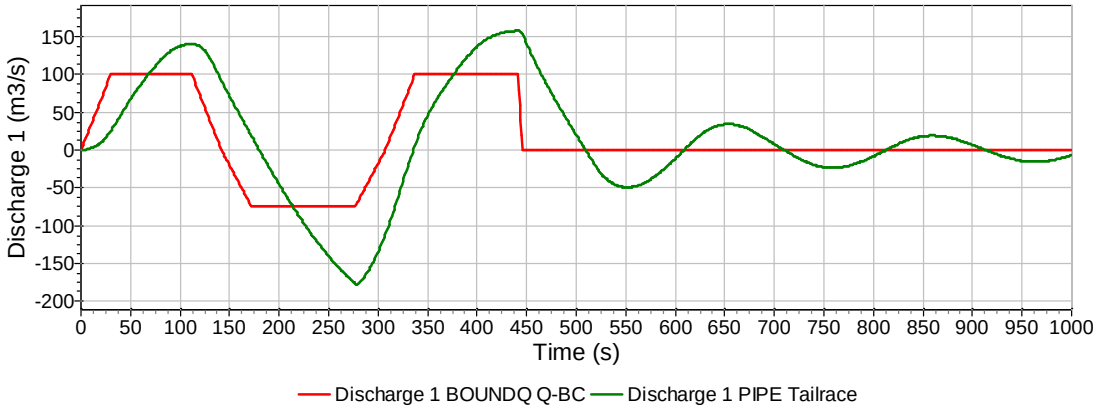

Figure 5.2: *Pump and Tailrace discharge for a load shedding scenario*

5.2 Turbine

In order to show the sizing of a turbine, the representative design flow of 100 m³/s is examined.
Two Francis turbines with 50 m³/s admission flow each have been chosen for this project. With a drop height of approximately 600 m the Francis turbines are close to their upper limit of usability according to figure 3.9.

5.2.1 Pre-dimensioning

Usually a pre-dimensioning is done with shell schemes. If those schemes are not available, the specific rotation speed $n_{q,max}$ (Equation 5.1) and therefore the overall impeller diameter D_3 can be determined using the half-empirical formula according to Mosonyi (Equation 5.5). This diameter is the initial value for the turbine size.

$$n_{q,max} = \frac{638}{H_0^{0.512}} \qquad [min^{-1}] \tag{5.1}$$

With equation 5.2 the rotational speed n of the turbine is calculated. Afterwards the synchronous speed n_{syn} can be determined with table 5.2 by rounding the rotational speed to the closest value. The synchronous speed for a 50 Hz electric power grid has to be chosen, since its the common utility frequency f_u in Europe and large parts of the world. In contrast, the 60 Hz frequency is used in America and parts of Asia. Railway systems use a unique utility frequency as well.

$$n = n_q * \frac{H_0^{0.75}}{\sqrt{Q_M}} \qquad [min^{-1}] \tag{5.2}$$

Table 5.2: *Synchronous speed n_{syn} with the according number of poles and pole pairs [9]*

Number of poles - $2p$	6	8	10	24	48	60
Number of pole pairs - p	3	4	5	12	24	30
n_{syn} $[min^{-1}]$ for $f_u = 50Hz$	1000	750	600	250	125	100
n_{syn} $[min^{-1}]$ for $f_u = 60Hz$	1200	900	720	300	150	120

Once the rotational and synchronous speeds are determined, the coefficient for Francis turbines $k_{u,F}$ and the speed of rotation u_3 have to be calculated. For this equations 5.3 and 5.4 are used. Afterwards the impeller diameter can be determined with equation 5.5.

$$k_{u,F} = 0.293 + 0.0081 * n_q \qquad [-] \tag{5.3}$$

$$u_3 = k_{u,F} * \sqrt{2 * g * H_0} \qquad [m/s] \tag{5.4}$$

$$D_3 = \frac{60 * u_3}{\pi * n} = 84.6 * \frac{k_{u,F}}{n} * \sqrt{H_0} \qquad [m] \tag{5.5}$$

With the determined impeller diameter the remaining dimensions can be calculated according to figure 5.3. These values are shown in table 5.4.

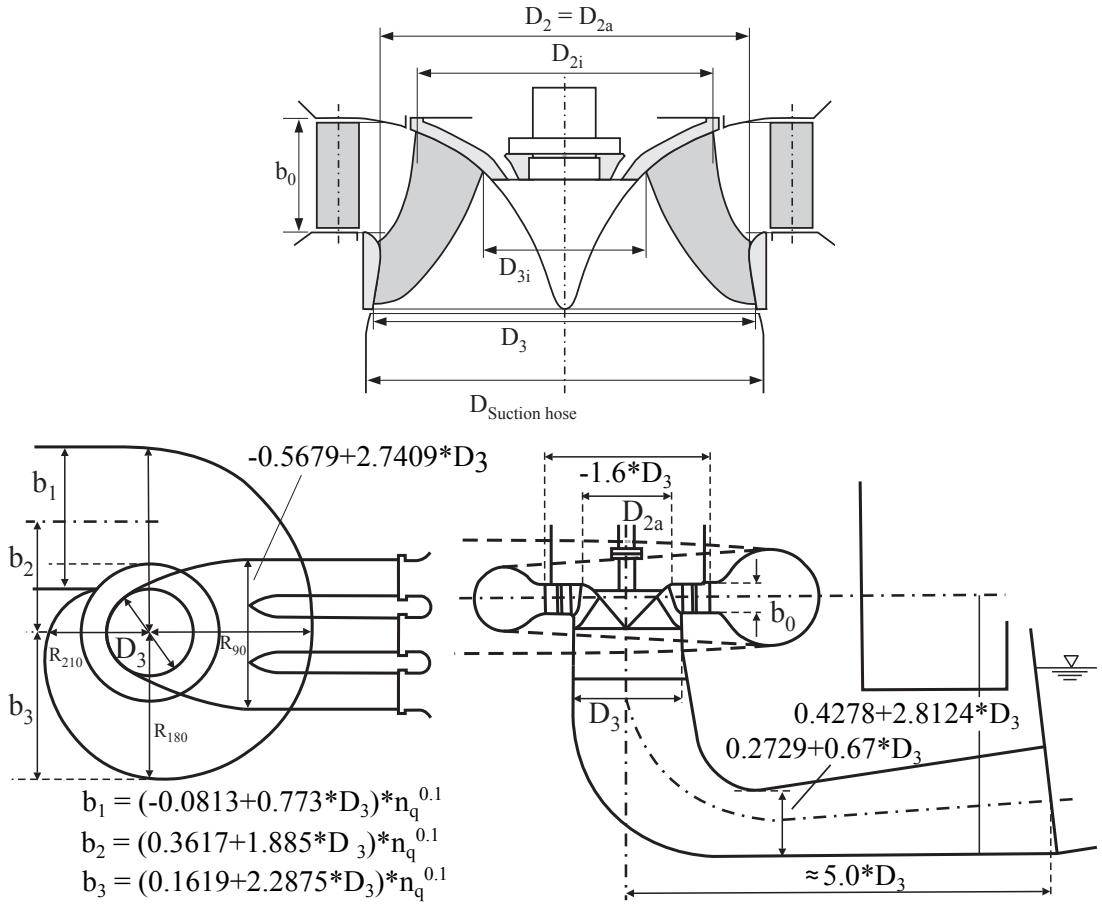

Figure 5.3: *Scheme sections of a Francis turbine [9]*

Table 5.3: *Calculated turbine parameters*

Turbine parameters

$n_{q,max} =$	24.1	[1/min]	Specific rotational speed
$n =$	413.6	[1/min]	Rotational speed
$n_{syn} =$	250	[1/min]	Synchronous speed
$k_{u,F} =$	0.488	[-]	Turbine coefficient
$u_3 =$	53	[m/s]	Speed of rotation
$D_3 =$	2.45	[m]	Overall impeller diameter

Table 5.4: *Calculated turbine dimensions*

Turbine dimensions

$b_1 =$	2.49	[m]	
$b_2 =$	6.85	[m]	
$b_3 =$	7.92	[m]	
$R_{90} =$	6.14	[m]	
$1.6 * D_3$ =	3.92	[m]	
$l =$	12.24	[m]	Suction hose length
$D_S =$	1.91	[m]	Suction hose min. diameter

6 The two chamber surge tank

6.1 Modelling and Analysis

In order to see the influences of certain construction parts three different models have been created for the variant analysis. All simulations have been performed with discharges reaching from 20 m³/s up to 100 m³/s. These three models use the same surge tank type but differ in certain construction parts.

6.1.1 Boundary conditions

The ternary units are modelled with a simple *boundQ* element. With the help of the action table input the discharge with respect to time is taken into account. With this element the different load case scenarios as mentioned in chapter 5 are defined.

In the model, the river Danube is represented by a *boundH* component. This boundary condition has a constant head at any time. Water level fluctuations of a river are hard to design in a hydraulic model and do not have a very big influence on the outcome, therefore they are negligible.

6.1.2 Tailrace

The tailrace is modelled with a *pressurized pipe* element. Friction is based on the wall roughness model. The roughness factor k is chosen, being 0.2 mm (according to [3]) for new concrete pressure tunnels.
The tailrace head must not drop below pipe level in order to prevent cavitation. The highest danger is to be found right next to the surge tank (beginning of the tailrace) due to the fact that this is where the strongest pressure fluctuations are.
The maximum head, together with the ground conditions and mountain water table, determine the sizing as well as the type of the lining.
As mentioned in chapter 3.1.2 the ideal diameter is determined by the cost of hydraulic losses and construction costs. In this case the diameter gets designated by a maximum velocity of 3.80 m/s, which is coupled to both of these conditions. With the continuity equation (Equation 6.1) the diameter can be calculated (Equation 6.2). Table 6.1 shows that bigger head losses come with smaller diameters and therefore confirms the cost of energy losses from figure 3.3.

$$Q = v * A \qquad [m^3/s] \tag{6.1}$$

$$\Rightarrow d = \sqrt{\frac{4Q}{v\pi}} \qquad [m] \tag{6.2}$$

Table 6.1: *Tailrace diameter and head loss*

Turbine	Pump	Tailrace diameter	Head loss
[m³/s]	[m³/s]	[m]	[m]
20	14.9	2.6	15.70
30	22.3	3.2	11.67
40	29.7	3.7	9.56
50	37.1	4.1	8.64
60	44.5	4.5	7.58
70	51.9	4.9	6.55
80	59.3	5.2	6.23
90	66.7	5.5	5.85
100	74.1	5.8	5.44

6.1.3 Trifurcation

The hydraulic losses of the trifurcation are compensated with two *resist 2-way quadr.xi* elements. In order to take both flow directions into account, those elements have to be arranged before and after the surge tank *H-node* as seen in figure 6.1.

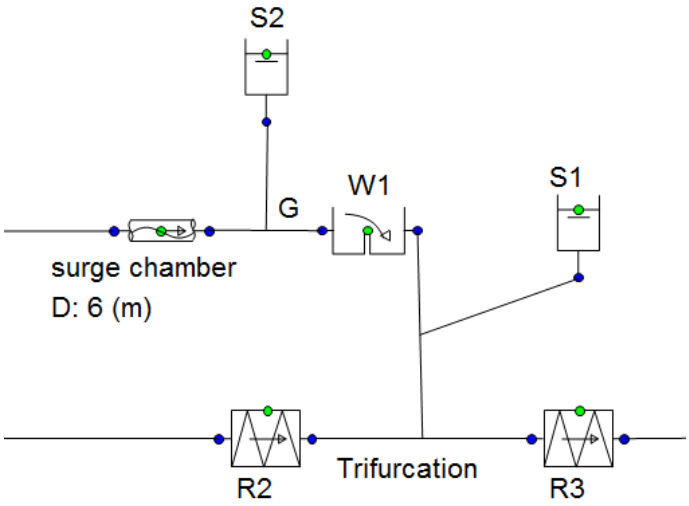

Figure 6.1: *Trifurcation model*

6.1.4 Surge shaft

The *surge shaft* input device is an action table with specified height and an according diameter. Its size is determined by the stability criterion while elevation depends on the operation levels. The stability criterion is calculated according to equations 3.2 and 3.3.

The results of these equations are shown in table 6.2 along with the chosen diameters for the surge shaft. Diameters had to be chosen bigger for the simulation in order to ensure enough water mass for the compensation. These final diameters got determined by various trial simulations.
The Thoma area differs with a factor of approximately 1,5 from the Svee area, which is exactly the Thoma factor γ_{Th}. This leads back to the big tailrace length and the consequential convergence of the value as already mentioned in section 3.1.3.2.

Table 6.2: *Surge shaft diameter*

Design flow - turbine	**Thoma**	**Svee**	**Chosen diameter**
[m³/s]	[m]	[m]	[m]
20	1.85	1.52	3.00
30	2.59	2.12	4.00
40	3.28	2.68	4.50
50	3.87	3.16	5.00
60	4.49	3.67	7.50
70	5.14	4.20	7.50
80	5.65	4.62	7.50
90	6.18	5.05	7.50
100	6.72	5.49	8.00

6.1.5 Surge chambers

Both surge chambers are modelled with a *free surface flow conduit* in order to simulate the filling and emptying of the surge tank.
In addition to the free surface flow conduit the lower chamber has a two-directional *weir* to simulate water overflow. By adding this weir, overflow losses are taken into account. Anyhow, the lower surge chamber may not run empty at any point of the simulation. In that case the head would go below tailrace level and therefore might lead to cavitation. This is ensured as long as the tailrace head stays above 169 m a.s.l.
Unlike the lower one, the upper surge chamber is not allowed to run full at any point of the simulation. Once this chamber is close to run empty the differential effect like mentioned in chapter 3.1.3.1 kicks in. As an example figure 6.2 shows this effect for a design flow of 100 m³/s. At 468 seconds in the simulation the shaft water level drops below edge level (250 m.a.s.l.) while there is still a decent amount of water in the upper chamber.
To ensure these boundary conditions of the surge chambers, the volume is multiplied by a safety factor of 1.25.

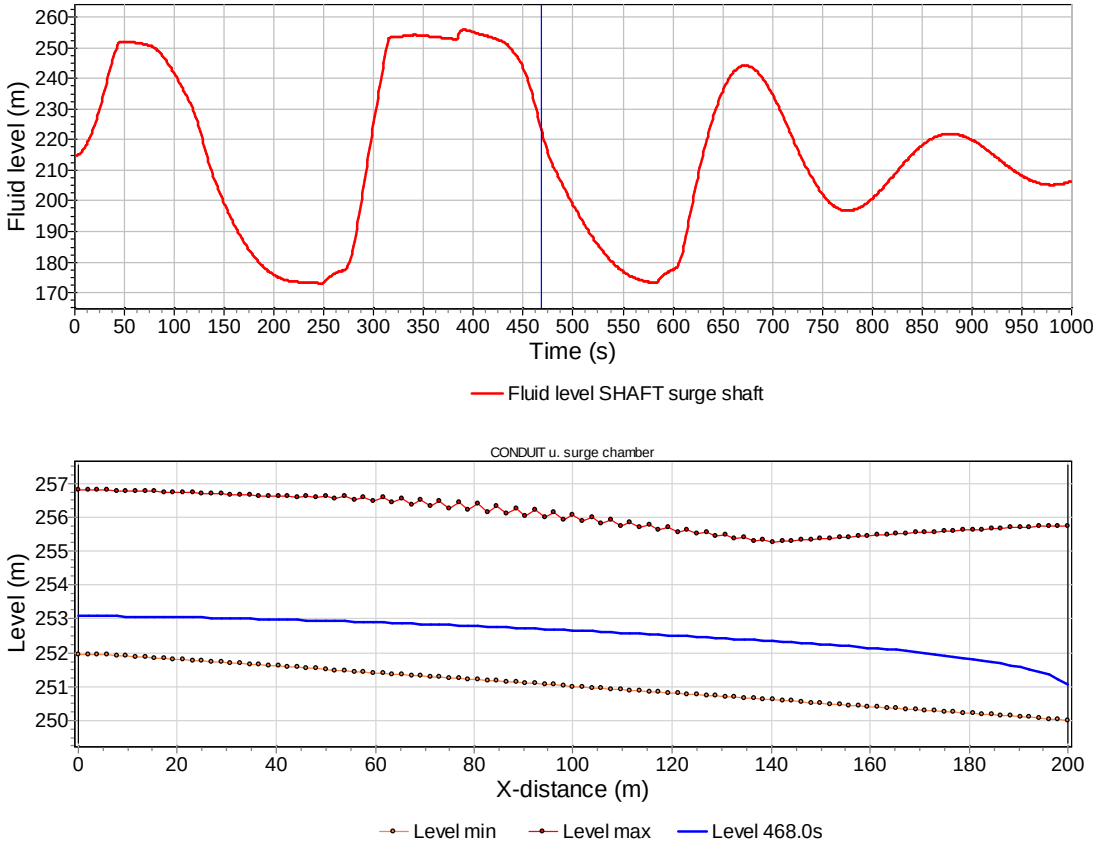

Figure 6.2: *Differential effect of the upper surge chamber*

Figure 6.3 shows that for this example the ridge would be at 258.00 m a.s.l. and the maximum water level would be at about 256.90 m a.s.l. This ensures that the whole system is free from pressure surges caused by a full-filling of the surge tank.

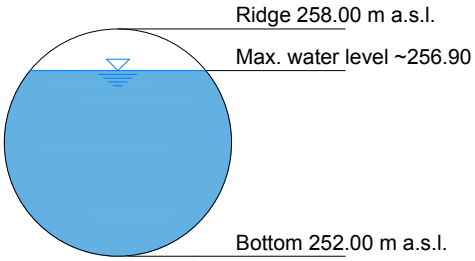

Figure 6.3: *Cross-section of the upper surge chamber at top end*

6.2 Type 1 - Surge tank without throttle

Model type 1 (Figure 6.4) is modelled without a throttle. For lower design flow rates a throttle is not mandatory. The main purpose of this model is to show the significance of a throttle for high design flow rates with regard to hydraulic and economical aspects. Subsequently all nine different design flow rates are shown. For each flow rate both main loading cases are observed and the results are compared in tables and graphs.

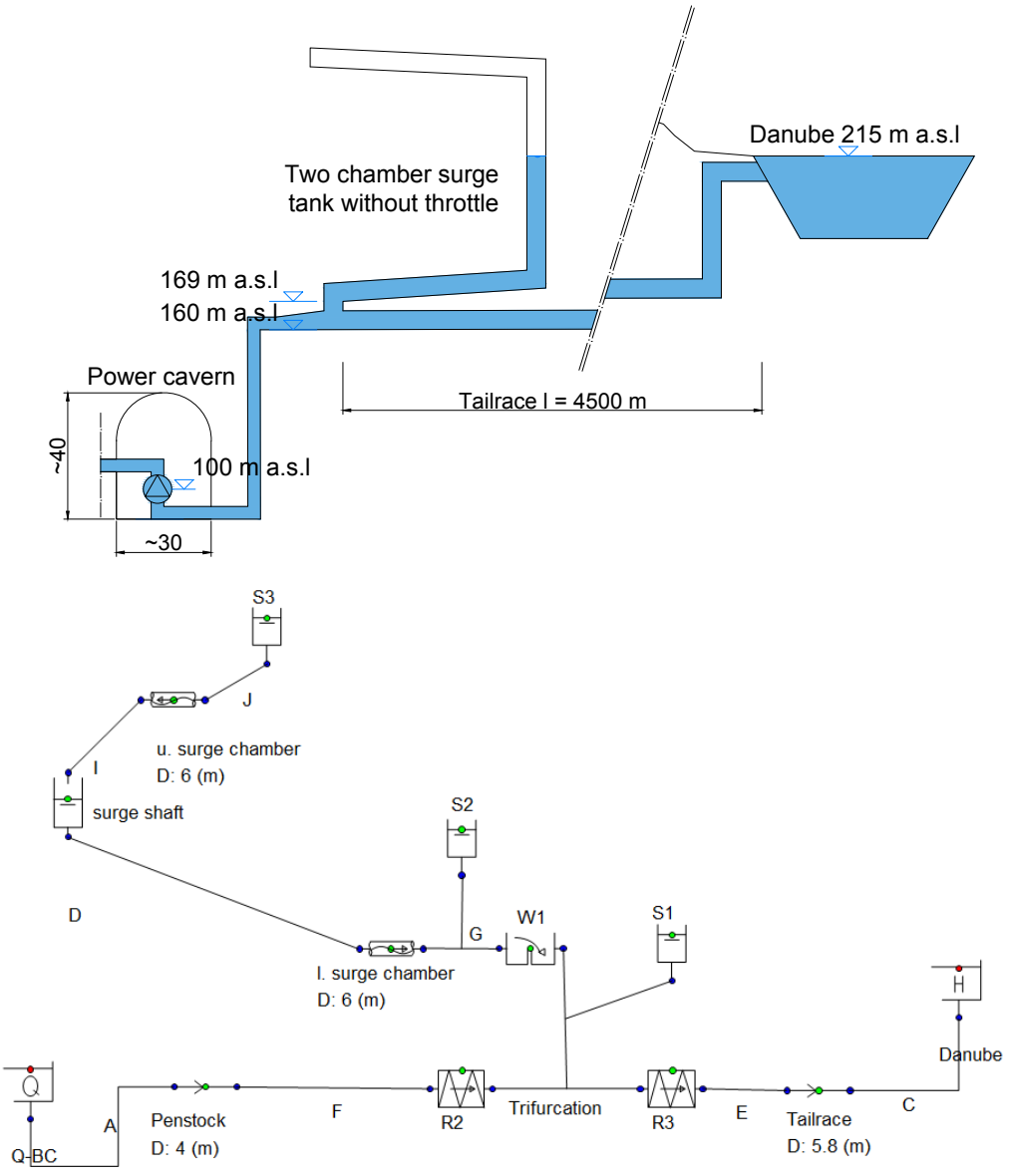

Figure 6.4: *Physical (top) and 1-D numerical model (bottom): Type 1 (turbine design flow = 100 m³/s)*

6.2.1 Type 1 - Turbine design flow rates

Turbine design flow rate Q = 20 m³/s

20 m³/s is the lowest observed design flow rate, which should fit especially this model type rather well. Due to the low flow rate a smaller amplification and surge tank size can be expected.
Figure 6.5 shows that both loading cases react quite similar Amplification also hardly differs from each other. The only difference is a slightly stronger negative flow amplification during the load changes. Both loading cases show a stable hydraulic behaviour.
In figure 6.7 the tailrace head of both loading cases is illustrated. None of those two graphs shows a head lower than 169 m.a.s.l., this means that the danger of cavitation is neglectable in this area. The load changes have a little bit smaller head than the load shed, but it is still above the lower chamber edge level.
The two loading cases correlate with one another, as mentioned in chapter 5.1. Therefore only one surge tank size is determined. This excavation size is designed for the maximum up- and down swing of the water column. Then the size of the upper and lower surge chambers is increased by 25 % for safety reasons.
Figure 6.6 is only shown once, since the tailrace length stays the same, only the diameter changes with the turbine design flow rate.

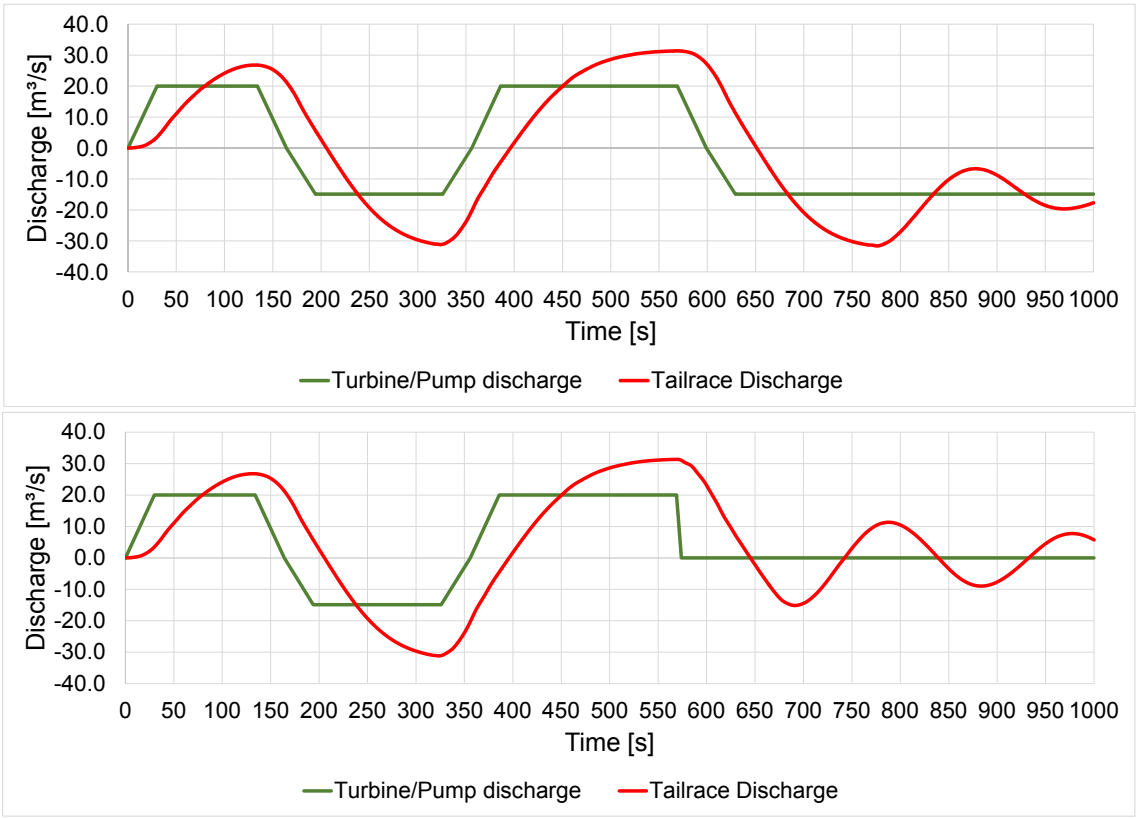

Figure 6.5: *Model type 1 - 20 m³/s - Comparison of the tailrace discharge (load changes top, load shed bottom)*

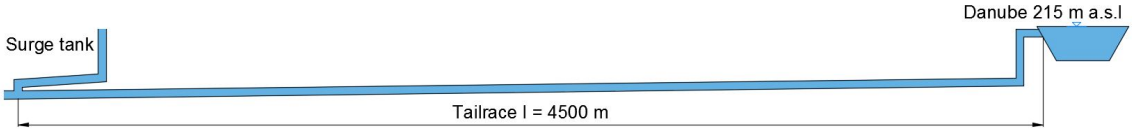

Figure 6.6: *Physical model for the tailrace*

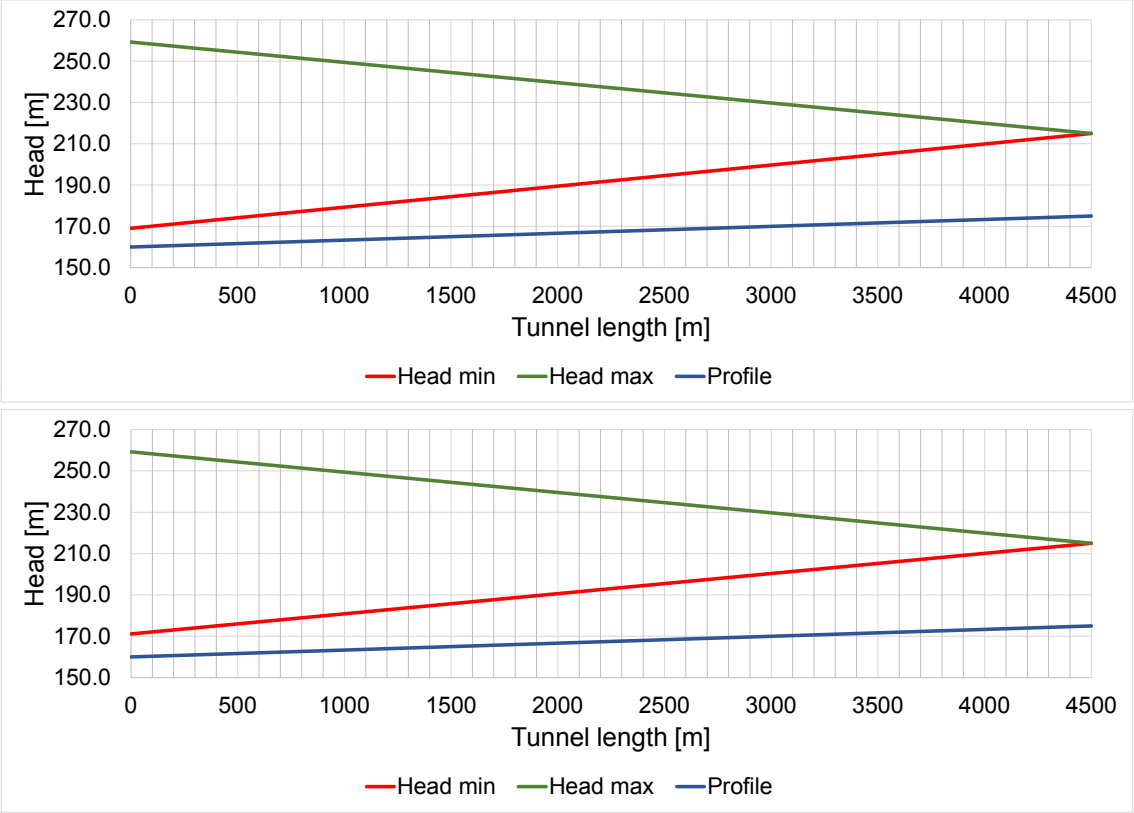

Figure 6.7: *Model type 1 - 20 m³/s - Comparison of the tailrace head (load changes top, load shed bottom)*

Table 6.3: *Model type 1 - 20 m³/s - Data comparison of the main loading cases*

Model type 1 - Q = 20 m³/s						
Load case	Qmax	Qmin	Amp+	Amp-	Head min	Head max
	[m³/s]	[m³/s]	[-]	[-]	[m.a.s.l.]	[m.a.s.l.]
Load changes	31.36	-31.61	1.57	2.12	169.06	259.25
Load shed	31.35	-31.18	1.57	2.09	171.12	259.23

Table 6.4: *Model type 1 - 20 m³/s - Surge tank construction parts and their sizes*

Model type 1 - 20 m³/s - Surge tank size	
Construction part	Excavation size
	[m³]
Lower chamber	1237
Surge tank	551
Upper chamber	1555
Sum	3343
Sum +25%	4041

Turbine design flow rate Q = 30 m³/s

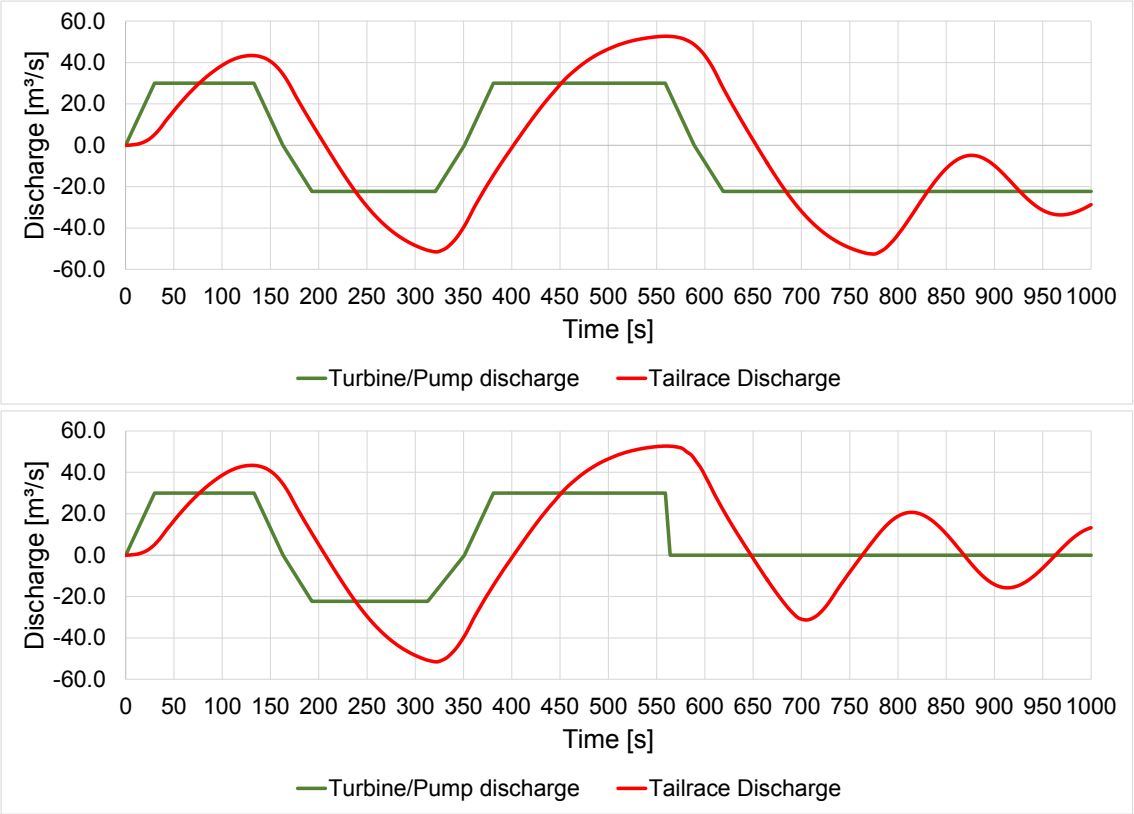

Figure 6.8: *Model type 1 - 30 m³/s - Comparison of the tailrace discharge (load changes top, load shed bottom)*

Figure 6.8 shows no special characteristics. Again only a small change of inflow amplification can be observed. Both loading cases show a stable hydraulic behaviour.
Figure 6.9 illustrates that this model is also safe from cavitation, due to the fact that the minimum head within the tailrace does not drop below profile height.
Table 6.6 lists the size of each construction part of the surge tank.

Table 6.5: *Model type 1 - 30 m³/s - Data comparison of the main loading cases*

Model type 1 - Q = 30 m³/s						
Load case	Qmax	Qmin	Amp+	Amp-	Head min	Head max
	[m³/s]	[m³/s]	[-]	[-]	[m.a.s.l.]	[m.a.s.l.]
Load changes	52.69	-52.60	1.76	2.36	171.02	256.84
Load shed	52.69	-51.56	1.76	2.31	172.02	256.81

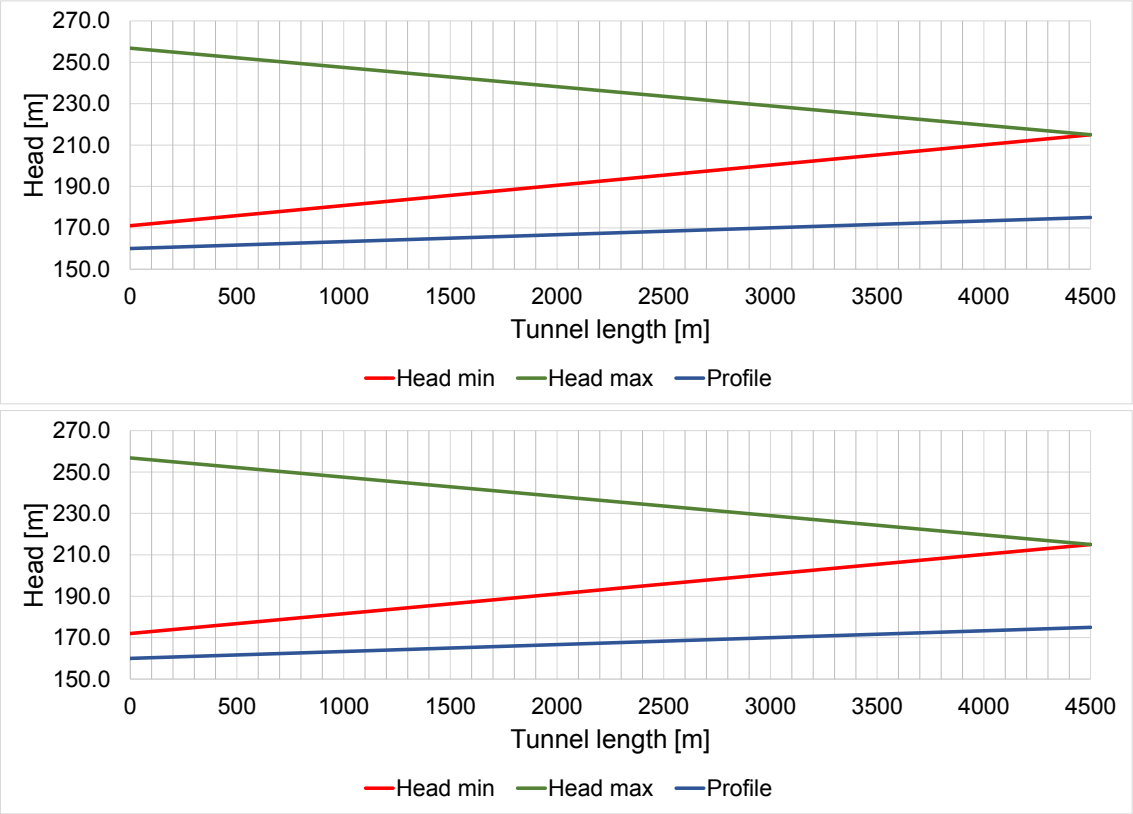

Figure 6.9: *Model type 1 - 30 m³/s - Comparison of the tailrace head (load changes top, load shed bottom)*

Table 6.6: *Model type 1 - 30 m³/s - Surge tank construction parts and their sizes*

Model type 1 - 30 m³/s - Surge tank size	
Construction part	Excavation size
	[m³]
Lower chamber	1885
Surge tank	980
Upper chamber	2513
Sum	5378
Sum +25%	6478

Turbine design flow rate Q = 40 m³/s

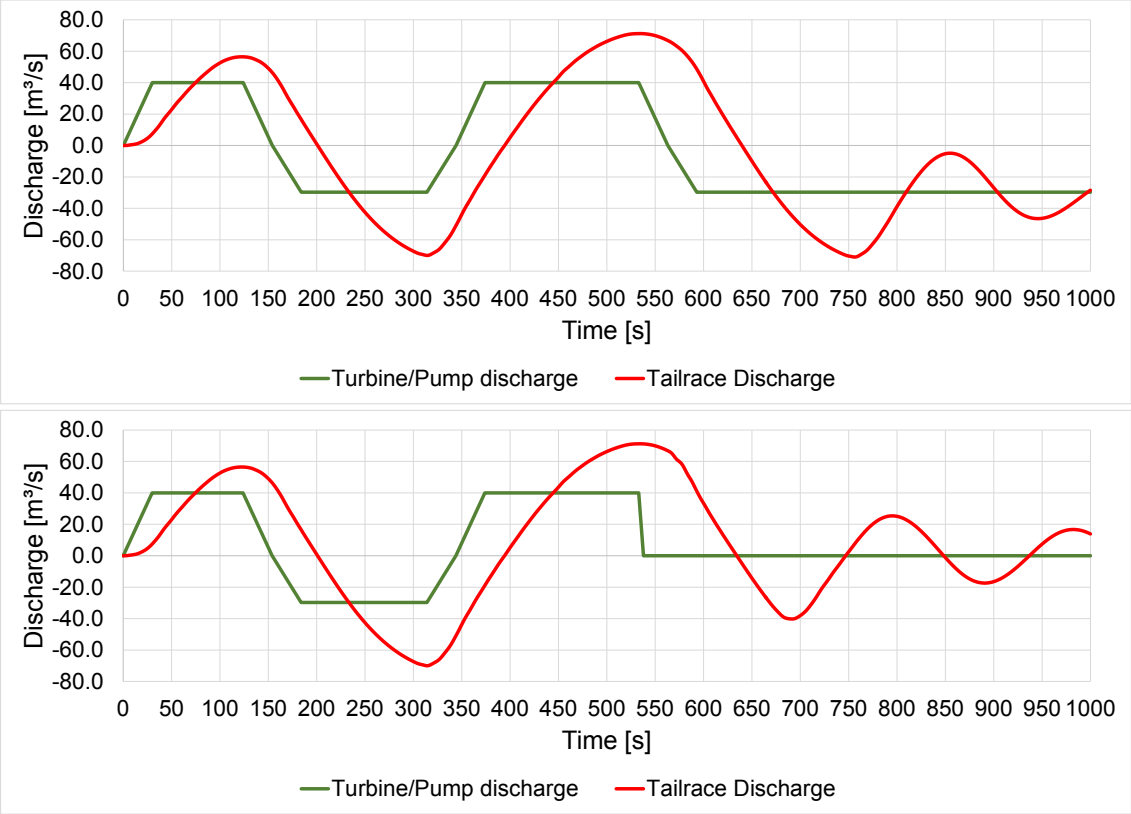

Figure 6.10: *Model type 1 - 40 m³/s - Comparison of the tailrace discharge (load changes top, load shed bottom)*

With the data shown in table 6.7 a trend can be observed. The negative amplification factor is slightly higher for each one of the design flow rates so far investigated. The biggest down-swing of the tailrace discharge is located after the last total load change. At this time step only the loading case - load changes can be decisive.

Table 6.7: *Model type 1 - 40 m³/s - Data comparison of the main loading cases*

Model type 1 - Q = 40 m³/s						
Load case	Qmax	Qmin	Amp+	Amp-	Head min	Head max
	[m³/s]	[m³/s]	[-]	[-]	[m.a.s.l.]	[m.a.s.l.]
Load changes	71.25	-70.97	1.78	2.39	173.11	257.36
Load shed	71.25	-69.96	1.78	2.36	172.70	257.36

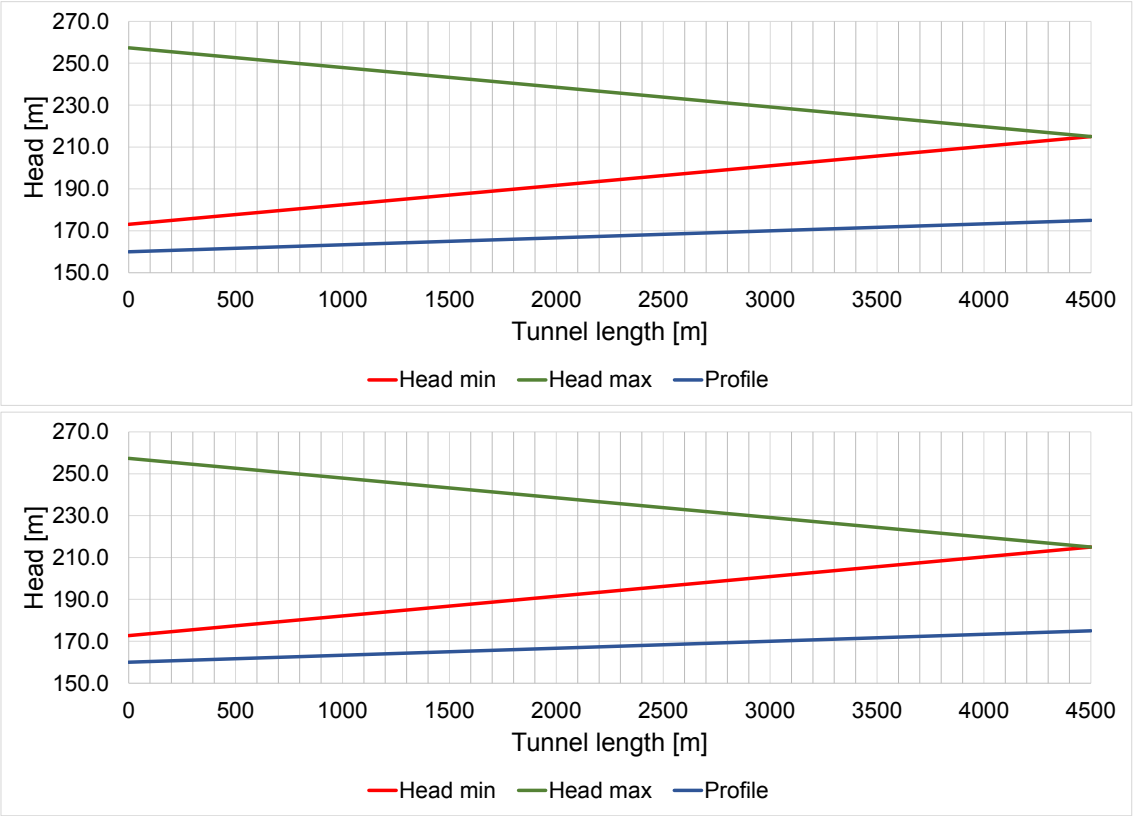

Figure 6.11: *Model type 1 - 40 m³/s - Comparison of the tailrace head (load changes top, load shed bottom)*

Table 6.8: *Model type 1 - 40 m³/s - Surge tank construction parts and their sizes*

Model type 1 - 40 m³/s - Surge tank size	
Construction part	Excavation size
	[m³]
Lower chamber	3578
Surge tank	1225
Upper chamber	3578
Sum	8382
Sum +25%	10171

Turbine design flow rate Q = 50 m³/s

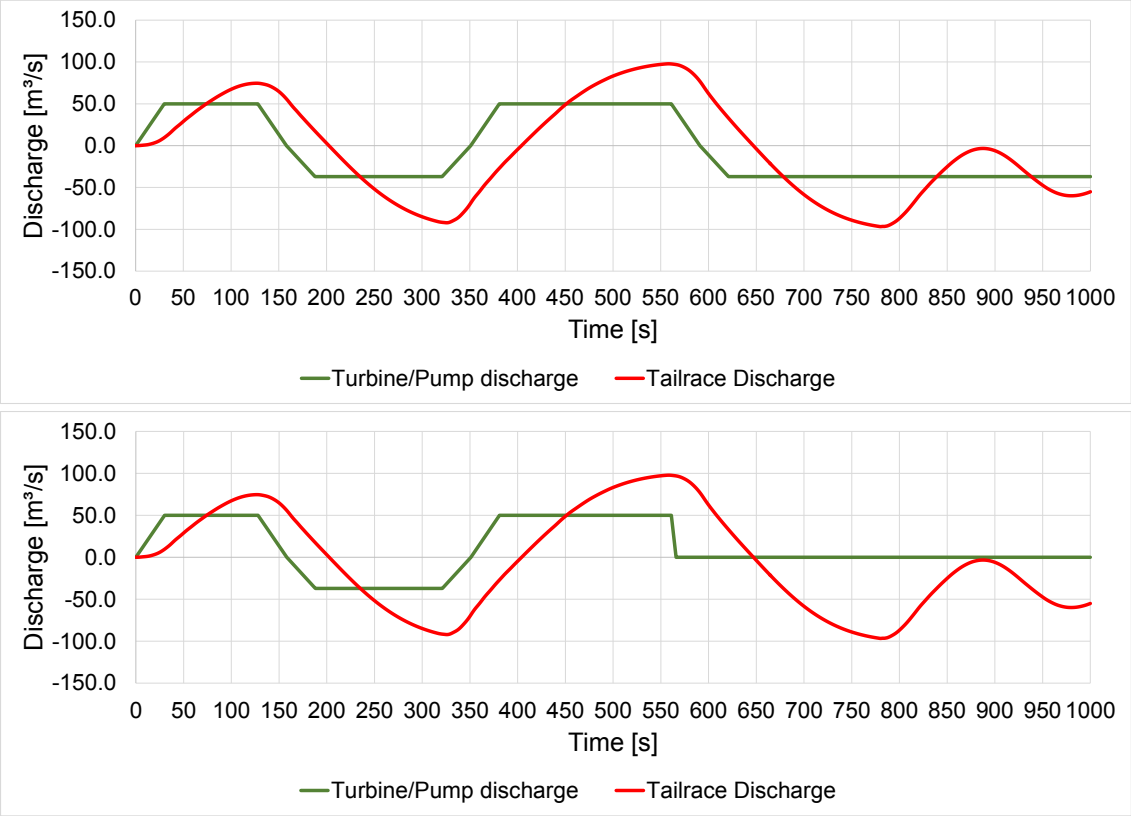

Figure 6.12: *Model type 1 - 50 m³/s - Comparison of the tailrace discharge (load changes top, load shed bottom)*

Table 6.9: *Model type 1 - 50 m³/s - Data comparison of the main loading cases*

Model type 1 - Q = 50 m³/s						
Load case	Qmax	Qmin	Amp+	Amp-	Head min	Head max
	[m³/s]	[m³/s]	[-]	[-]	[m.a.s.l.]	[m.a.s.l.]
Load changes	89.67	-73.82	1.96	2.61	172.23	259.59
Load shed	89.67	-73.82	1.96	2.61	172.23	259.58

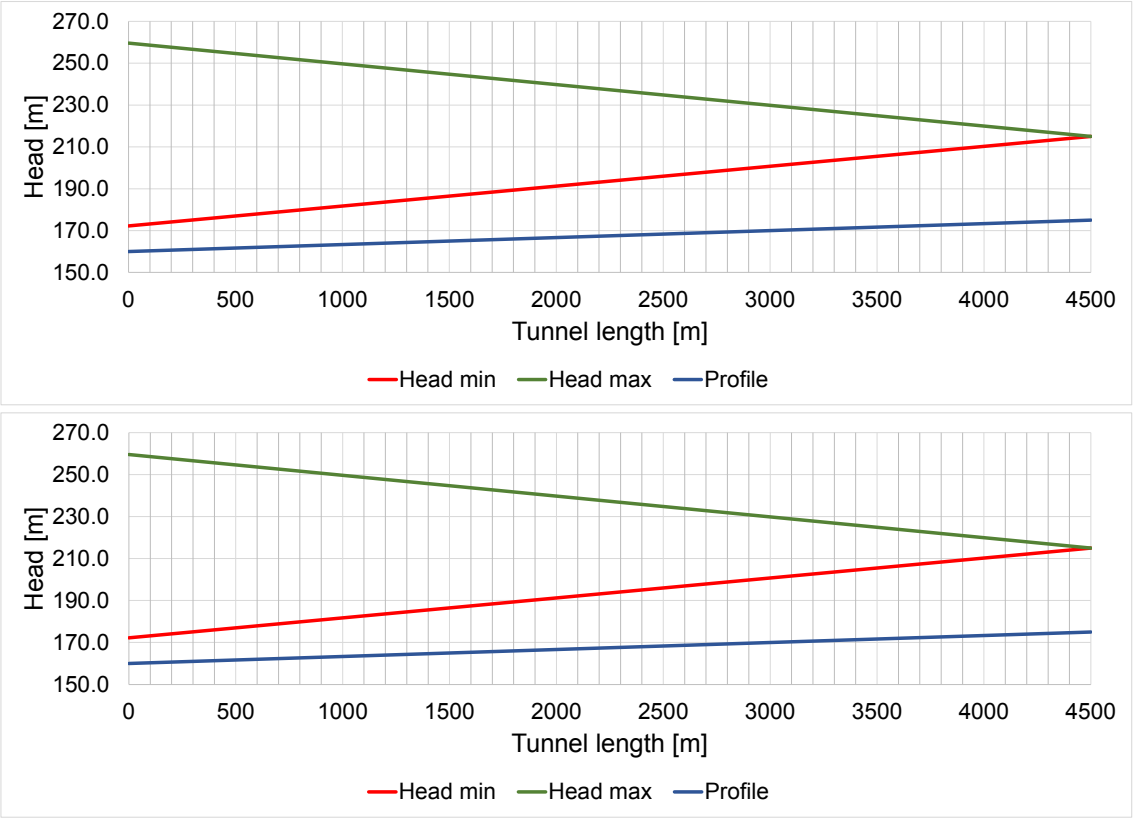

Figure 6.13: *Model type 1 - 50 m³/s - Comparison of the tailrace head (load changes top, load shed bottom)*

Table 6.10: *Model type 1 - 50 m³/s - Surge tank construction parts and their sizes*

Model type 1 - 50 m³/s - Surge tank size	
Construction part	Excavation size
	[m³]
Lower chamber	4418
Surge tank	1502
Upper chamber	4909
Sum	10829
Sum +25%	13160

Turbine design flow rate Q = 60 m³/s

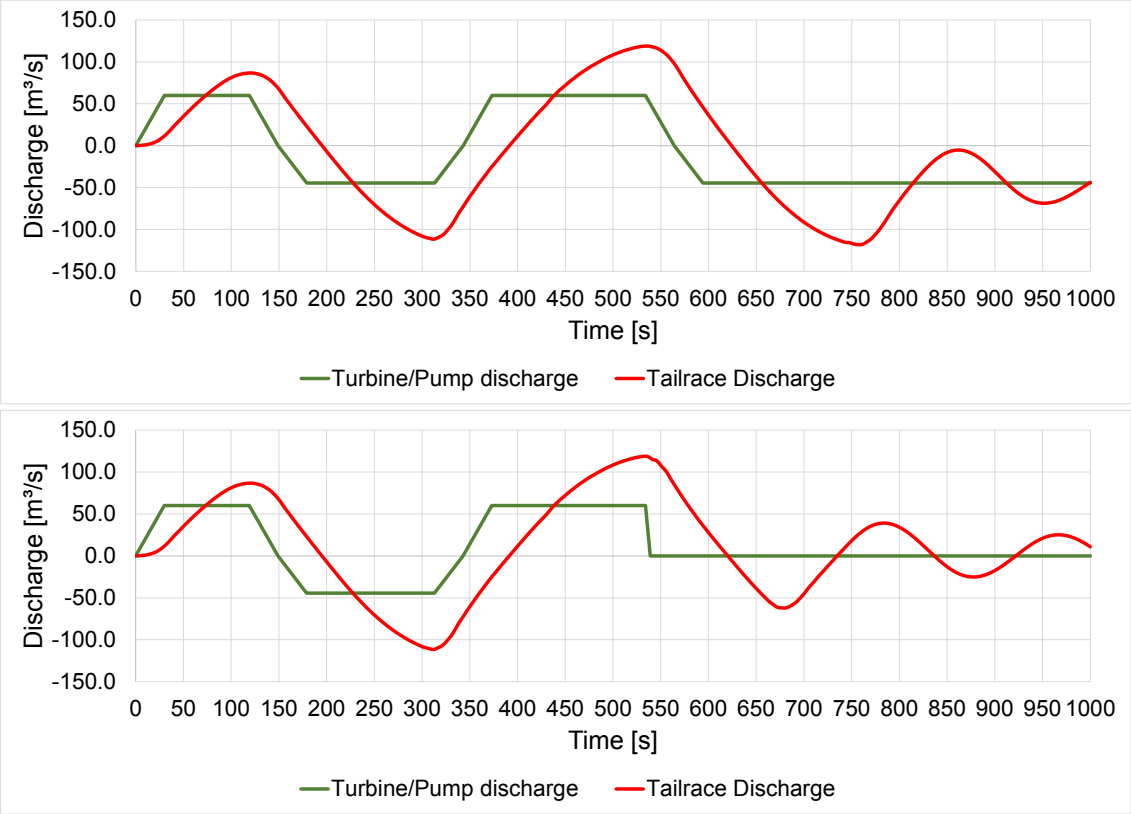

Figure 6.14: *Model type 1 - 60 m³/s - Comparison of the tailrace discharge (load changes top, load shed bottom)*

At a discharge of 60 m³/s it is obvious that the maximum inflow is nearly as high as the maximum outflow. This could be caused by a rather big surge shaft expansion. Due to this the load changes are now the decisive load case with much stronger inflow amplifications. Table 6.11 and figure 6.14 show this data.
At this point of the simulations it can clearly be seen that the maximum inflow amplification occurs after the third total load change. Therefore this is the decisive loading case.

Table 6.11: *Model type 1 - 60 m³/s - Data comparison of the main loading cases*

Model type 1 - Q = 60 m³/s						
Load case	Qmax	Qmin	Amp+	Amp-	Head min	Head max
	[m³/s]	[m³/s]	[-]	[-]	[m.a.s.l.]	[m.a.s.l.]
Load changes	118.85	-118.17	1.98	2.66	171.84	261.59
Load shed	118.82	-111.60	1.98	2.51	173.83	261.53

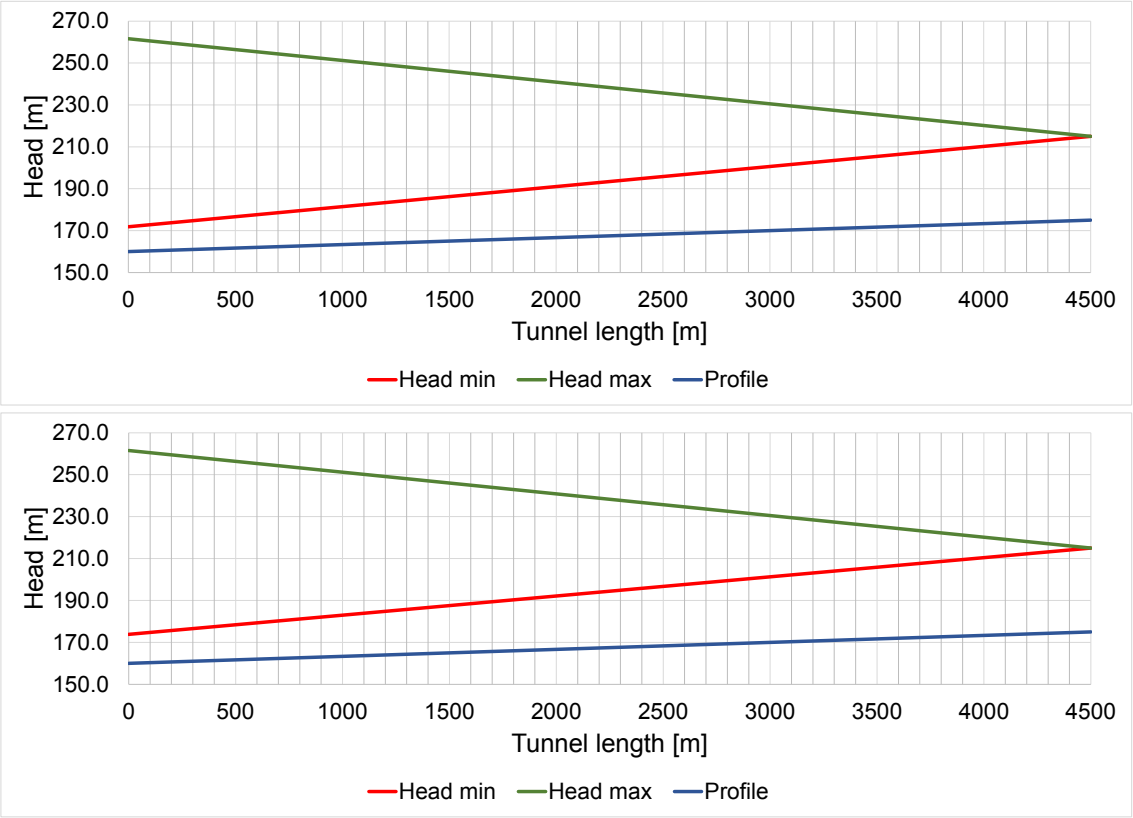

Figure 6.15: *Model type 1 - 60 m³/s - Comparison of the tailrace head (load changes top, load shed bottom)*

Table 6.12: *Model type 1 - 60 m³/s - Surge tank construction parts and their sizes*

Model type 1 - 60 m³/s - Surge tank size	
Construction part	Excavation size
	[m³]
Lower chamber	4418
Surge tank	3402
Upper chamber	4418
Sum	12237
Sum +25%	14446

Turbine design flow rate Q = 70 m³/s

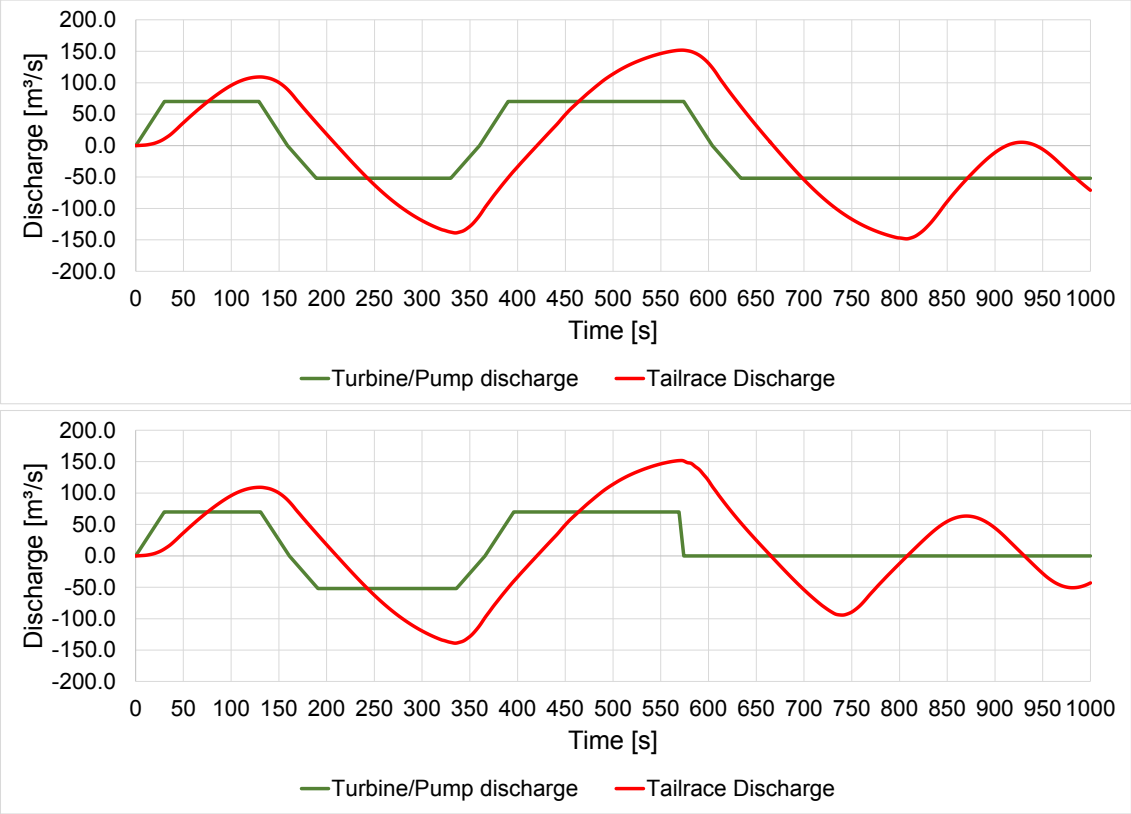

Figure 6.16: *Model type 1 - 70 m³/s - Comparison of the tailrace discharge (load changes top, load shed bottom)*

This model seems quite similar to the one before. All values show the same tendency even though the surge chambers are bigger compared to the surge tank.

Table 6.13: *Model type 1 - 70 m³/s - Data comparison of the main loading cases*

Model type 1 - Q = 70 m³/s						
Load case	Qmax	Qmin	Amp+	Amp-	Head min	Head max
	[m³/s]	[m³/s]	[-]	[-]	[m.a.s.l.]	[m.a.s.l.]
Load changes	151.85	-148.37	2.17	2.86	171.80	261.64
Load shed	151.83	-138.95	2.17	2.68	174.37	261.64

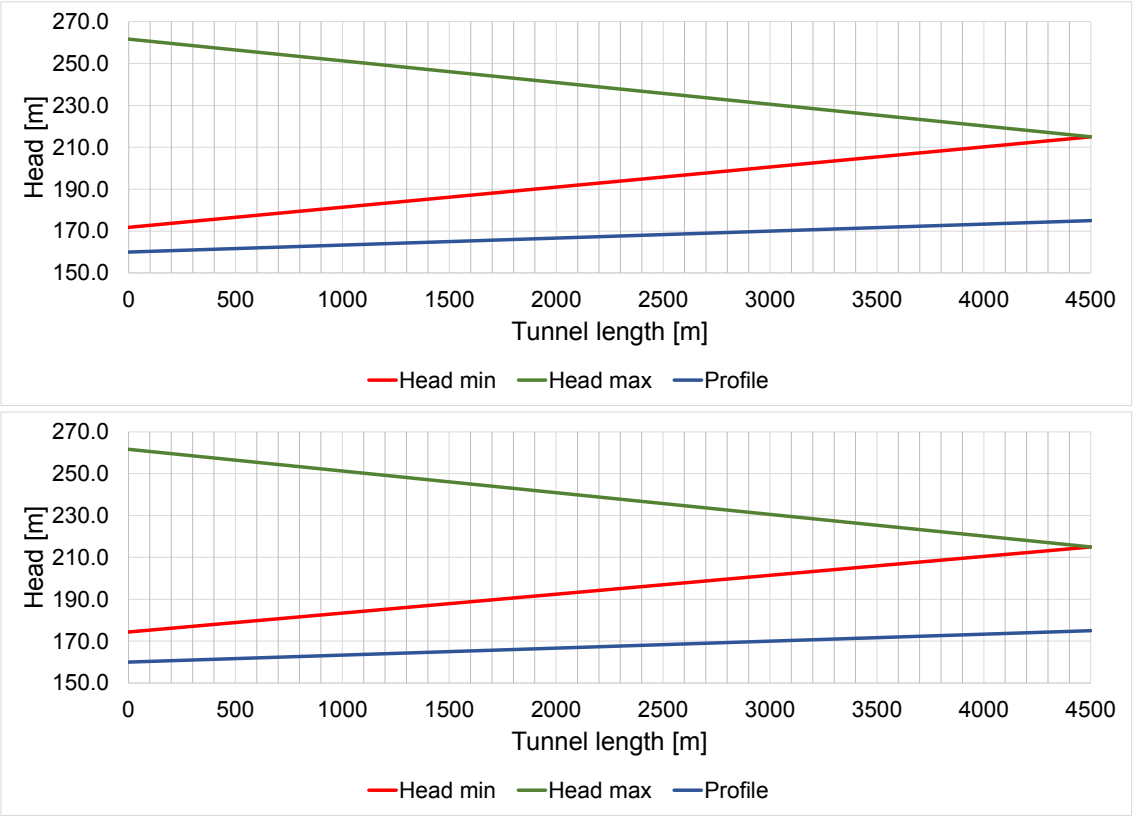

Figure 6.17: *Model type 1 - 70 m³/s - Comparison of the tailrace head (load changes top, load shed bottom)*

Table 6.14: *Model type 1 - 70 m³/s - Surge tank construction parts and their sizes*

Model type 1 - 70 m³/s - Surge tank size	
Construction part	Excavation size
	[m³]
Lower chamber	7134
Surge tank	2963
Upper chamber	7466
Sum	17564
Sum +25%	21214

Turbine design flow rate Q = 80 m³/s

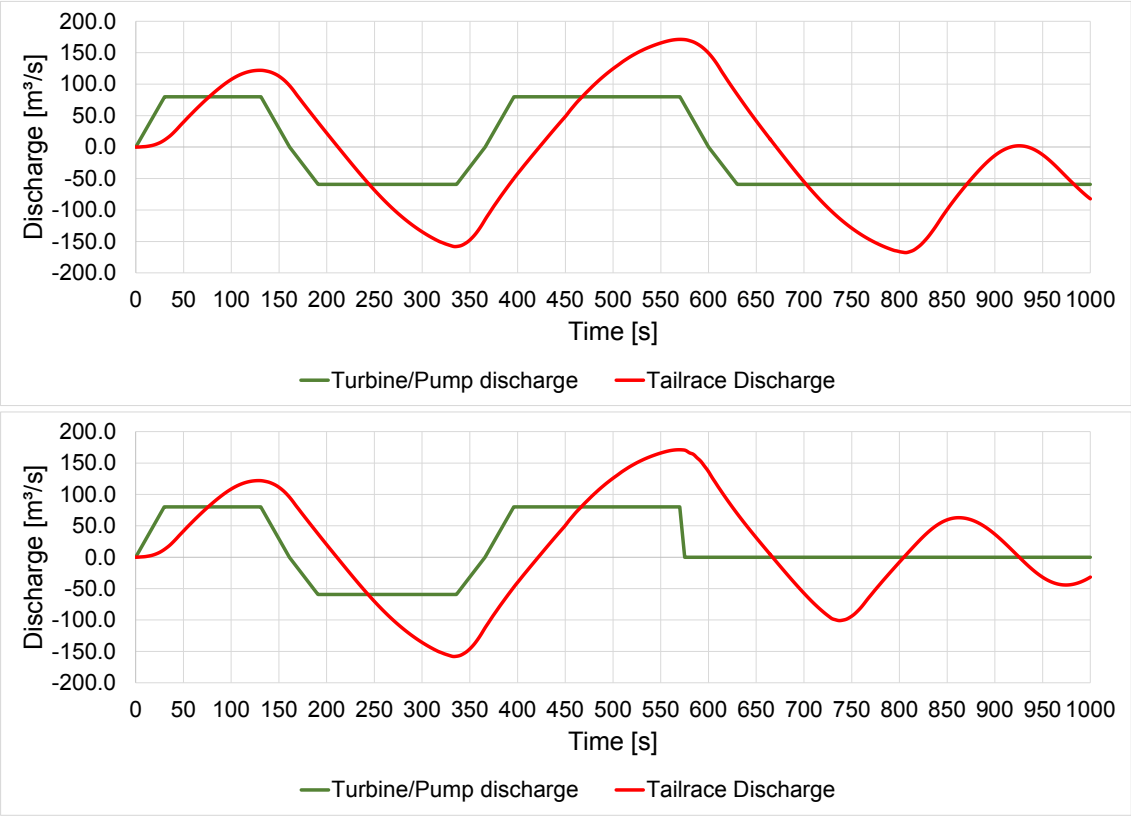

Figure 6.18: *Model type 1 - 80 m³/s - Comparison of the tailrace discharge (load changes top, load shed bottom)*

Table 6.15: *Model type 1 - 80 m³/s - Data comparison of the main loading cases*

Model type 1 - Q = 80 m³/s						
Load case	Qmax	Qmin	Amp+	Amp-	Head min	Head max
	[m³/s]	[m³/s]	[-]	[-]	[m.a.s.l.]	[m.a.s.l.]
Load changes	171.16	-167.72	2.14	2.83	172.77	261.71
Load shed	171.16	-158.16	2.14	2.67	174.37	261.64

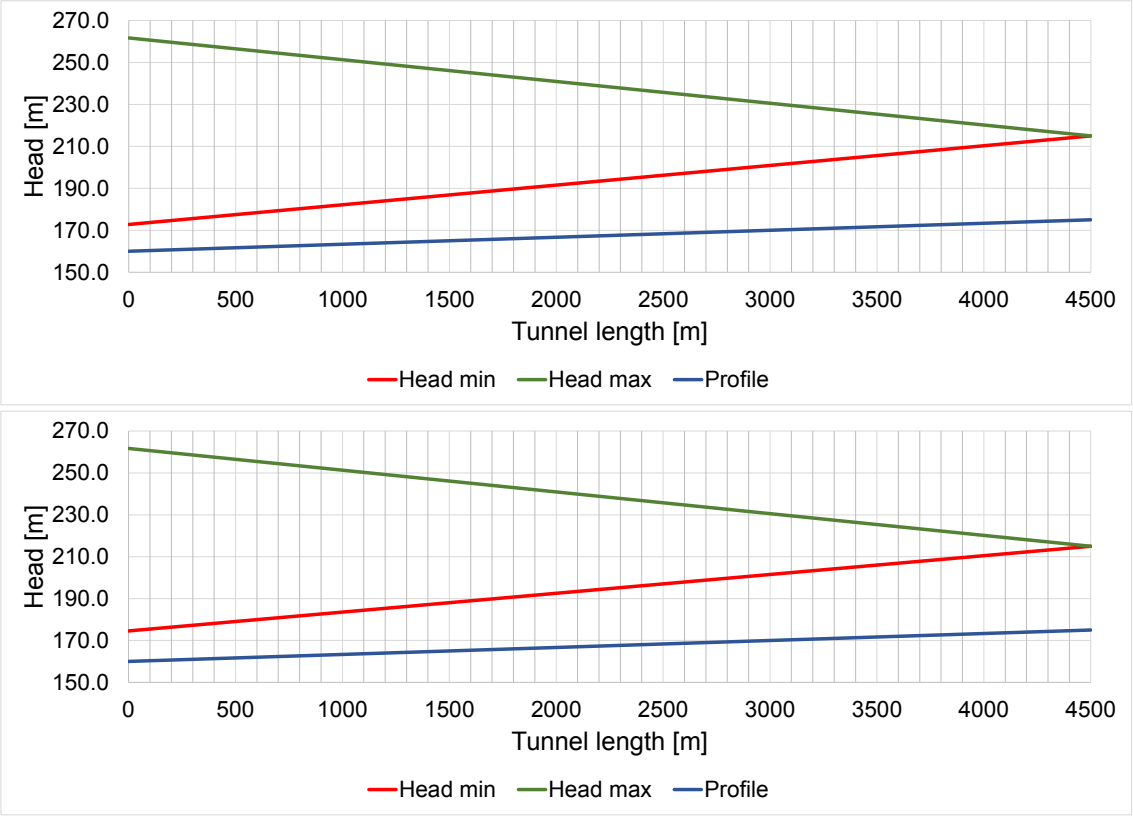

Figure 6.19: *Model type 1 - 80 m³/s - Comparison of the tailrace head (load changes top, load shed bottom)*

Table 6.16: *Model type 1 - 80 m³/s - Surge tank construction parts and their sizes*

Model type 1 - 80 m³/s - Surge tank size	
Construction part	Excavation size
	[m³]
Lower chamber	7697
Surge tank	3402
Upper chamber	9236
Sum	20335
Sum +25%	24568

Turbine design flow rate Q = 90 m³/s

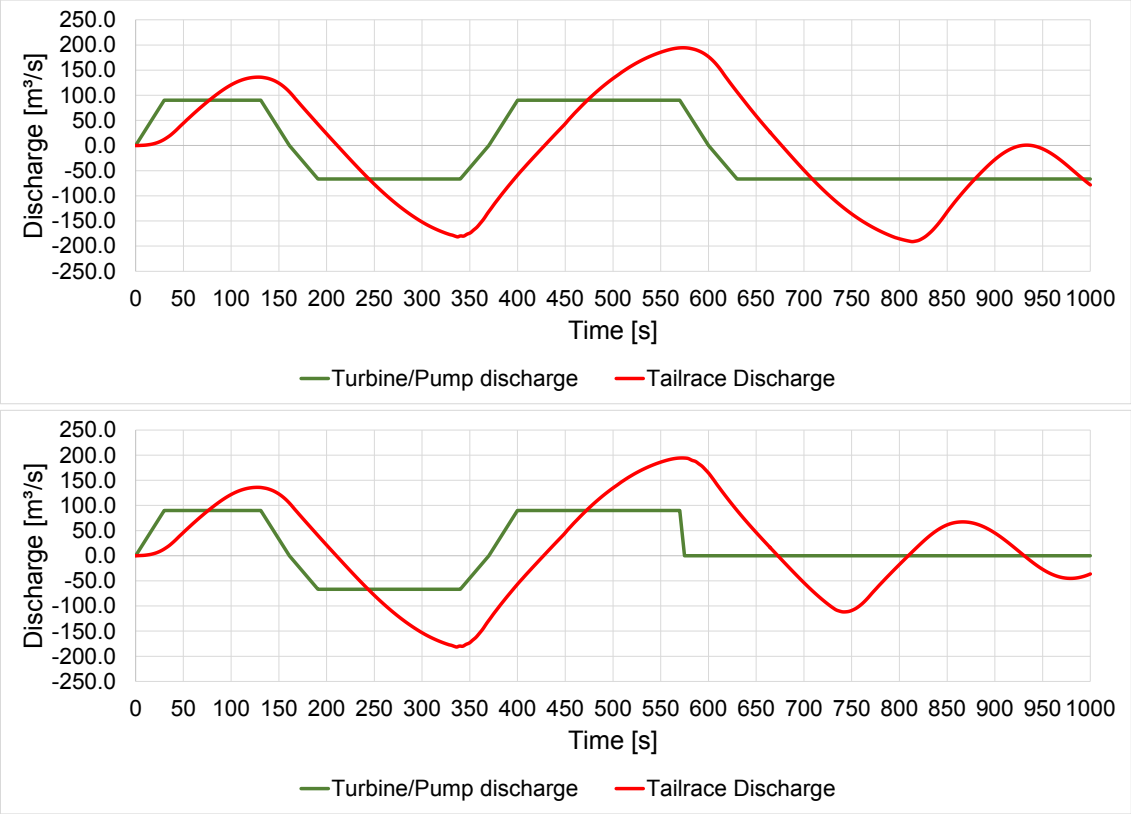

Figure 6.20: *Model type 1 - 90 m³/s - Comparison of the tailrace discharge (load changes top, load shed bottom)*

Table 6.17: *Model type 1 - 90 m³/s - Data comparison of the main loading cases*

Model type 1 - Q = 90 m³/s						
Load case	Qmax	Qmin	Amp+	Amp-	Head min	Head max
	[m³/s]	[m³/s]	[-]	[-]	[m.a.s.l.]	[m.a.s.l.]
Load changes	194.50	-191.04	2.16	2.86	175.78	263.00
Load shed	194.50	-181.58	2.16	2.72	175.08	260.79

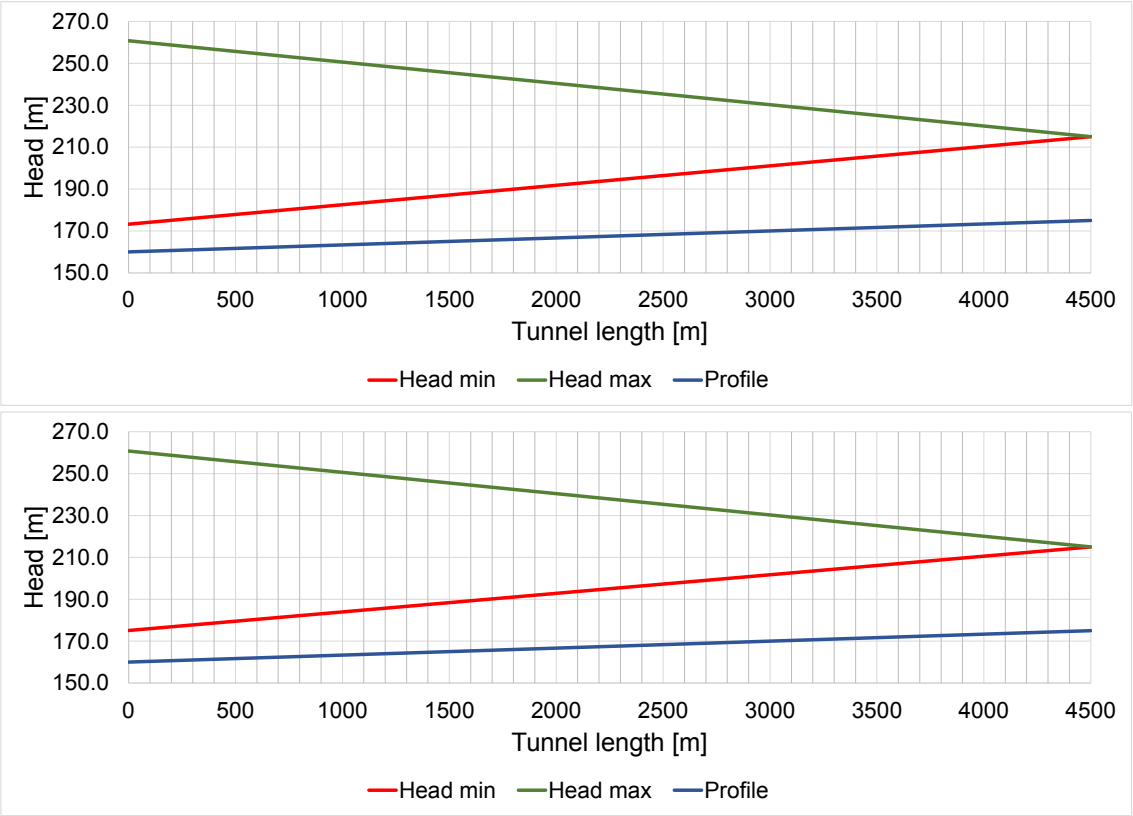

Figure 6.21: *Model type 1 - 90 m³/s - Comparison of the tailrace head (load changes top, load shed bottom)*

Table 6.18: *Model type 1 - 90 m³/s - Surge tank construction parts and their sizes*

Model type 1 - 90 m³/s - Surge tank size	
Construction part	Excavation size
	[m³]
Lower chamber	10053
Surge tank	3921
Upper chamber	11310
Sum	25284
Sum +25%	30624

Turbine design flow rate Q = 100 m³/s

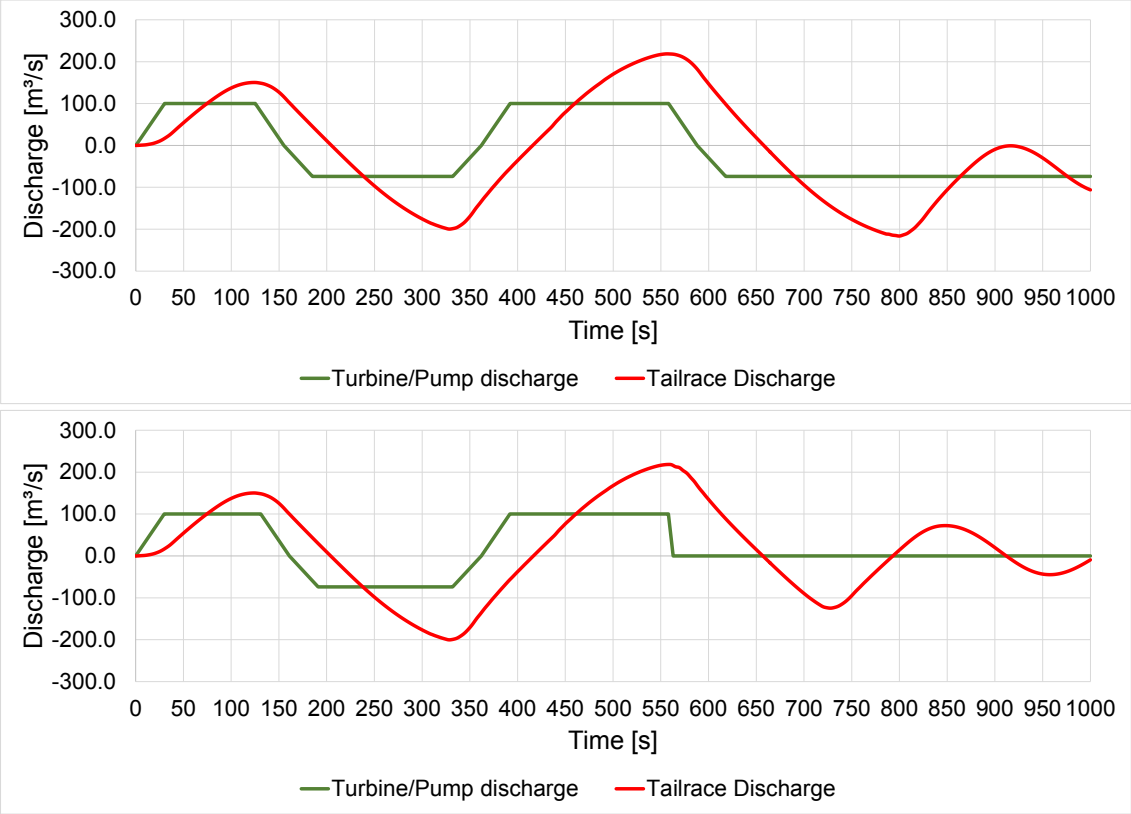

Figure 6.22: *Model type 1 - 100 m³/s - Comparison of the tailrace discharge (load changes top, load shed bottom)*

At a design flow rate of 100 m³/s a minor model error occurs, which amounts to a scale of approximately 0.11 %. The reason for this could be a digit mistake in the hydraulic model.
An error of this size can easily be neglected, and therefore the computations do not have to be repeated.

Table 6.19: *Model type 1 - 100 m³/s - Data comparison of the main loading cases*

Model type 1 - Q = 100 m³/s						
Load case	Qmax	Qmin	Amp+	Amp-	Head min	Head max
	[m³/s]	[m³/s]	[-]	[-]	[m.a.s.l.]	[m.a.s.l.]
Load changes	218.57	-216.30	2.19	2.92	173.81	264.06
Load shed	218.32	-200.24	2.18	2.70	175.78	263.00

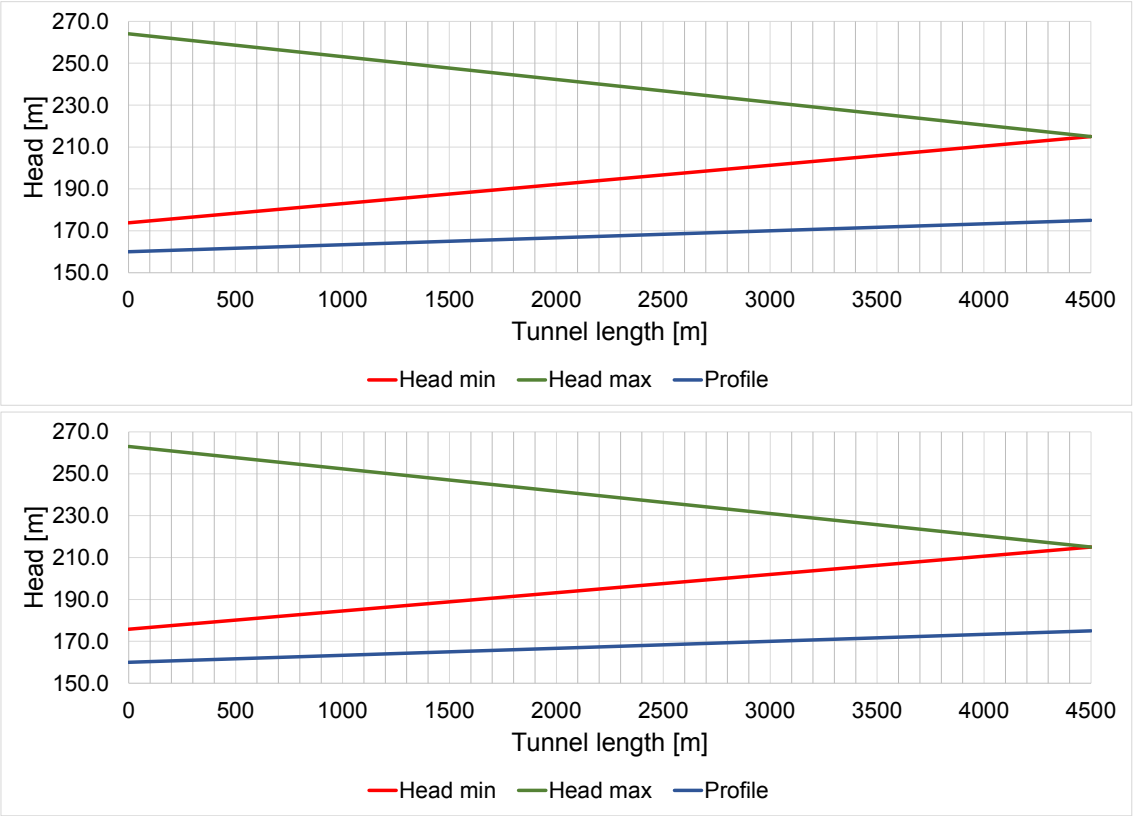

Figure 6.23: *Model type 1 - 100 m³/s - Comparison of the tailrace head (load changes top, load shed bottom)*

Table 6.20: *Model type 1 - 100 m³/s - Surge tank construction parts and their sizes*

Model type 1 - 100 m³/s - Surge tank size	
Construction part	Excavation size
	[m³]
Lower chamber	12566
Surge tank	3883
Upper chamber	12064
Sum	28513
Sum +25%	34671

6.3 Type 2 - Surge tank with throttle

In model type 2 (Figure 6.24) a throttle is built in the lower surge chamber right below the riser duct. This throttle should regulate the inflow and outflow to the surge shaft in order to reduce the size of the overall surge tank for higher design flow rates. The throttle has a 1:3 ratio between inflow and outflow. The actual dampening factor is calculated with the impact loss formula according to chapter 3.1.4.

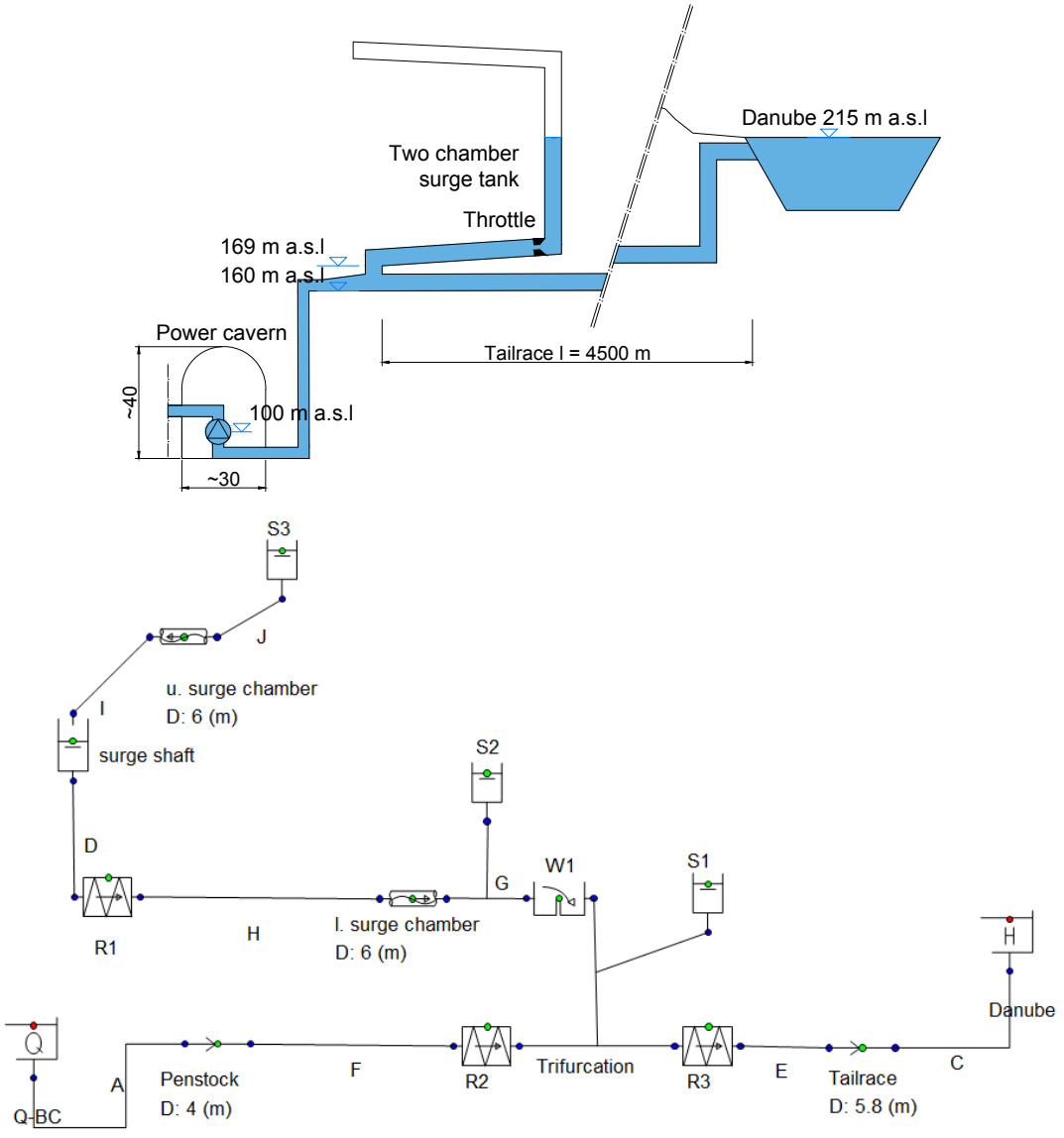

Figure 6.24: *Physical (top) and 1-D numerical model (bottom): Type 2*

6.3.1 Type 2 - Turbine design flow rates

Turbine design flow rate Q = 20 m³/s

In figure 6.25 it can already be seen that this type of surge tank has a stronger dampening effect due to the throttle used. Fluctuations after the last load change decrease quite fast. Table 6.21 shows that both loading cases have exactly the same amplifications, therefore no model errors occurred, but this also means that the maximum negative amplification occurs after the first load change. The reason for this could be mass oscillation during the dampening within the surge chamber.
The negative amplification is approximately 150 % of the positive one. Usually a close to equal amplification for both, inflow and outflow should be aimed at. With different overall boundary conditions values with various amplification factors can be pursued.

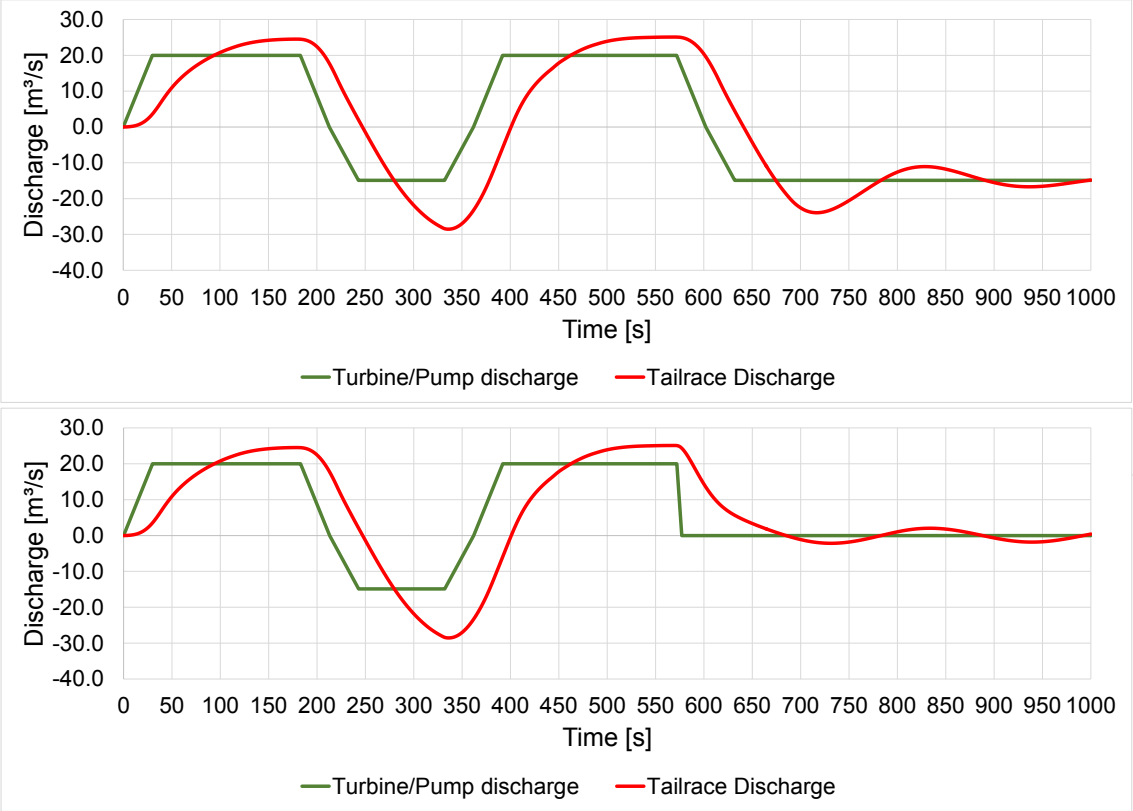

Figure 6.25: *Model type 2 - 20 m³/s - Comparison of the tailrace discharge (load changes top, load shed bottom)*

This model type has the same tailrace profile and therefore the same boundary conditions for cavitation risk. As can be seen in table 6.21 both loading cases have the same head within the tailrace. Therefore only one graph is illustrated here as long as the values are totally equal.

Figure 6.27 shows a comparison of flow rates between the surge tank and the tailrace. It can be observed that the maximum flows are a bit shifted. The reason for that is the differential effect of the throttle.

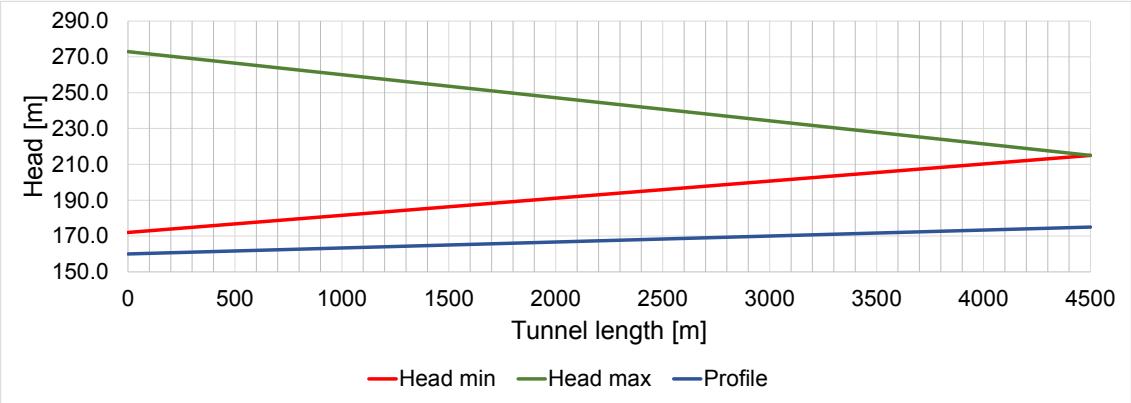

Figure 6.26: *Model type 2 - 20 m³/s - Tailrace head*

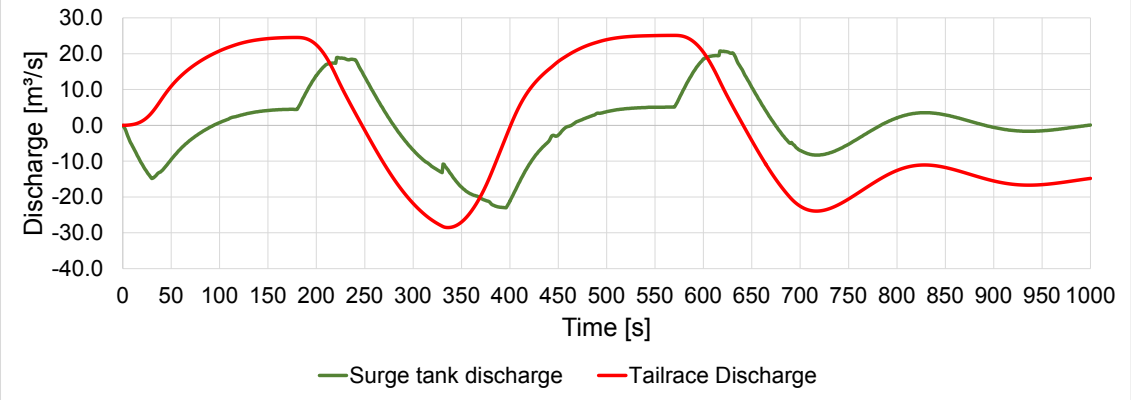

Figure 6.27: *Flow comparison of the surge tank and tailrace*

Table 6.21: *Model type 2 - 20 m³/s - Data comparison of the main loading cases*

Model type 2 - Q = 20 m³/s						
Load case	Qmax	Qmin	Amp+	Amp-	Head min	Head max
	[m³/s]	[m³/s]	[-]	[-]	[m.a.s.l.]	[m.a.s.l.]
Load changes	25.10	-28.54	1.26	1.92	171.99	272.92
Load shed	25.10	-28.54	1.26	1.92	171.99	272.92

Table 6.22: *Model type 2 - 20 m³/s - Surge tank construction parts and their sizes*

Model type 2 - 20 m³/s - Surge tank size	
Construction part	Excavation size
	[m³]
Lower chamber	1443
Surge tank	669
Upper chamber	1203
Sum	3314
Sum +25%	3976

Turbine design flow rate Q = 30 m³/s

At this point of the analysis it can already be seen that the dampening effect of this model types is significantly stronger than in model type 1. After the last load change or the load shedding, the discharge oscillates just slightly around the actual design flow. This means that the problem of dampening behaviour is satisfyingly solved.

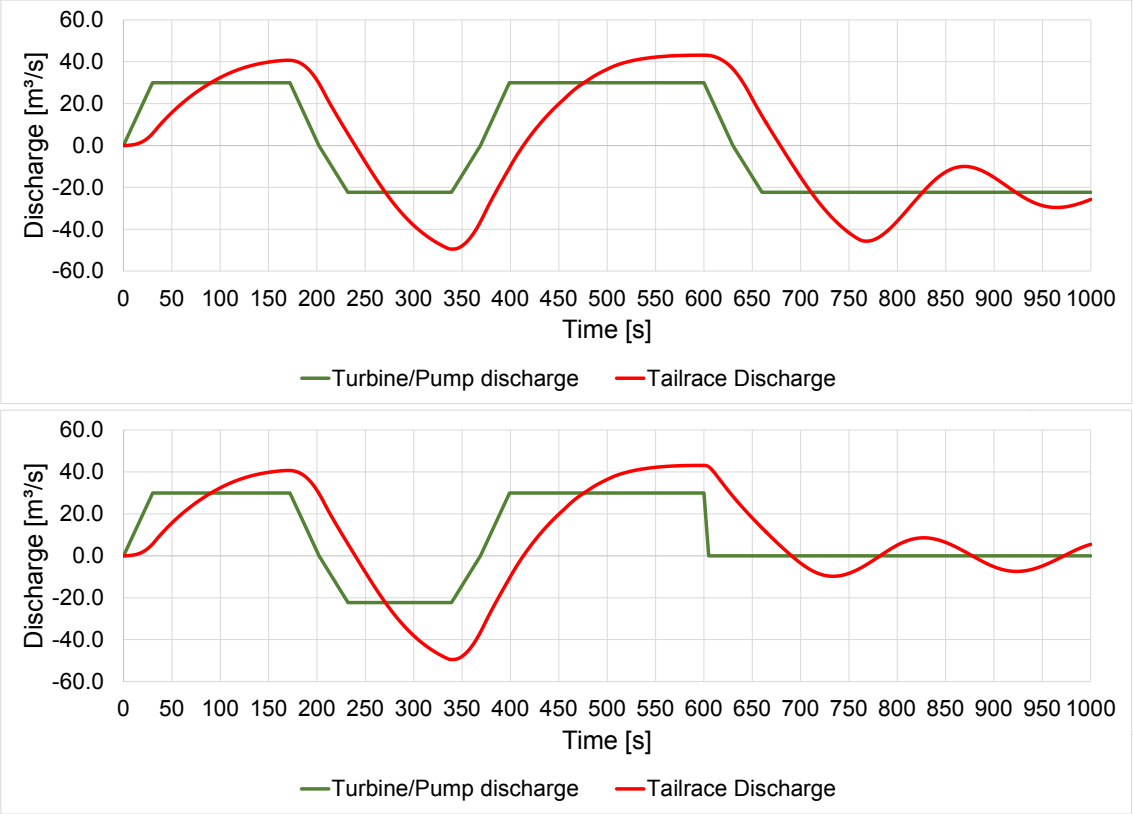

Figure 6.28: *Model type 2 - 30 m³/s - Comparison of the tailrace discharge (load changes top, load shed bottom)*

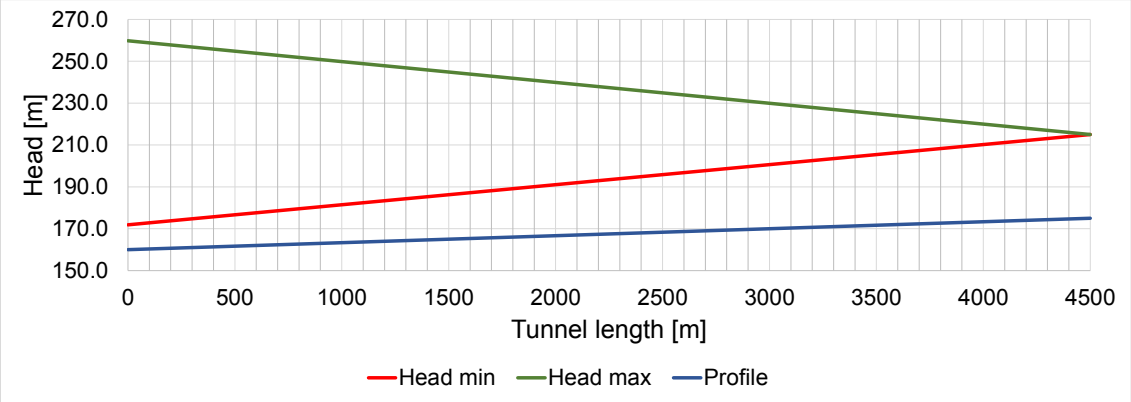

Figure 6.29: *Model type 2 - 30 m³/s - Tailrace head*

Table 6.23: *Model type 2 - 30 m³/s - Data comparison of the main loading case*

Model type 2 - Q = 30 m³/s						
Load case	Qmax	Qmin	Amp+	Amp-	Head min	Head max
	[m³/s]	[m³/s]	[-]	[-]	[m.a.s.l.]	[m.a.s.l.]
Load changes	43.13	-49.47	1.44	2.22	171.87	259.78
Load shed	43.13	-49.47	1.44	2.22	171.87	259.78

Table 6.24: *Model type 2 - 30 m³/s - Surge tank construction parts and their sizes*

Model type 2 - 30 m³/s - Surge tank size	
Construction part	Excavation size
	[m³]
Lower chamber	1885
Surge tank	873
Upper chamber	2513
Sum	5272
Sum +25%	6371

Turbine design flow rate Q = 40 m³/s

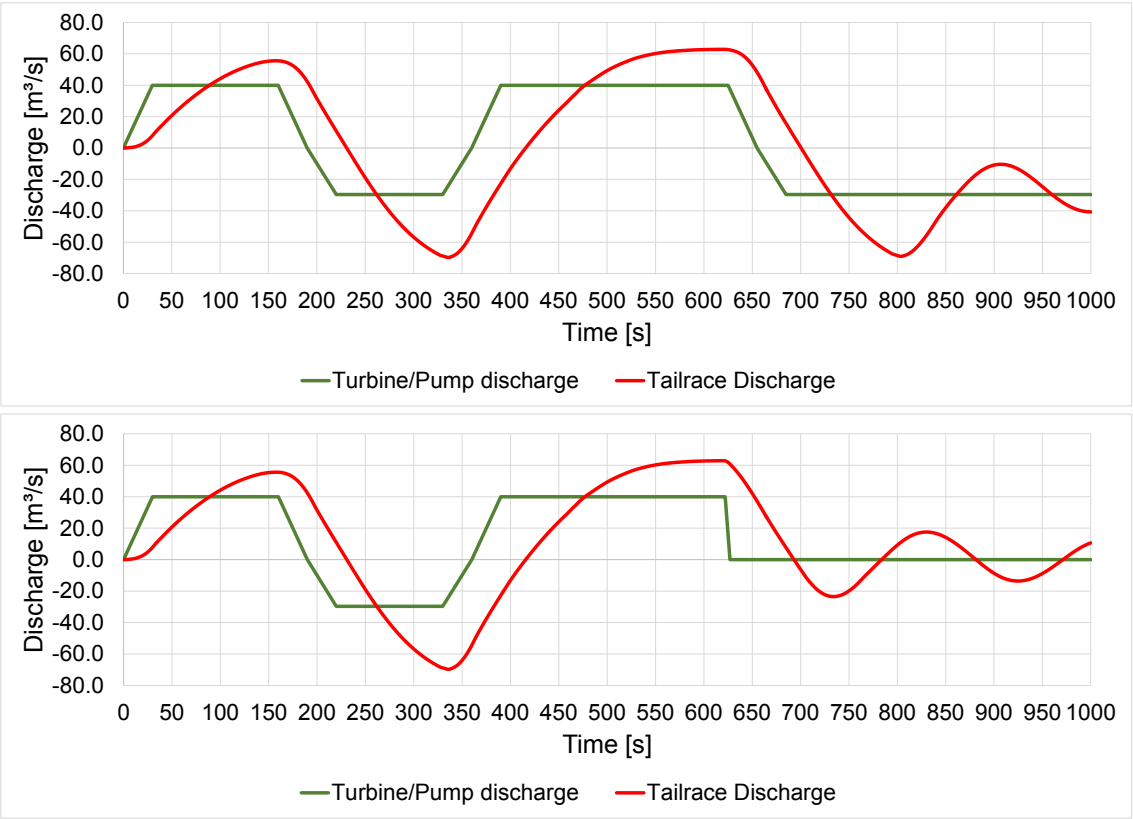

Figure 6.30: *Model type 2 - 40 m³/s - Comparison of the tailrace discharge (load changes top, load shed bottom)*

Table 6.25: *Model type 2 - 40 m³/s - Data comparison of the main loading cases*

Model type 2 - Q = 40 m³/s						
Load case	Qmax	Qmin	Amp+	Amp-	Head min	Head max
	[m³/s]	[m³/s]	[-]	[-]	[m.a.s.l.]	[m.a.s.l.]
Load changes	62.88	-69.74	1.57	2.35	172.05	254.46
Load shed	62.88	-69.74	1.57	2.35	172.05	254.46

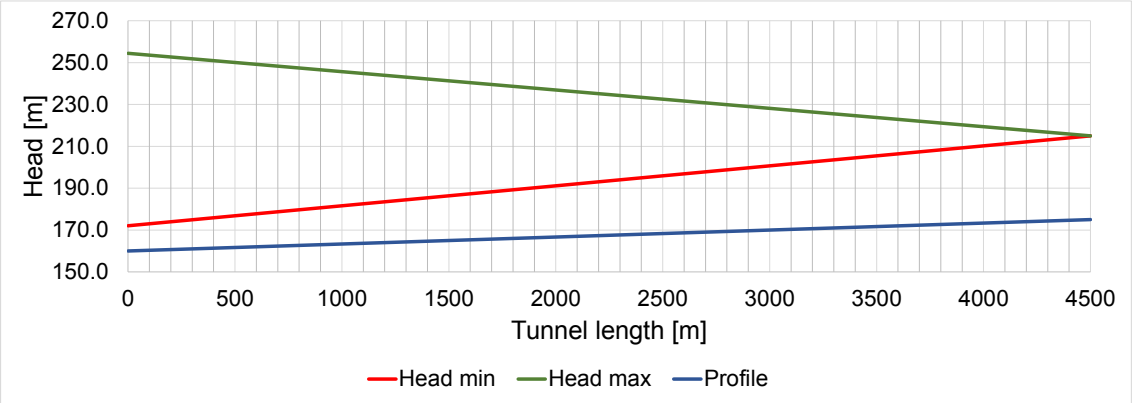

Figure 6.31: *Model type 2 - 40 m³/s - Tailrace head*

Table 6.26: *Model type 2 - 40 m³/s - Surge tank construction parts and their sizes*

Model type 2 - 40 m³/s - Surge tank size	
Construction part	Excavation size
	[m³]
Lower chamber	2386
Surge tank	1089
Upper chamber	3976
Sum	7451
Sum +25%	9042

Turbine design flow rate Q = 50 m³/s

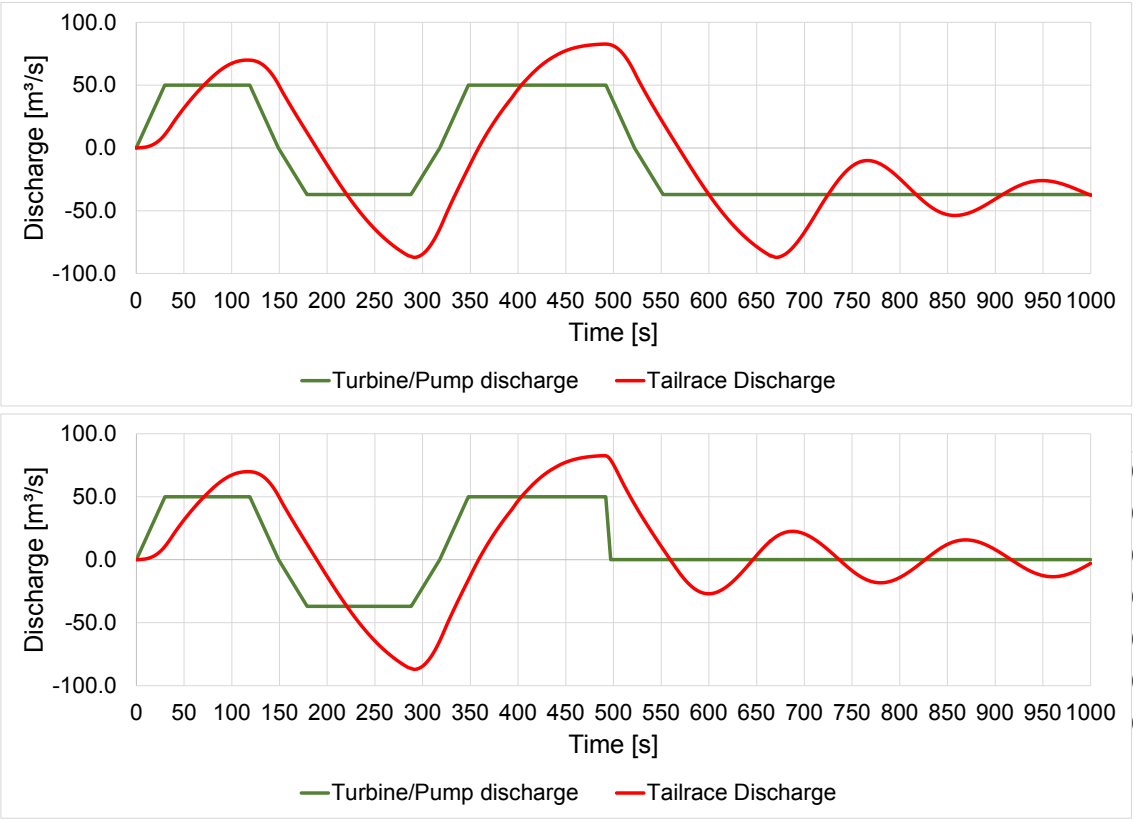

Figure 6.32: *Model type 2 - 50 m³/s - Comparison of the tailrace discharge (load changes top, load shed bottom)*

Table 6.27: *Model type 2 - 50 m³/s - Data comparison of the main loading cases*

Model type 2 - Q = 50 m³/s						
Load case	Qmax	Qmin	Amp+	Amp-	Head min	Head max
	[m³/s]	[m³/s]	[-]	[-]	[m.a.s.l.]	[m.a.s.l.]
Load changes	82.69	-87.10	1.65	2.35	172.48	267.39
Load shed	82.69	-87.10	1.65	2.35	172.48	267.39

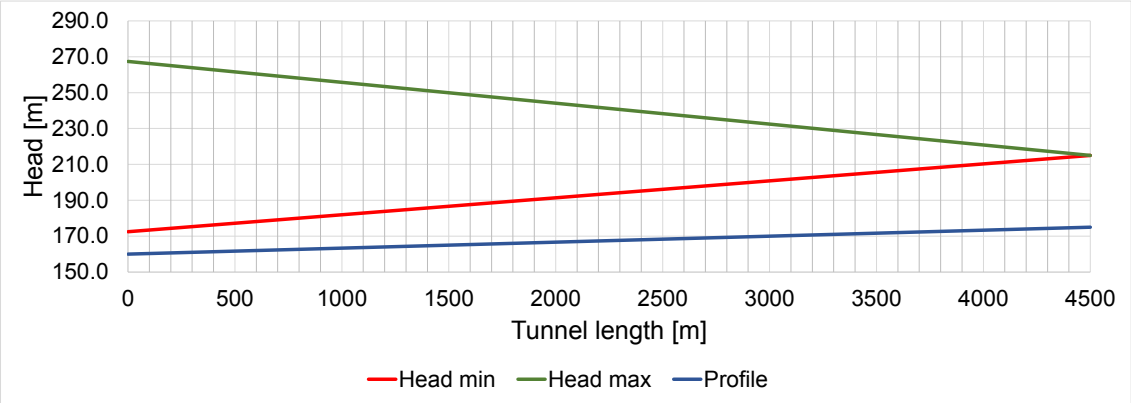

Figure 6.33: *Model type 2 - 50 m³/s - Tailrace head*

Table 6.28: *Model type 2 - 50 m³/s - Surge tank construction parts and their sizes*

Model type 2 - 50 m³/s - Surge tank size	
Construction part	Excavation size
	[m³]
Lower chamber	3436
Surge tank	1541
Upper chamber	2945
Sum	7923
Sum +25%	9518

Turbine design flow rate Q = 60 m³/s

At a design flow rate of 60 m³/s a minor model error can be observed. This error has a range of approximately 0.5 % and therefore is negligible.

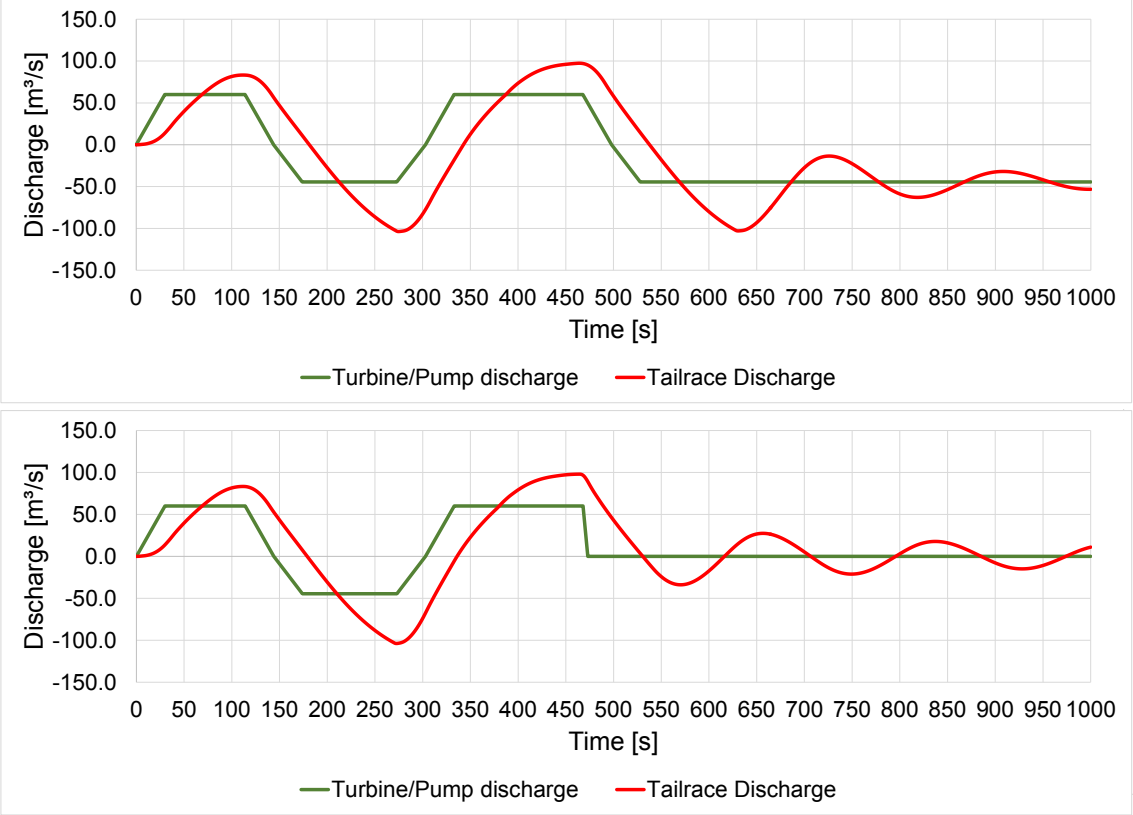

Figure 6.34: *Model type 2 - 60 m³/s - Comparison of the tailrace discharge (load changes top, load shed bottom)*

Table 6.29: *Model type 2 - 60 m³/s - Data comparison of the main loading cases*

Model type 2 - Q = 60 m³/s						
Load case	Qmax	Qmin	Amp+	Amp-	Head min	Head max
	[m³/s]	[m³/s]	[-]	[-]	[m.a.s.l.]	[m.a.s.l.]
Load changes	97.38	-103.70	1.62	2.33	172.08	269.16
Load shed	97.92	-103.79	1.63	2.33	172.05	271.65

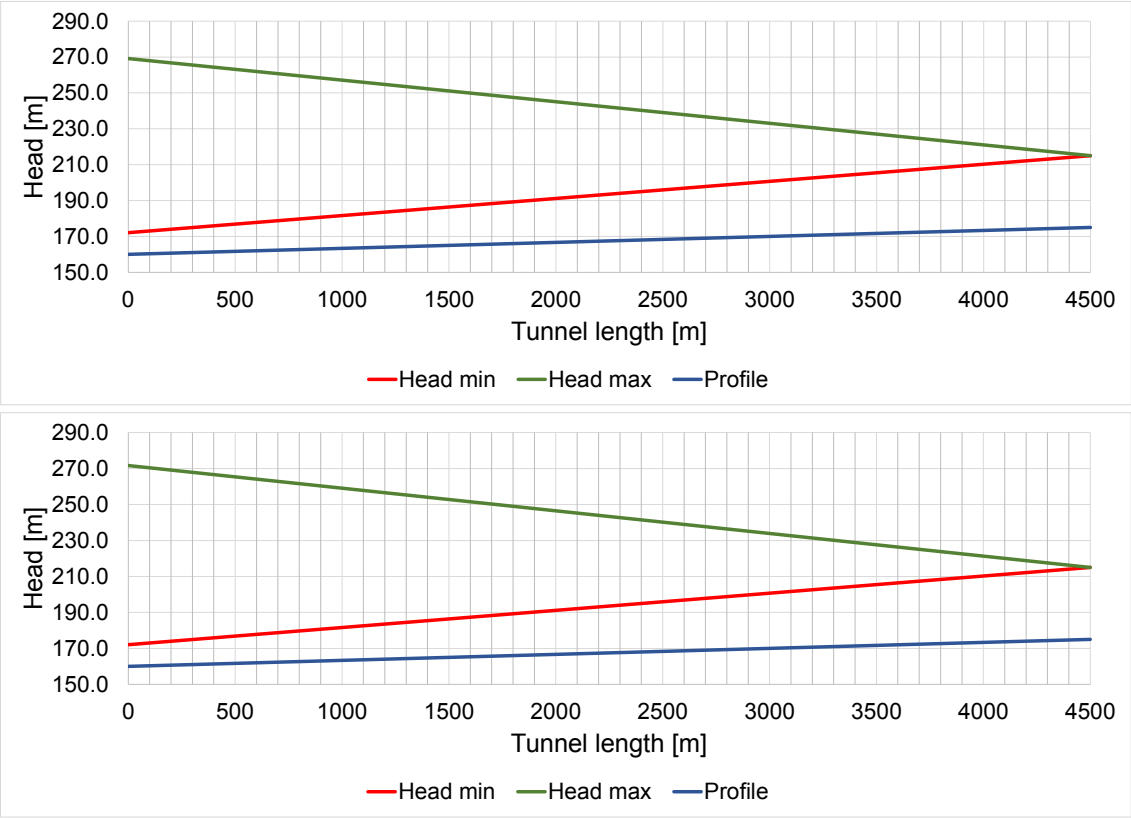

Figure 6.35: *Model type 2 - 60 m³/s - Comparison of the tailrace head (load changes top, load shed bottom)*

Table 6.30: *Model type 2 - 60 m³/s - Surge tank construction parts and their sizes*

Model type 2 - 60 m³/s - Surge tank size	
Construction part	Excavation size
	[m³]
Lower chamber	3927
Surge tank	1871
Upper chamber	2945
Sum	8743
Sum +25%	10461

Turbine design flow rate Q = 70 m³/s

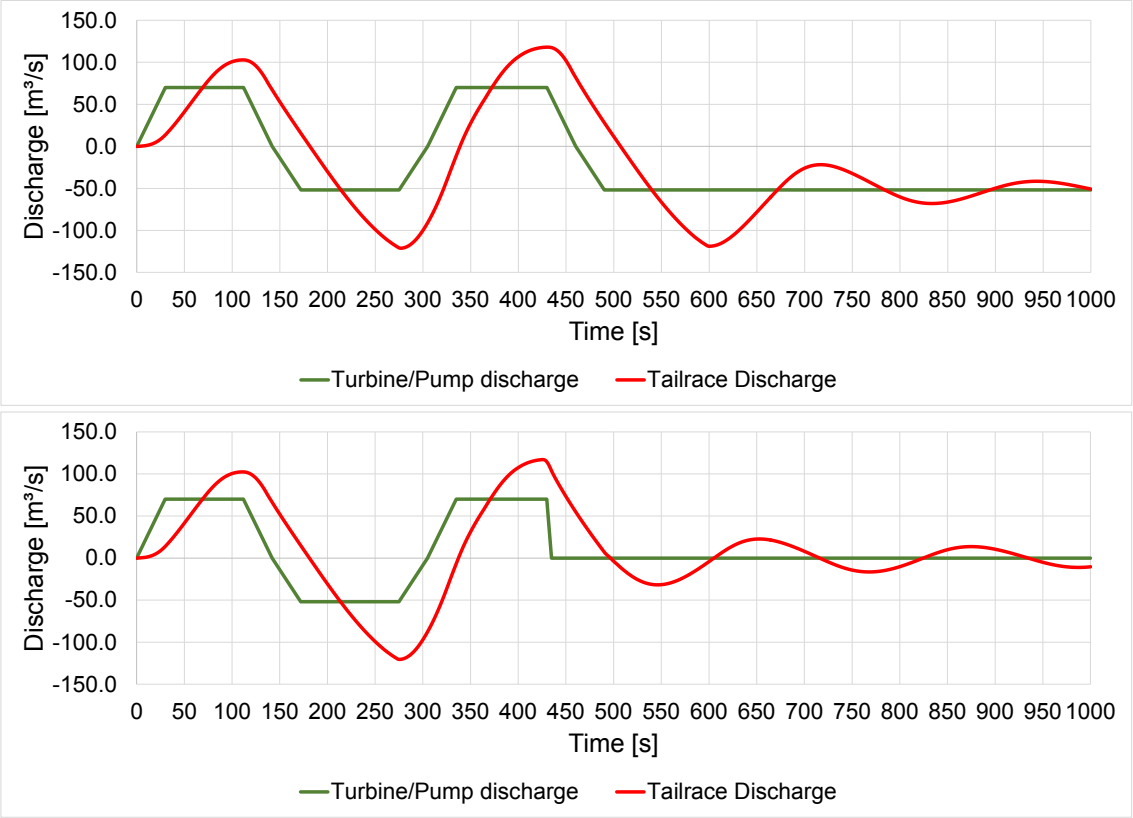

Figure 6.36: *Model type 2 - 70 m³/s - Comparison of the tailrace discharge (load changes top, load shed bottom)*

Table 6.31: *Model type 2 - 70 m³/s - Data comparison of the main loading cases*

Model type 2 - Q = 70 m³/s						
Load case	Qmax	Qmin	Amp+	Amp-	Head min	Head max
	[m³/s]	[m³/s]	[-]	[-]	[m.a.s.l.]	[m.a.s.l.]
Load changes	118.04	-121.17	1.69	2.33	174.44	287.20
Load shed	117.05	-120.45	1.67	2.32	169.65	287.64

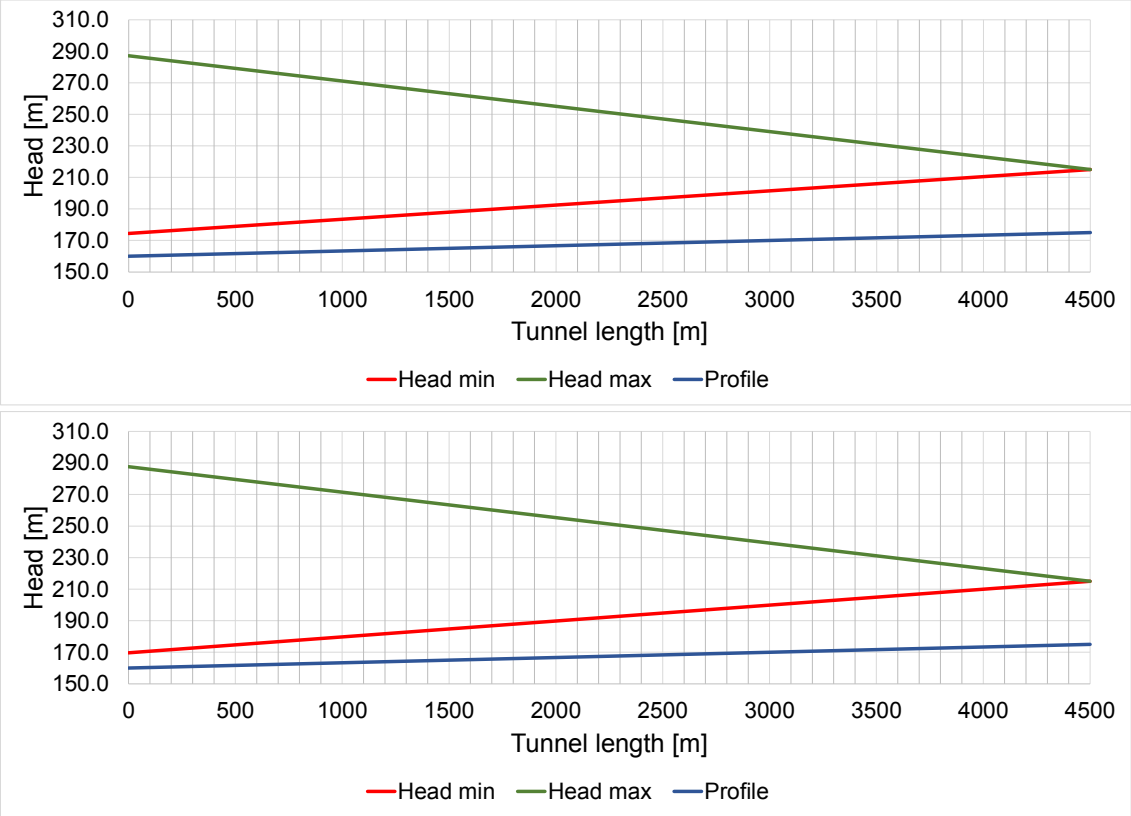

Figure 6.37: *Model type 2 - 70 m³/s - Comparison of the tailrace head (load changes top, load shed bottom)*

Table 6.32: *Model type 2 - 70 m³/s - Surge tank construction parts and their sizes*

Model type 2 - 70 m³/s - Surge tank size	
Construction part	Excavation size
	[m³]
Lower chamber	2827
Surge tank	3866
Upper chamber	4948
Sum	11641
Sum +25%	13585

Turbine design flow rate Q = 80 m³/s

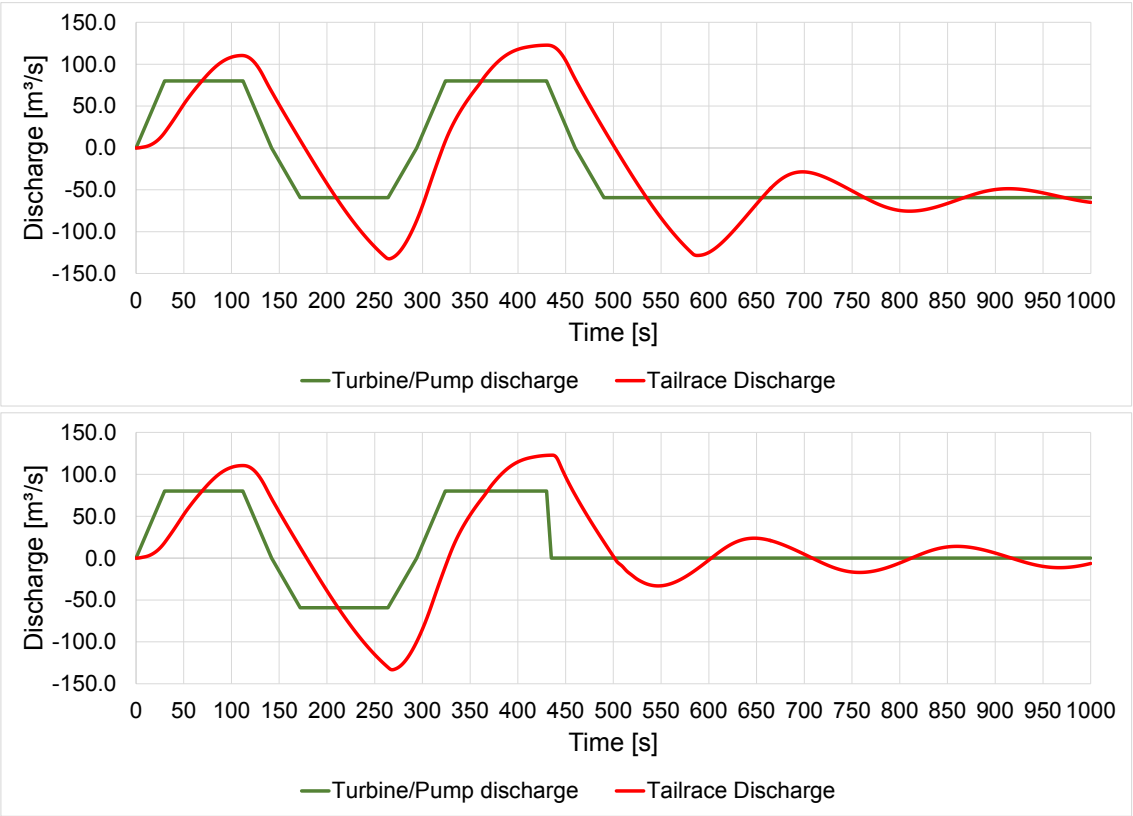

Figure 6.38: *Model type 2 - 80 m³/s - Comparison of the tailrace discharge (load changes top, load shed bottom)*

Table 6.33: *Model type 2 - 80 m³/s - Data comparison of the main loading cases*

Model type 2 - Q = 80 m³/s						
Load case	Qmax	Qmin	Amp+	Amp-	Head min	Head max
	[m³/s]	[m³/s]	[-]	[-]	[m.a.s.l.]	[m.a.s.l.]
Load changes	122.76	-132.36	1.53	2.23	173.88	286.32
Load shed	122.90	-133.26	1.54	2.25	170.18	284.18

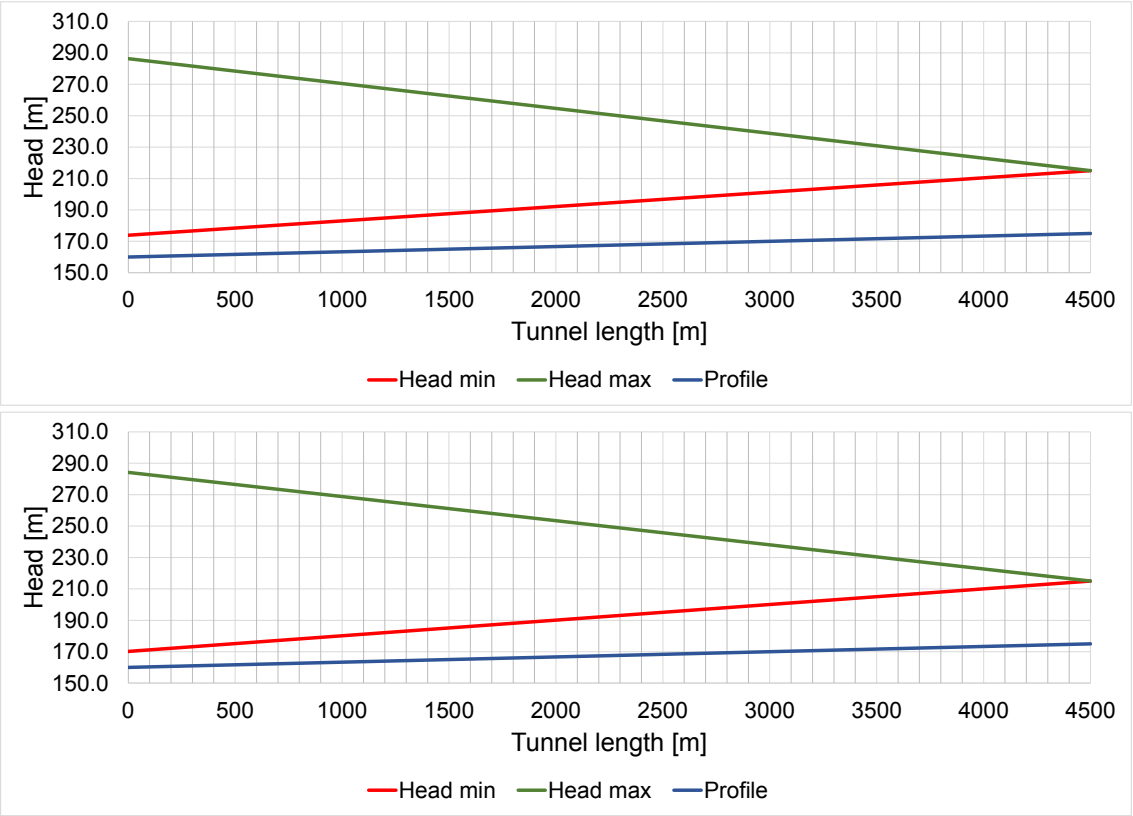

Figure 6.39: *Model type 2 - 80 m³/s - Comparison of the tailrace head (load changes top, load shed bottom)*

Table 6.34: *Model type 2 - 80 m³/s - Surge tank construction parts and their sizes*

Model type 2 - 80 m³/s - Surge tank size	
Construction part	Excavation size
	[m³]
Lower chamber	4752
Surge tank	3446
Upper chamber	3564
Sum	11761
Sum +25%	13840

Turbine design flow rate Q = 90 m³/s

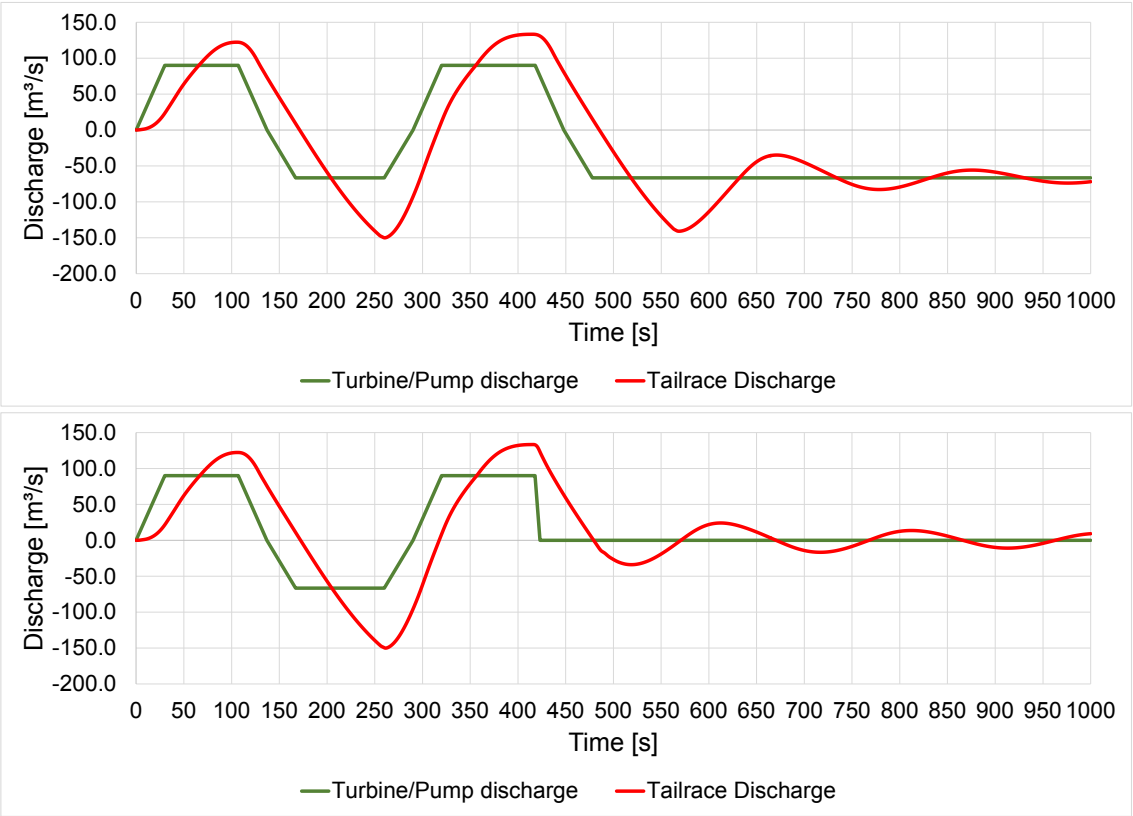

Figure 6.40: *Model type 2 - 90 m³/s - Comparison of the tailrace discharge (load changes top, load shed bottom)*

Table 6.35: *Model type 2 - 90 m³/s - Data comparison of the main loading cases*

Model type 2 - Q = 90 m³/s						
Load case	Qmax	Qmin	Amp+	Amp-	Head min	Head max
	[m³/s]	[m³/s]	[-]	[-]	[m.a.s.l.]	[m.a.s.l.]
Load changes	133.29	-150.09	1.48	2.25	174.11	284.59
Load shed	133.29	-150.09	1.48	2.25	174.11	284.59

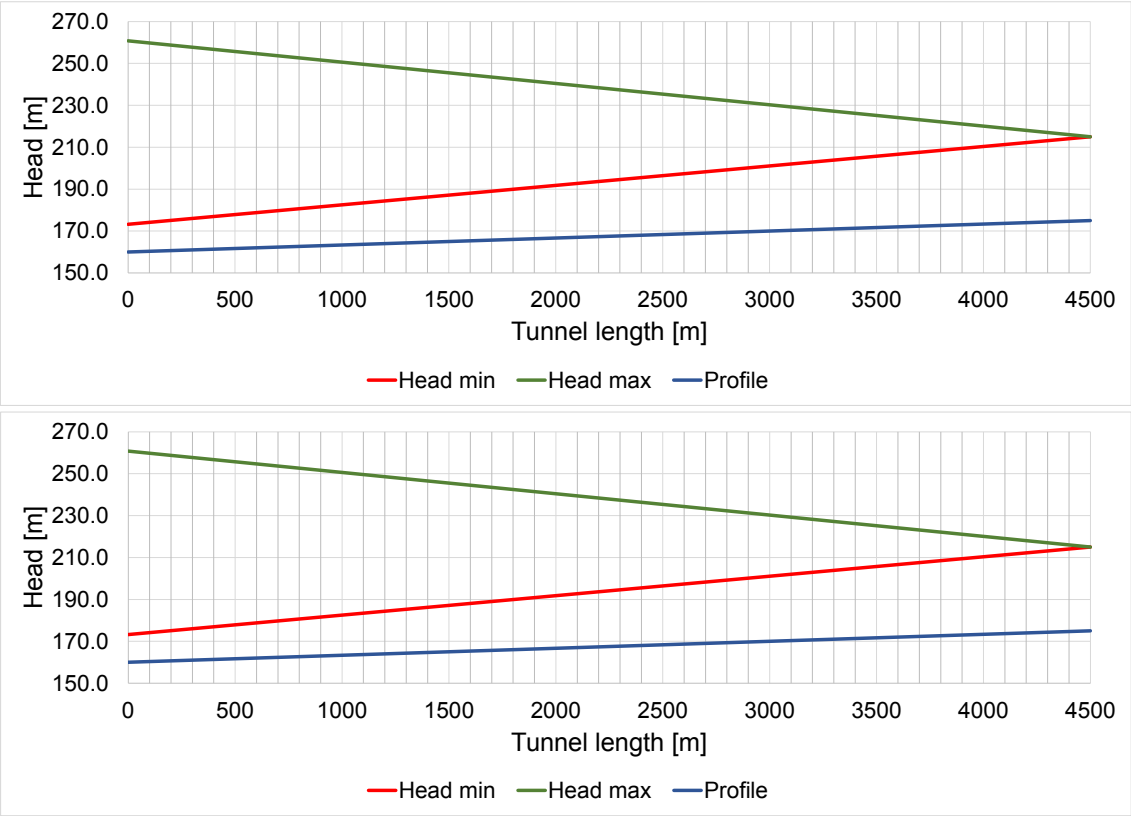

Figure 6.41: *Model type 2 - 90 m³/s - Comparison of the tailrace head (load changes top, load shed bottom)*

Table 6.36: *Model type 2 - 90 m³/s - Surge tank construction parts and their sizes*

Model type 2 - 90 m³/s - Surge tank size	
Construction part	Excavation size
	[m³]
Lower chamber	4948
Surge tank	3446
Upper chamber	4241
Sum	12635
Sum +25%	14932

Turbine design flow rate Q = 100 m³/s

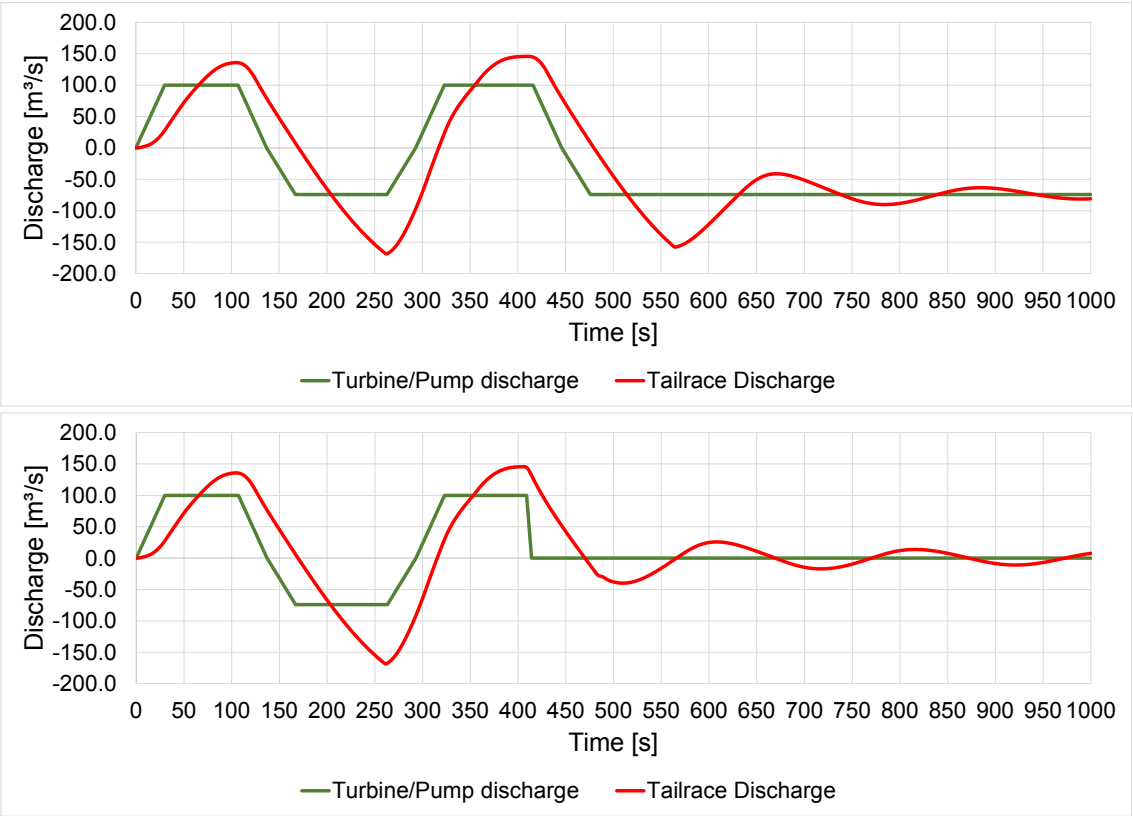

Figure 6.42: *Model type 2 - 100 m³/s - Comparison of the tailrace discharge (load changes top, load shed bottom)*

Table 6.37: *Model type 2 - 100 m³/s - Data comparison of the main loading cases*

Model type 2 - Q = 100 m³/s						
Load case	Qmax	Qmin	Amp+	Amp-	Head min	Head max
	[m³/s]	[m³/s]	[-]	[-]	[m.a.s.l.]	[m.a.s.l.]
Load changes	145.79	-168.53	1.46	2.27	174.27	288.05
Load shed	145.69	-168.35	1.46	2.27	171.77	288.72

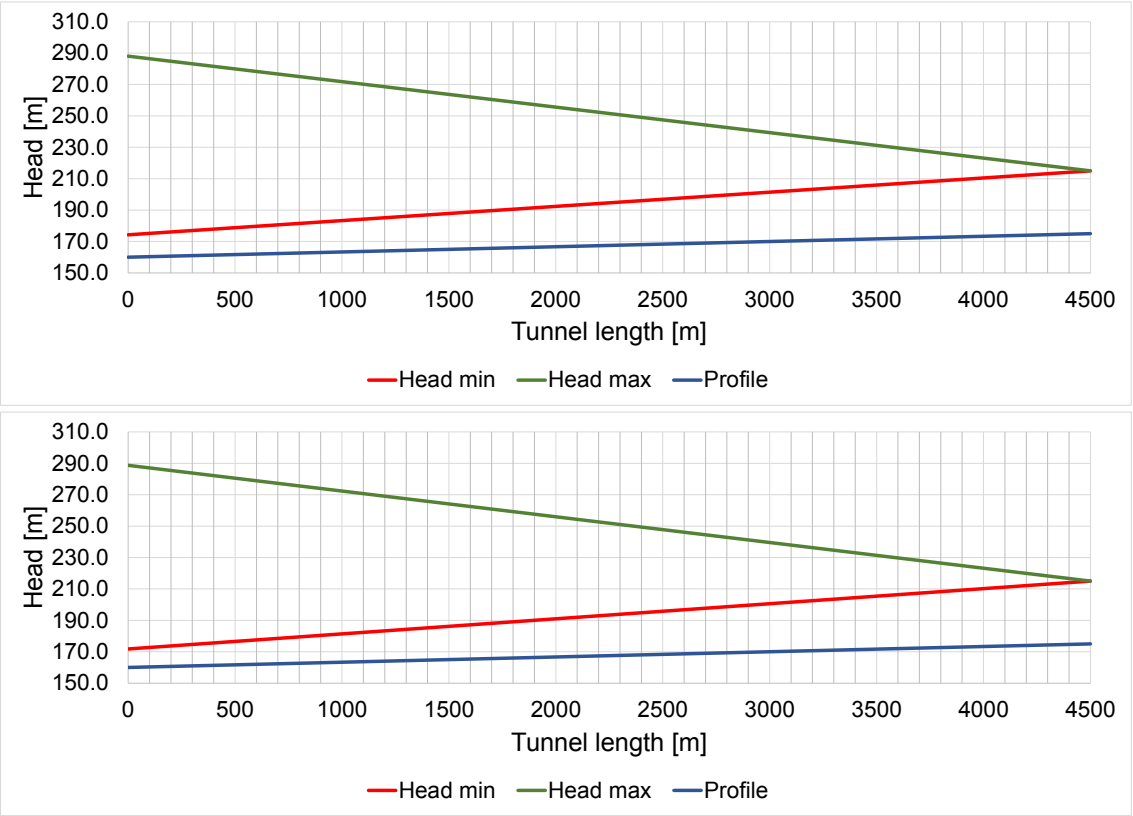

Figure 6.43: *Model type 2 - 100 m³/s - Comparison of the tailrace head (load changes top, load shed bottom)*

Table 6.38: *Model type 2 - 100 m³/s - Surge tank construction parts and their sizes*

Model type 2 - 100 m³/s - Surge tank size	
Construction part	Excavation size
	[m³]
Lower chamber	9189
Surge tank	3920
Upper chamber	3817
Sum	16927
Sum +25%	20178

6.4 Type 3 - Surge tank with aerated throttle

The third model type (Figure 6.44) is equipped with an aeration at the throttle, in order to show the significance of hydraulic losses that come with such an important construction part. Model type 3 is probably the model closest to reality.

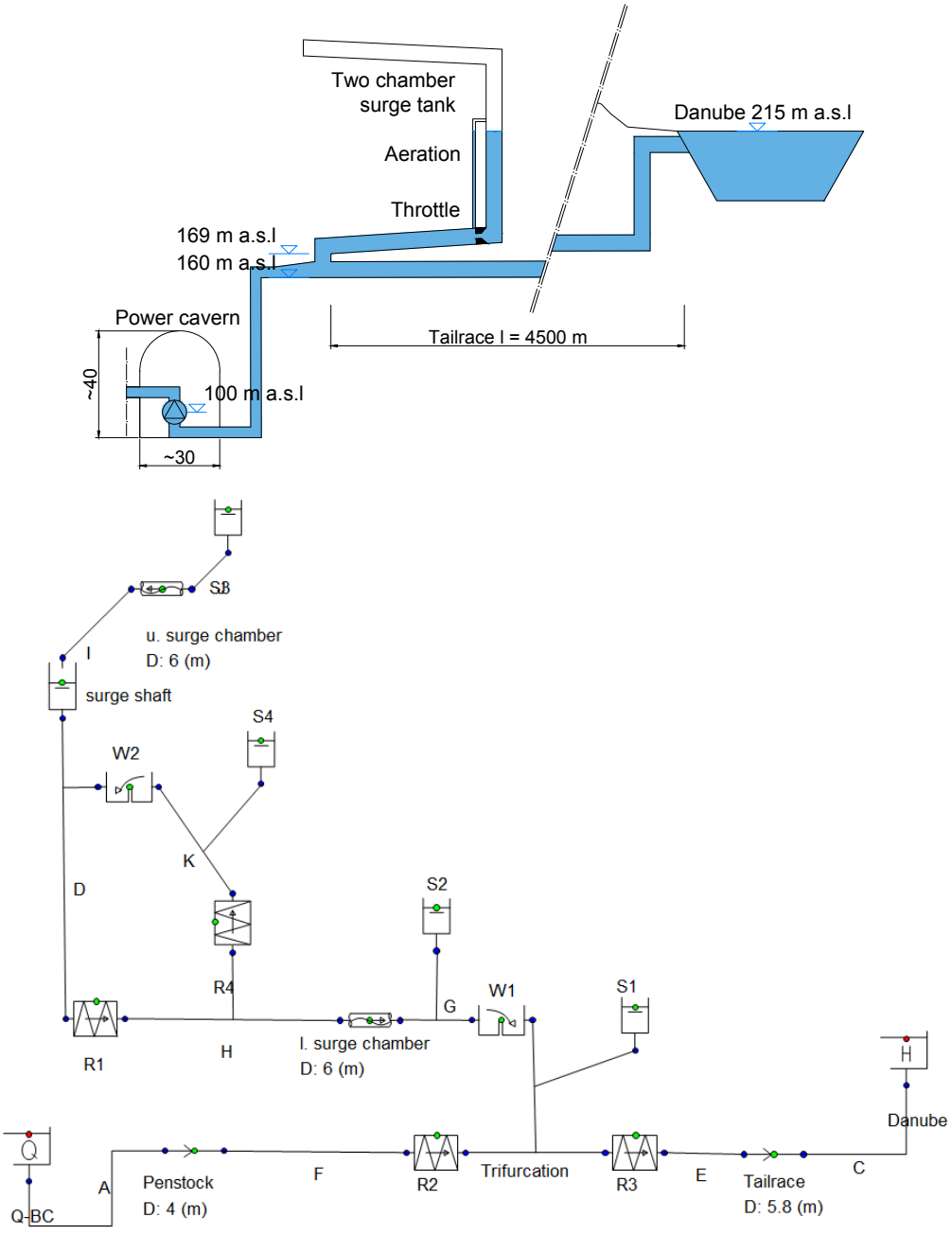

Figure 6.44: *Physical (top) and 1-D numerical model (bottom): Type 3*

6.4.1 Type 3 - Turbine design flow rates

Turbine design flow rate Q = 20 m³/s

In this model the biggest negative amplification again occurs after the first load change, therefore the values as seen in table 6.39 are the same for both loading cases. This happens due to the fact that until this point of the simulation both loading cases are equal. As long as the head stays the same for both loading cases only one graph is illustrated.

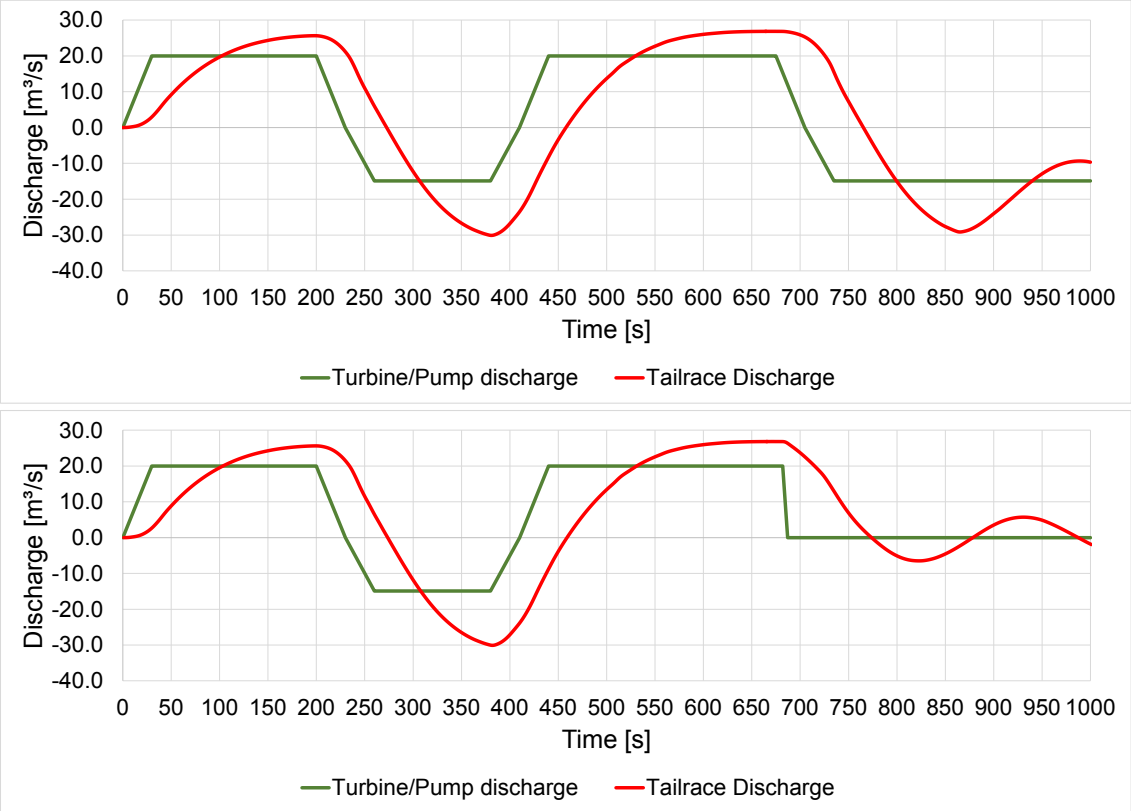

Figure 6.45: *Model type 3 - 20 m³/s - Comparison of the tailrace discharge (load changes top, load shed bottom)*

Table 6.39: *Model type 3 - 20 m³/s - Data comparison of the main loading cases*

Model type 3 - Q = 20 m³/s						
Load case	Qmax	Qmin	Amp+	Amp-	Head min	Head max
	[m³/s]	[m³/s]	[-]	[-]	[m.a.s.l.]	[m.a.s.l.]
Load changes	26.84	-30.09	1.34	2.02	170.43	257.24
Load shed	26.84	-30.09	1.34	2.02	170.43	257.24

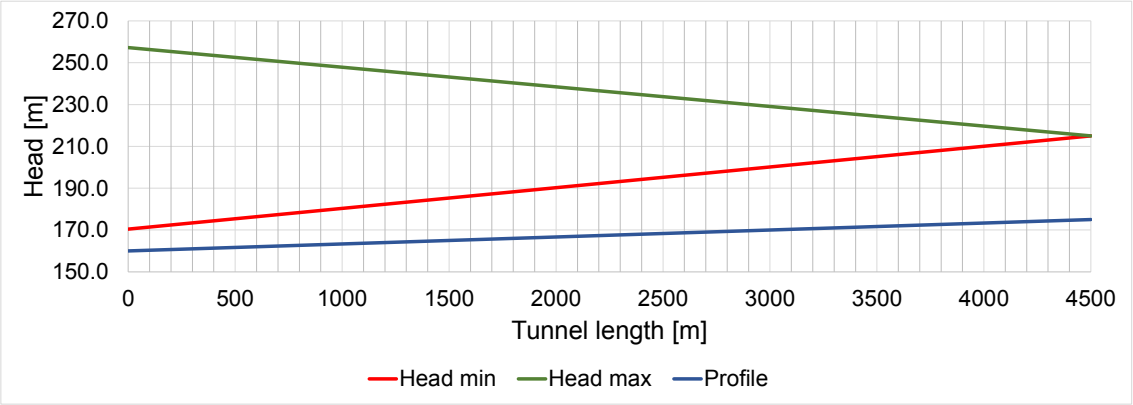

Figure 6.46: *Model type 3 - 20 m³/s - Tailrace head*

Table 6.40: *Model type 3 - 20 m³/s - Surge tank construction parts and their sizes*

Model type 3 - 20 m³/s - Surge tank size	
Construction part	Excavation size
	[m³]
Lower chamber	1924
Surge tank	644
Upper chamber	1684
Sum	4253
Sum +25%	5155

Turbine design flow rate Q = 30 m³/s

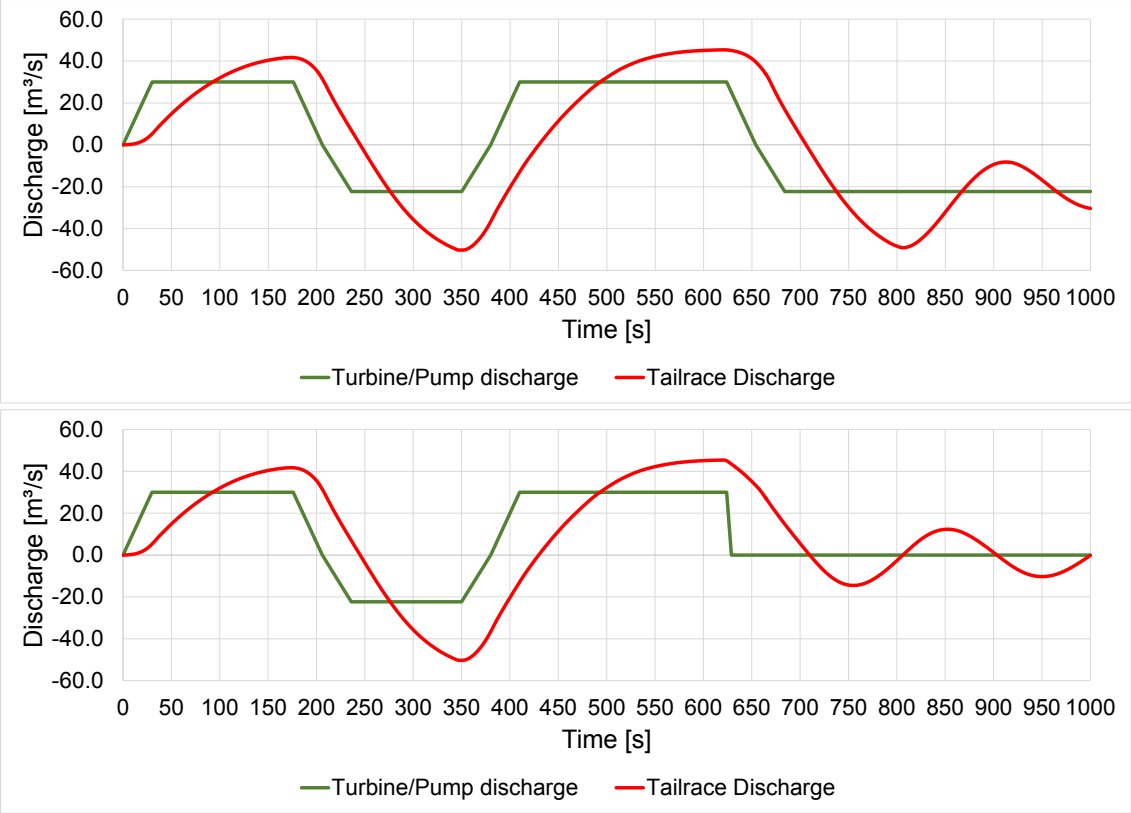

Figure 6.47: *Model type 3 - 30 m³/s - Comparison of the tailrace discharge (load changes top, load shed bottom)*

Table 6.41: *Model type 3 - 30 m³/s - Data comparison of the main loading cases*

Model type 3 - Q = 30 m³/s						
Load case	Qmax	Qmin	Amp+	Amp-	Head min	Head max
	[m³/s]	[m³/s]	[-]	[-]	[m.a.s.l.]	[m.a.s.l.]
Load changes	45.38	-50.27	1.51	2.25	169.43	254.83
Load shed	45.37	-50.27	1.51	2.25	171.64	254.83

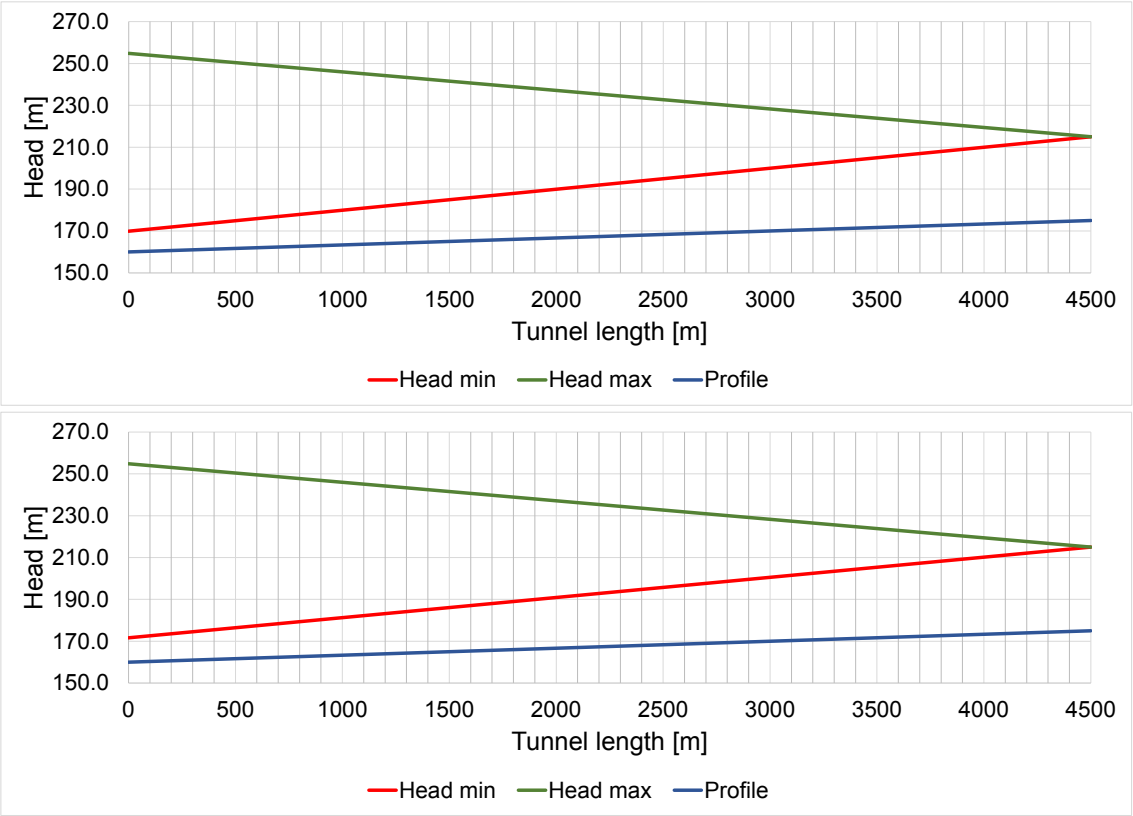

Figure 6.48: *Model type 3 - 30 m³/s - Comparison of the tailrace head (load changes top, load shed bottom)*

Table 6.42: *Model type 3 - 30 m³/s - Surge tank construction parts and their sizes*

Model type 3 - 30 m³/s - Surge tank size	
Construction part	Excavation size
	[m³]
Lower chamber	1885
Surge tank	873
Upper chamber	2827
Sum	5586
Sum +25%	6764

Turbine design flow rate Q = 40 m³/s

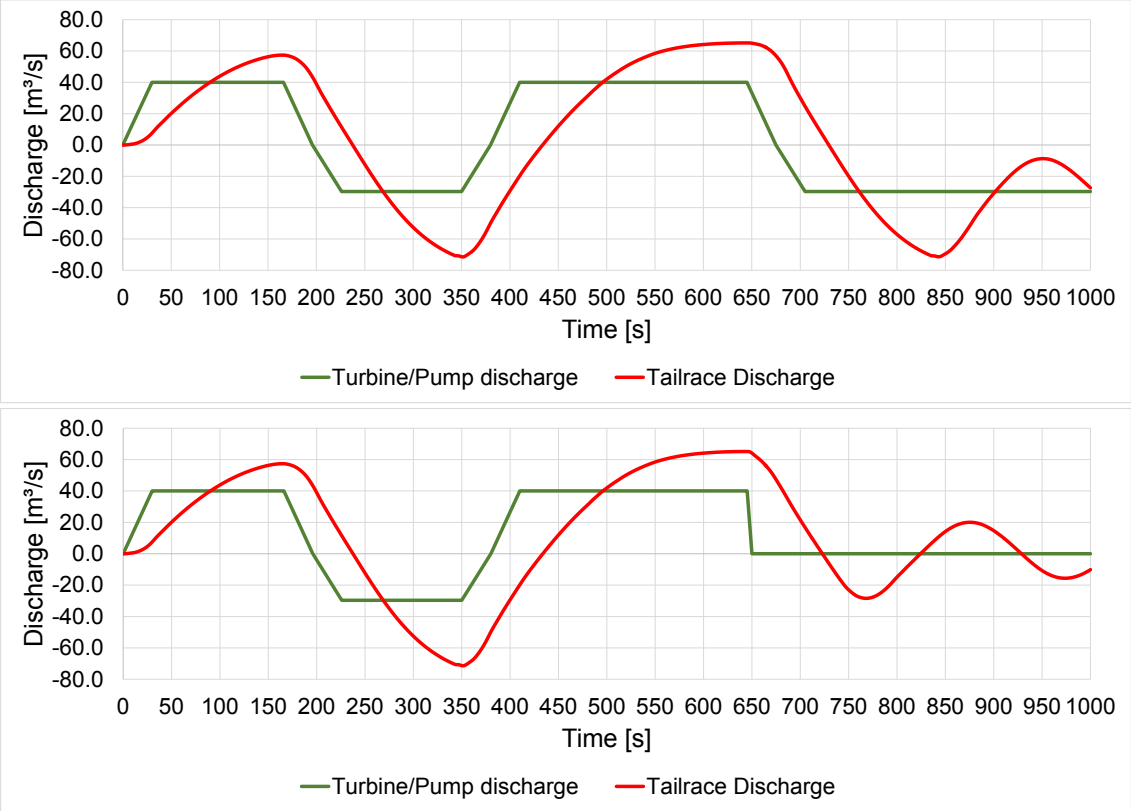

Figure 6.49: *Model type 3 - 40 m³/s - Comparison of the tailrace discharge (load changes top, load shed bottom)*

Table 6.43: *Model type 3 - 40 m³/s - Data comparison of the main loading cases*

Model type 3 - Q = 40 m³/s						
Load case	Qmax	Qmin	Amp+	Amp-	Head min	Head max
	[m³/s]	[m³/s]	[-]	[-]	[m.a.s.l.]	[m.a.s.l.]
Load changes	65.13	-71.40	1.63	2.40	172.58	253.01
Load shed	65.13	-71.40	1.63	2.40	172.58	253.01

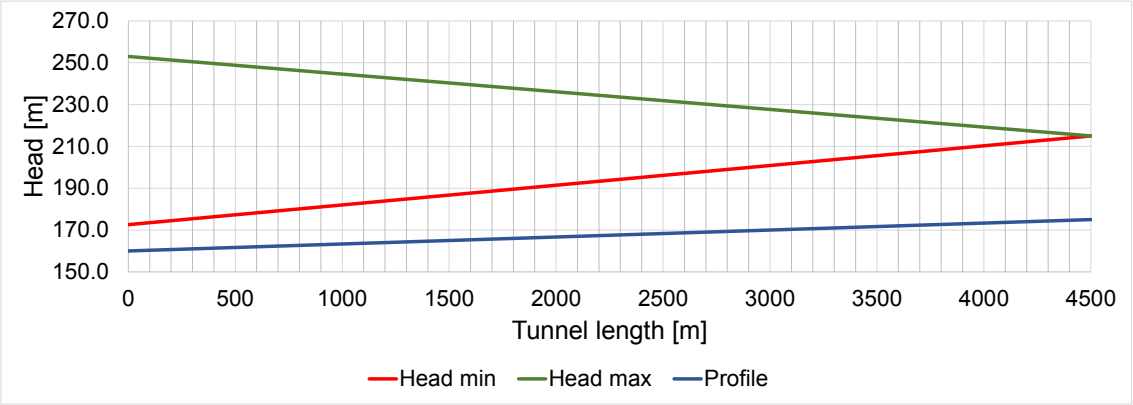

Figure 6.50: *Model type 3 - 40 m³/s - Tailrace head*

Table 6.44: *Model type 3 - 40 m³/s - Surge tank construction parts and their sizes*

Model type 3 - 40 m³/s - Surge tank size	
Construction part	Excavation size
	[m³]
Lower chamber	3181
Surge tank	1089
Upper chamber	4374
Sum	8644
Sum +25%	10533

Turbine design flow rate Q = 50 m³/s

This model again shows some difference in the positive amplification. As before this is due to a small model error.

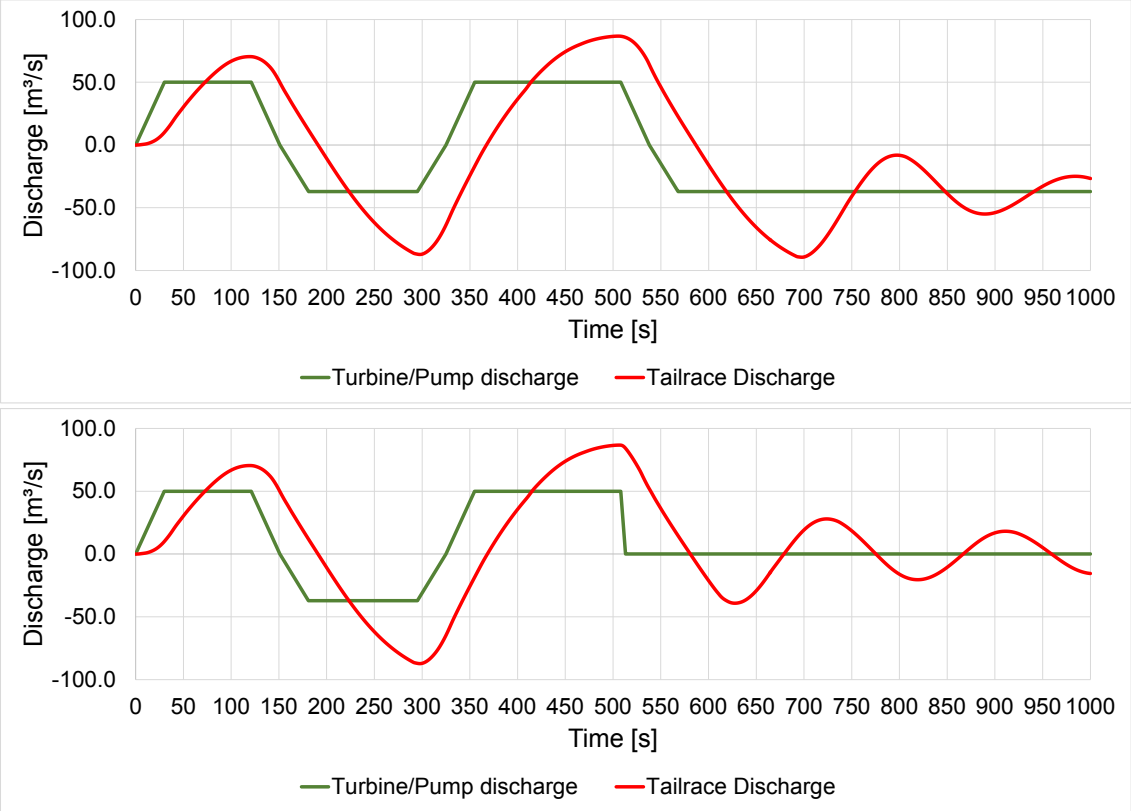

Figure 6.51: *Model type 3 - 50 m³/s - Comparison of the tailrace discharge (load changes top, load shed bottom)*

Table 6.45: *Model type 3 - 50 m³/s - Data comparison of the main loading cases*

Model type 3 - Q = 50 m³/s						
Load case	Qmax	Qmin	Amp+	Amp-	Head min	Head max
	[m³/s]	[m³/s]	[-]	[-]	[m.a.s.l.]	[m.a.s.l.]
Load changes	86.78	-89.42	1.74	2.41	172.54	264.92
Load shed	86.71	-87.22	1.73	2.35	173.07	264.46

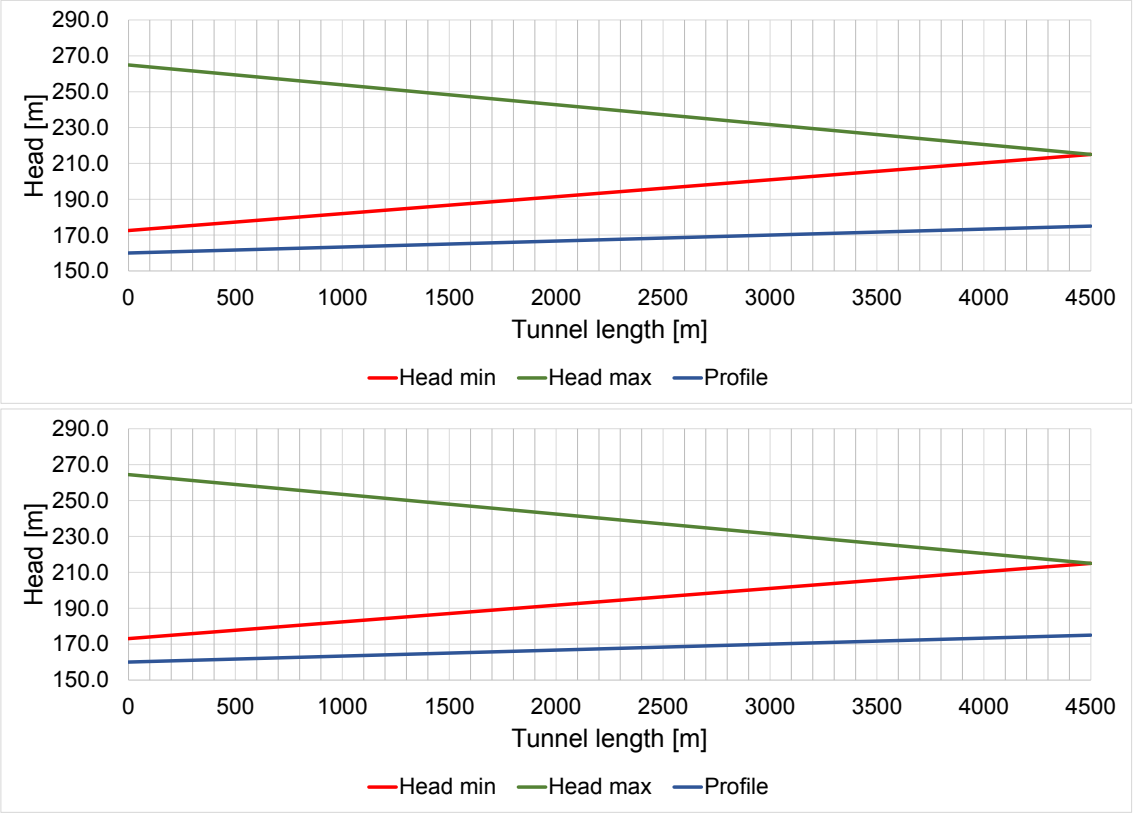

Figure 6.52: *Model type 3 - 50 m³/s - Comparison of the tailrace head (load changes top, load shed bottom)*

Table 6.46: *Model type 3 - 50 m³/s - Surge tank construction parts and their sizes*

Model type 3 - 50 m³/s - Surge tank size	
Construction part	Excavation size
	[m³]
Lower chamber	3927
Surge tank	1532
Upper chamber	3927
Sum	9386
Sum +25%	11349

Turbine design flow rate Q = 60 m³/s

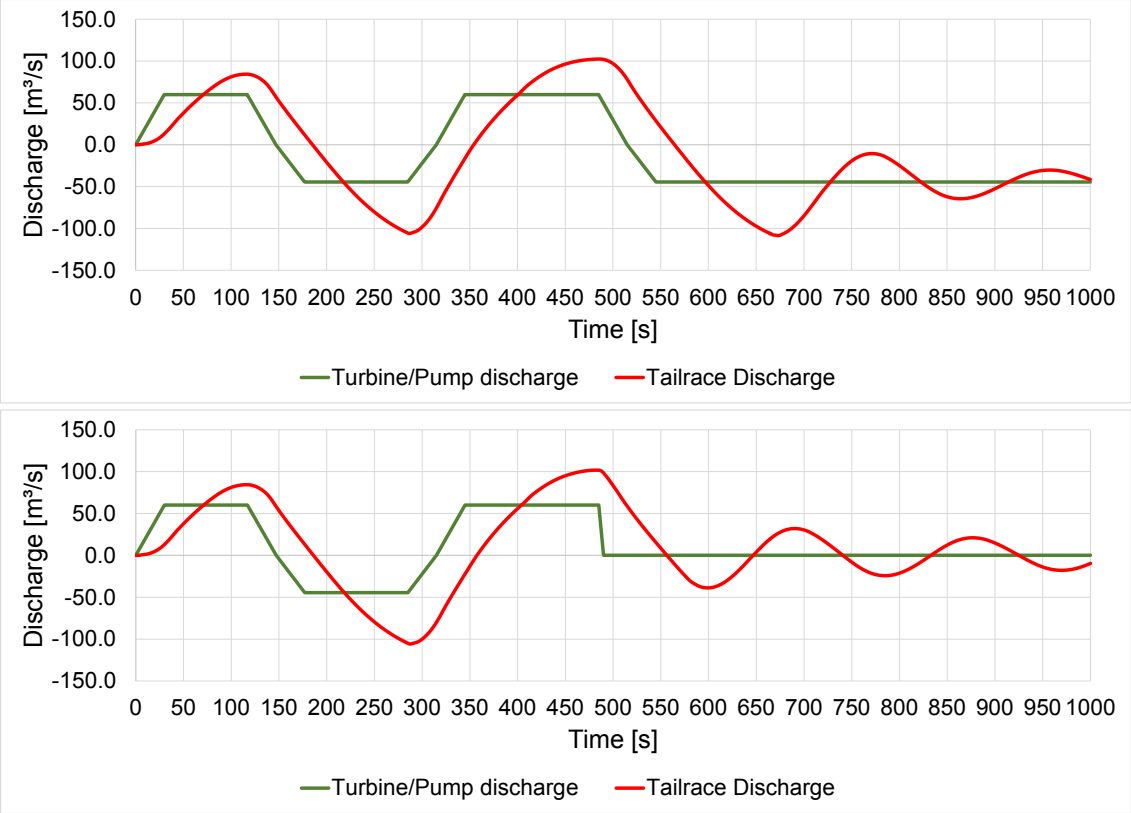

Figure 6.53: *Model type 3 - 60 m³/s - Comparison of the tailrace discharge (load changes top, load shed bottom)*

Table 6.47: *Model type 3 - 60 m³/s - Data comparison of the main loading cases*

Model type 3 - Q = 60 m³/s						
Load case	Qmax	Qmin	Amp+	Amp-	Head min	Head max
	[m³/s]	[m³/s]	[-]	[-]	[m.a.s.l.]	[m.a.s.l.]
Load changes	102.43	-108.53	1.71	2.44	172.76	268.63
Load shed	101.74	-105.83	1.70	2.38	173.43	267.29

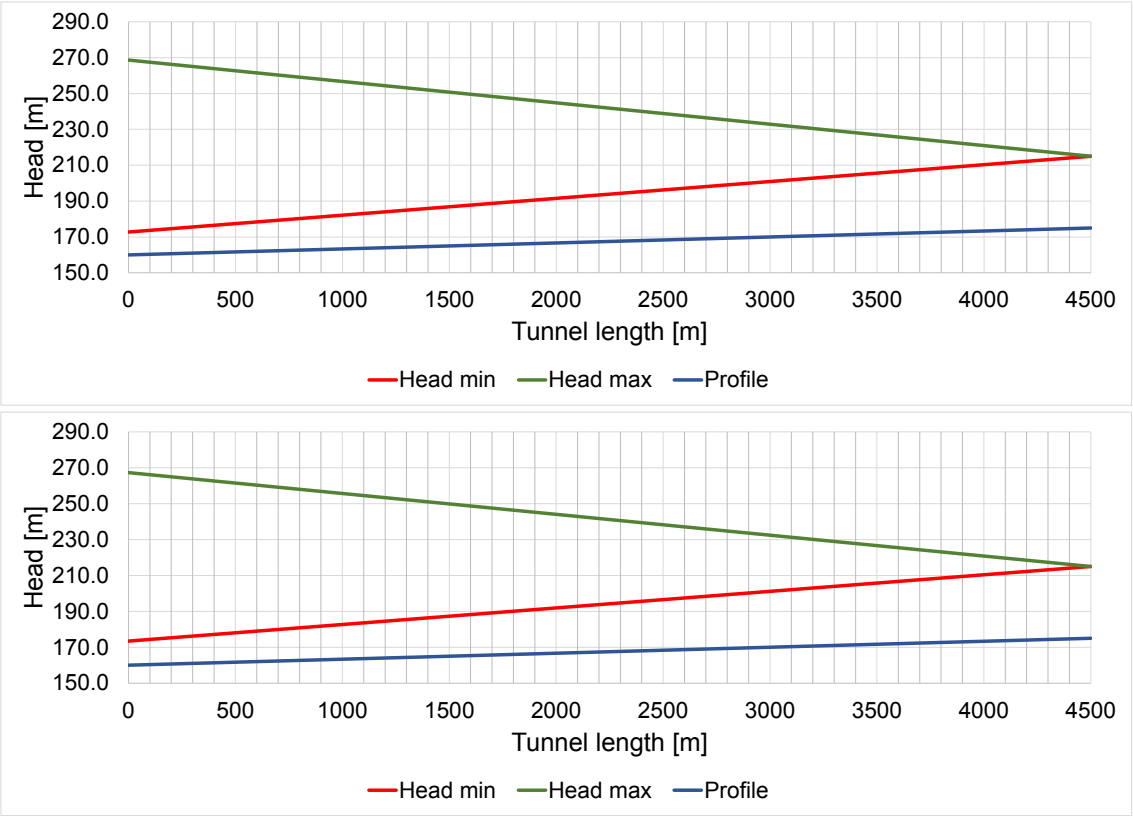

Figure 6.54: *Model type 3 - 60 m³/s - Comparison of the tailrace head (load changes top, load shed bottom)*

Table 6.48: *Model type 3 - 60 m³/s - Surge tank construction parts and their sizes*

Model type 3 - 60 m³/s - Surge tank size	
Construction part	Excavation size
	[m³]
Lower chamber	4712
Surge tank	1853
Upper chamber	4418
Sum	10983
Sum +25%	13266

Turbine design flow rate Q = 70 m³/s

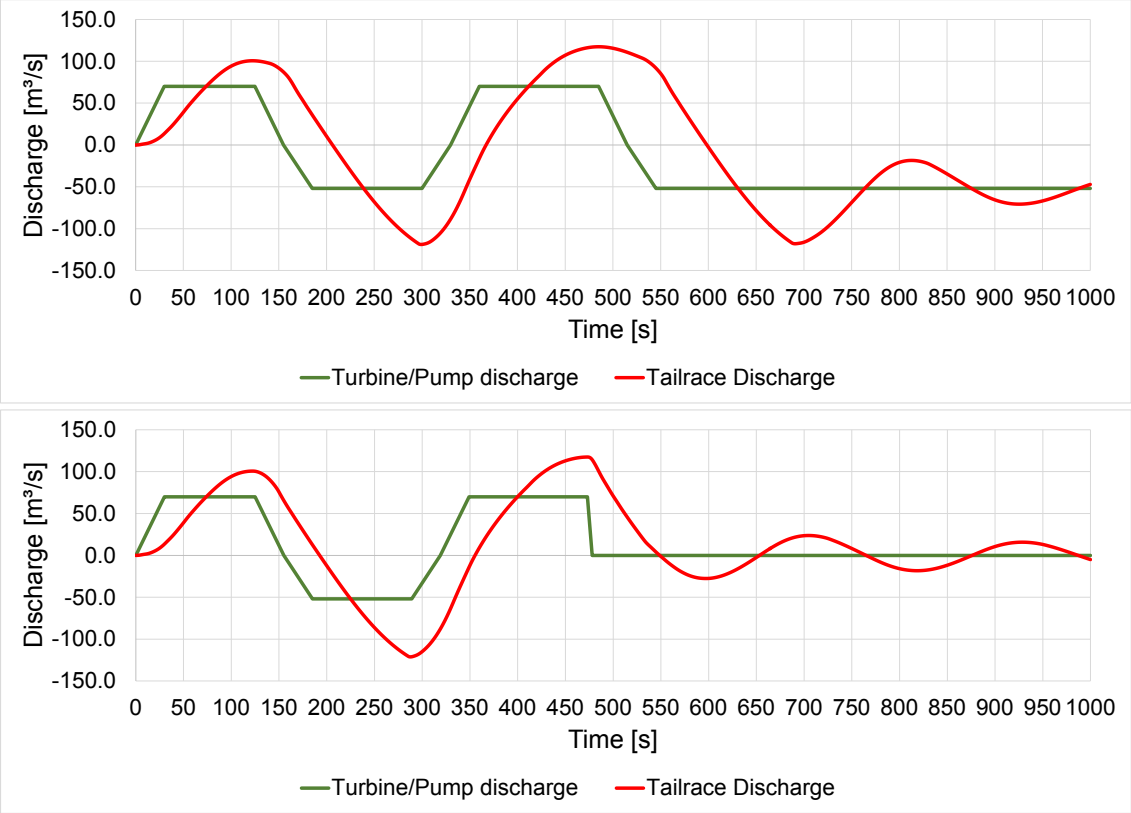

Figure 6.55: *Model type 3 - 70 m³/s - Comparison of the tailrace discharge (load changes top, load shed bottom)*

Table 6.49: *Model type 3 - 70 m³/s - Data comparison of the main loading cases*

Model type 3 - Q = 70 m³/s						
Load case	Qmax	Qmin	Amp+	Amp-	Head min	Head max
	[m³/s]	[m³/s]	[-]	[-]	[m.a.s.l.]	[m.a.s.l.]
Load changes	117.36	-118.84	1.68	2.29	173.06	275.60
Load shed	117.41	-121.17	1.68	2.33	173.37	275.99

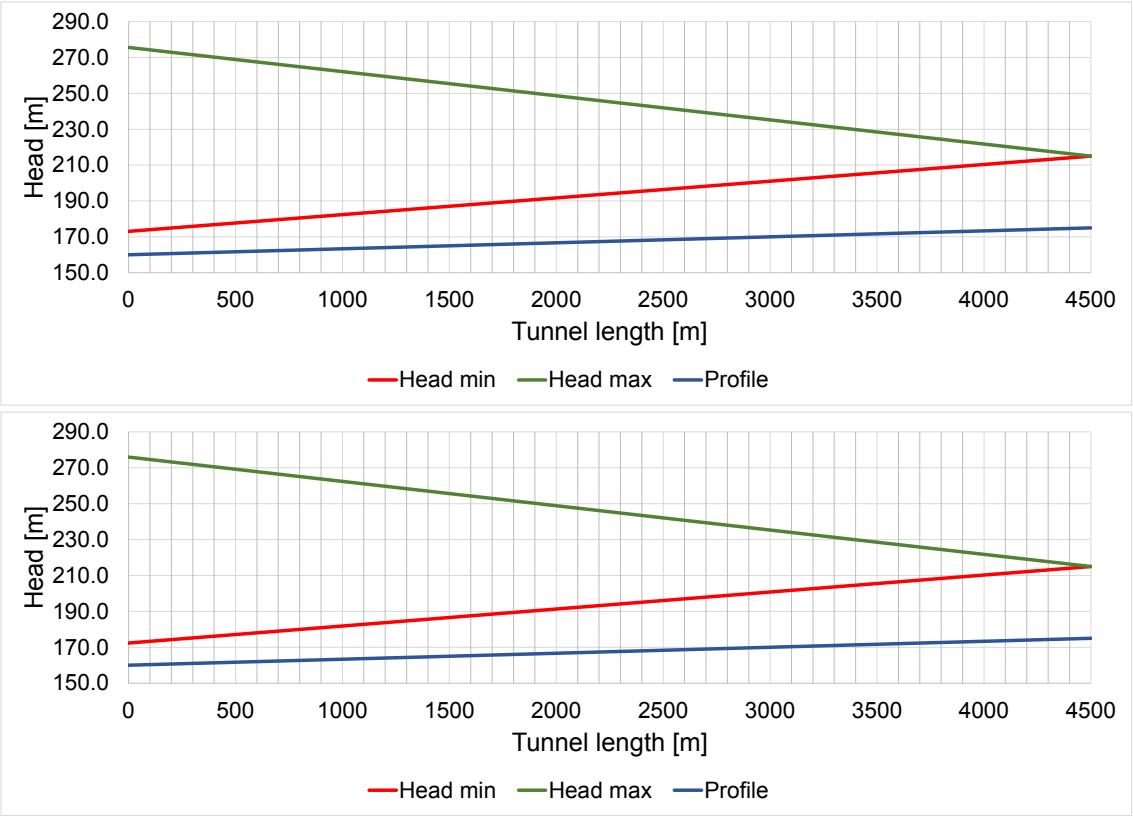

Figure 6.56: *Model type 3 - 70 m³/s - Comparison of the tailrace head (load changes top, load shed bottom)*

Table 6.50: *Model type 3 - 70 m³/s - Surge tank construction parts and their sizes*

Model type 3 - 70 m³/s - Surge tank size	
Construction part	Excavation size
	[m³]
Lower chamber	4418
Surge tank	3402
Upper chamber	4418
Sum	12237
Sum +25%	14446

Turbine design flow rate Q = 80 m³/s

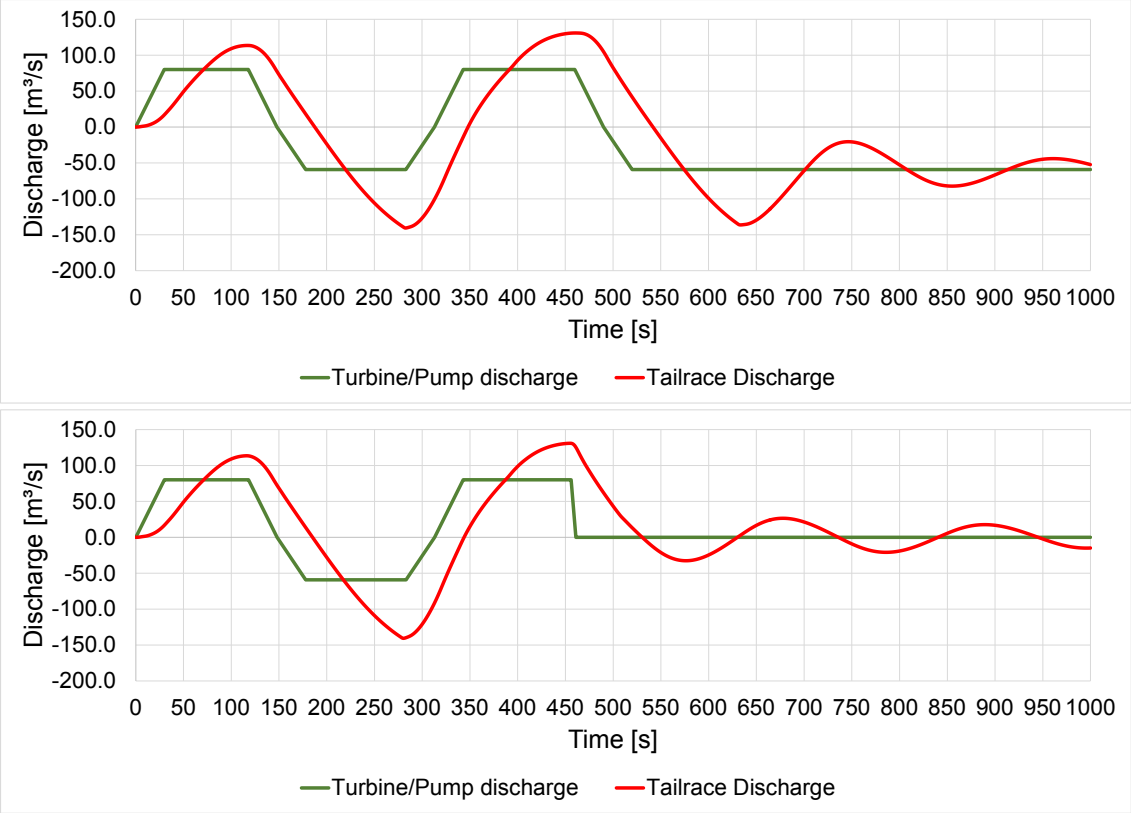

Figure 6.57: *Model type 3 - 80 m³/s - Comparison of the tailrace discharge (load changes top, load shed bottom)*

Table 6.51: *Model type 3 - 80 m³/s - Data comparison of the main loading cases*

Model type 3 - Q = 80 m³/s						
Load case	Qmax	Qmin	Amp+	Amp-	Head min	Head max
	[m³/s]	[m³/s]	[-]	[-]	[m.a.s.l.]	[m.a.s.l.]
Load changes	131.00	-140.62	1.64	2.37	173.78	277.60
Load shed	130.95	-140.66	1.64	2.37	172.82	279.12

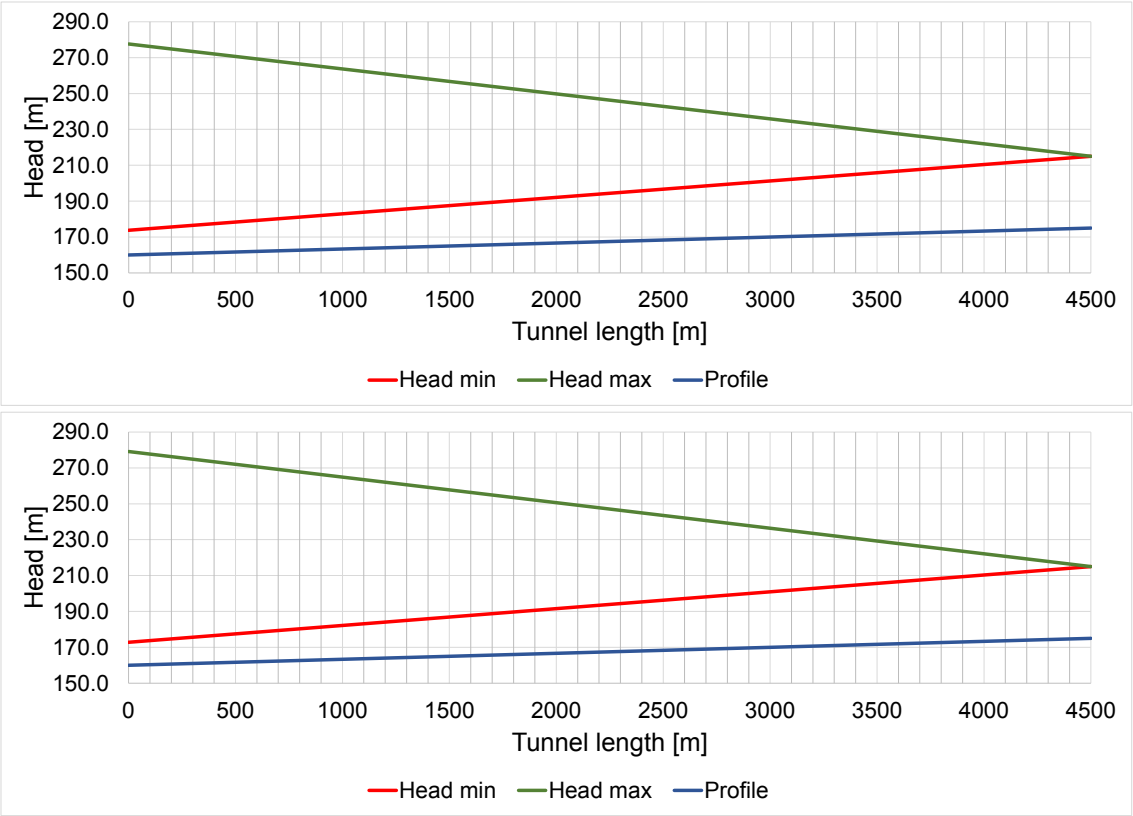

Figure 6.58: *Model type 3 - 80 m³/s - Comparison of the tailrace head (load changes top, load shed bottom)*

Table 6.52: *Model type 3 - 80 m³/s - Surge tank construction parts and their sizes*

Model type 3 - 80 m³/s - Surge tank size	
Construction part	Excavation size
	[m³]
Lower chamber	4989
Surge tank	3446
Upper chamber	4752
Sum	13187
Sum +25%	15622

Turbine design flow rate Q = 90 m³/s

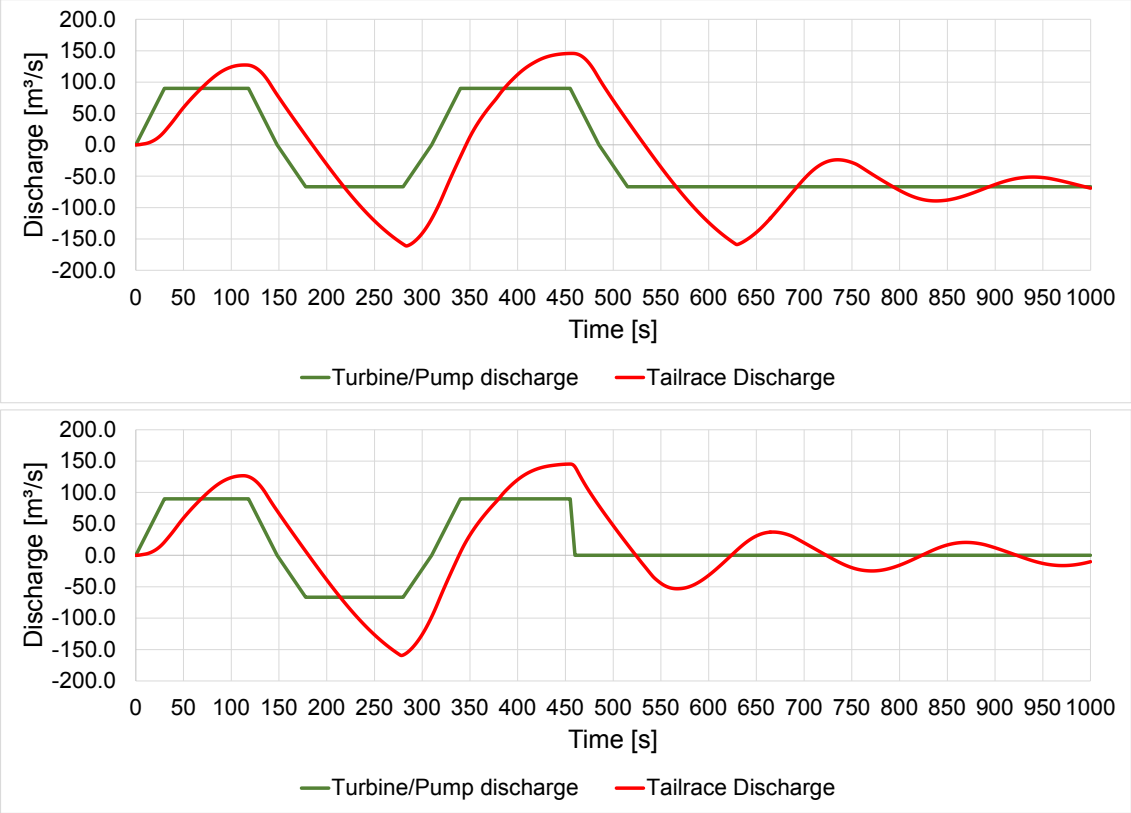

Figure 6.59: *Model type 3 - 90 m³/s - Comparison of the tailrace discharge (load changes top, load shed bottom)*

Table 6.53: *Model type 3 - 90 m³/s - Data comparison of the main loading cases*

Model type 3 - Q = 90 m³/s						
Load case	Qmax	Qmin	Amp+	Amp-	Head min	Head max
	[m³/s]	[m³/s]	[-]	[-]	[m.a.s.l.]	[m.a.s.l.]
Load changes	145.73	-161.00	1.62	2.41	173.91	279.81
Load shed	145.27	-159.43	1.61	2.39	173.16	281.54

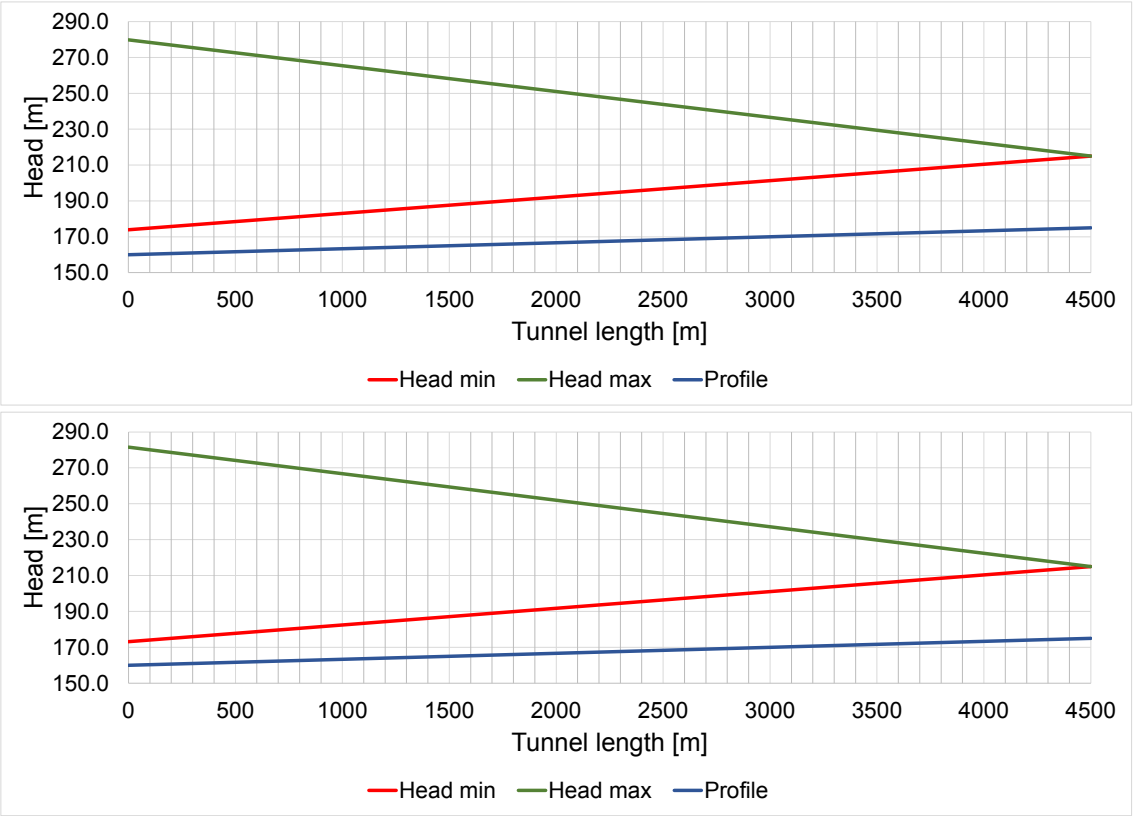

Figure 6.60: *Model type 3 - 90 m³/s - Comparison of the tailrace head (load changes top, load shed bottom)*

Table 6.54: *Model type 3 - 90 m³/s - Surge tank construction parts and their sizes*

Model type 3 - 90 m³/s - Surge tank size	
Construction part	Excavation size
	[m³]
Lower chamber	7069
Surge tank	3446
Upper chamber	4948
Sum	15463
Sum +25%	18467

Turbine design flow rate Q = 100 m³/s

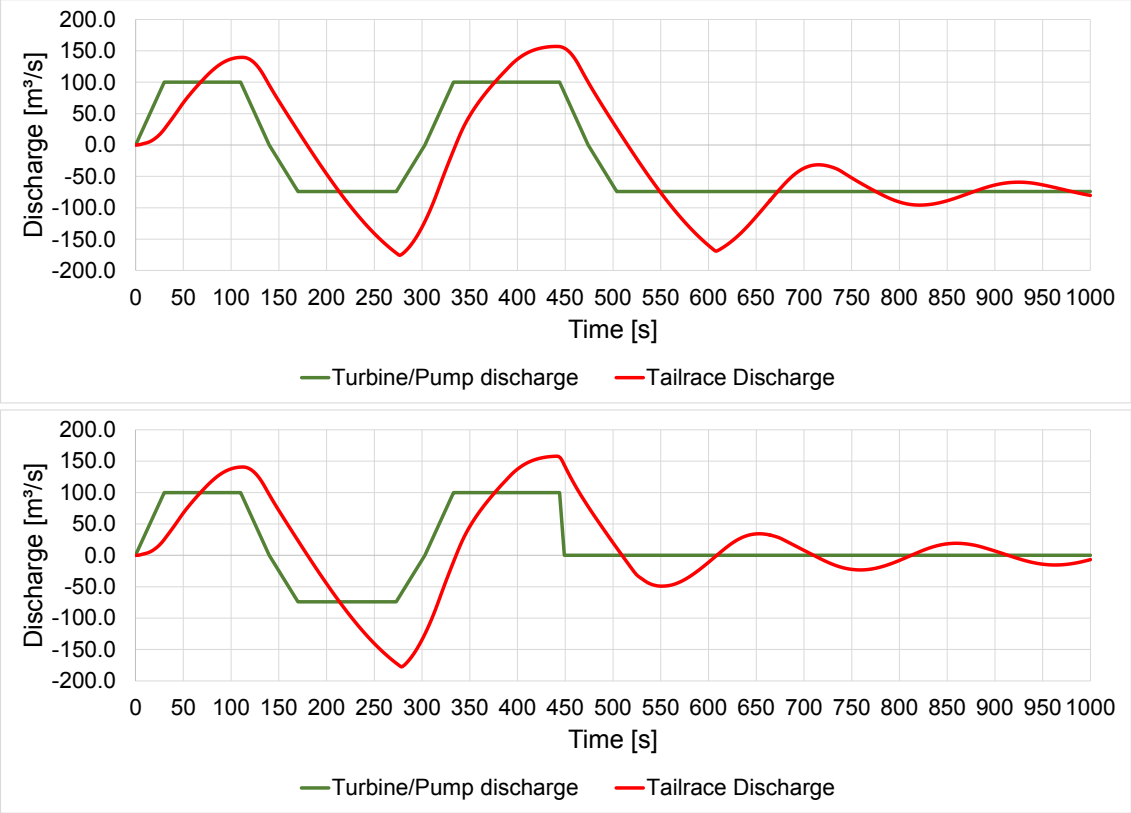

Figure 6.61: *Model type 3 - 100 m³/s - Comparison of the tailrace discharge (load changes top, load shed bottom)*

Table 6.55: *Model type 3 - 100 m³/s - Data comparison of the main loading cases*

Model type 3 - Q = 100 m³/s						
Load case	Qmax	Qmin	Amp+	Amp-	Head min	Head max
	[m³/s]	[m³/s]	[-]	[-]	[m.a.s.l.]	[m.a.s.l.]
Load changes	157.01	-175.60	1.57	2.37	174.13	283.82
Load shed	157.91	-177.44	1.58	2.39	173.03	285.28

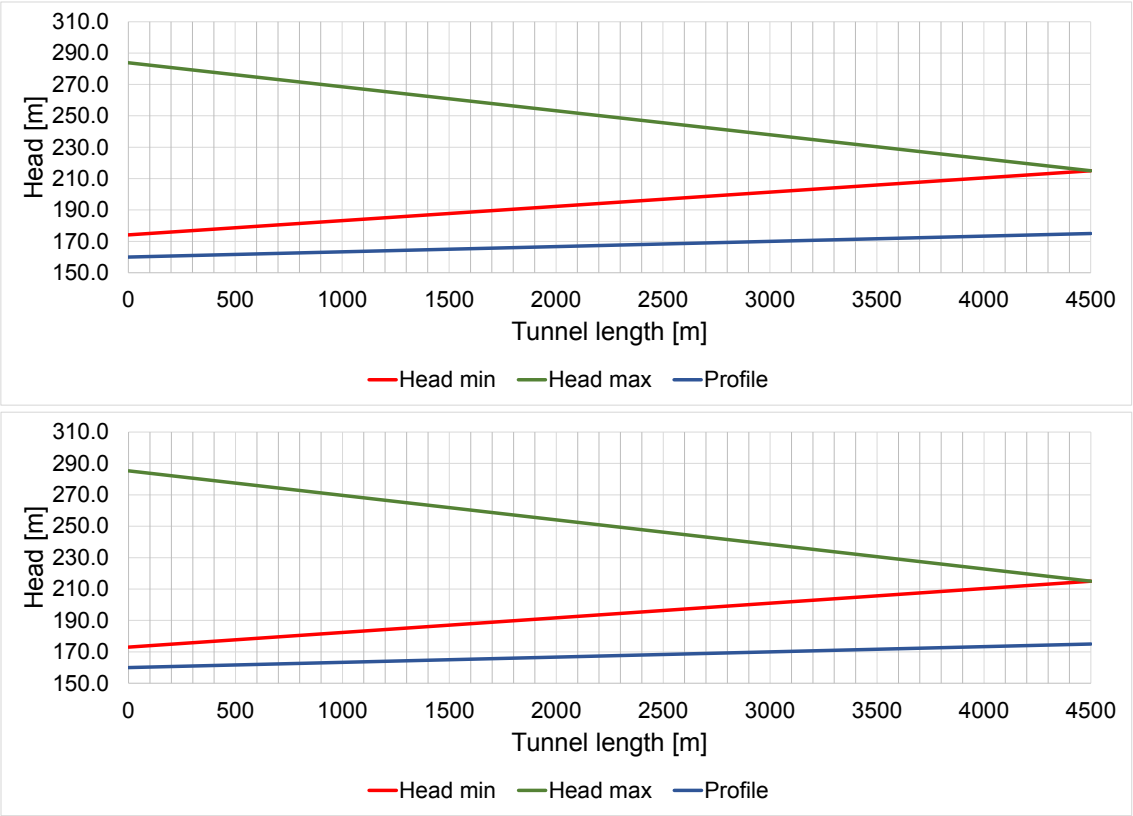

Figure 6.62: *Model type 3 - 100 m³/s - Comparison of the tailrace head (load changes top, load shed bottom)*

Table 6.56: *Model type 3 - 100 m³/s - Surge tank construction parts and their sizes*

Model type 3 - 100 m³/s - Surge tank size	
Construction part	Excavation size
	[m³]
Lower chamber	9189
Surge tank	3921
Upper chamber	5655
Sum	18765
Sum +25%	22476

6.5 Comparison

Figure 6.63 again shows the three different surge tank types. In figures 6.64 to 6.66 a comparison of these model types as a function of the turbine design flow is illustrated. Figures 6.64 and 6.65 show the difference of the surge tank volume. The tailrace discharge in relation to the design flow is shown in figure 6.66.

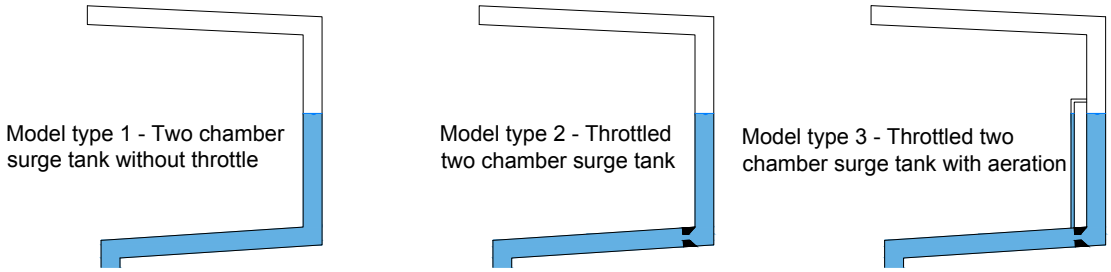

Figure 6.63: *The three different observed surge tank model types*

The following figures make it clear that the volume of a surge tank without a throttle has to be much higher, especially with bigger design flow rates, compared to one with a throttle. Figure 6.65 shows the surge tank size approximated with linear trend lines.
The divergence of model type 1 compared to the other two leads to the result that this surge tank design is not appropriate for higher design flow rates and therefore should not be considered for the main model.
These approximations show that the size difference caused by aeration is just a small change in gradient but leads to a separation value of about 1000 m³. This shows that aeration with respect to the losses is a considerable construction and modelling part of the hydraulic system and therefore can not be neglected.

By comparing the tailrace discharge results with the design flow rates, the amplification can be displayed, as shown in figure 6.66.
In figures 6.64 as well as 6.66 a rising divergence between model type 1 and the others can be observed. This leads to the result that along with a bigger design flow the necessity of a throttle becomes more essential.
Since model type 1 has already been ruled out due to the surge tank size, only model types 2 and 3 are compared. The data however is included for the sake of completeness. The two remaining models hardly show any differences until a design flow rate of 70 m³/s is reached. From this point onwards the results start to drift apart and therefore show significant differences in the tailrace discharge. This means that the results of model type 3 are decisive, since it is the closest model to reality. Therefore this type should be considered as the main model and used for further calculations/comparisons since the increase in excavation size is also not negligible.

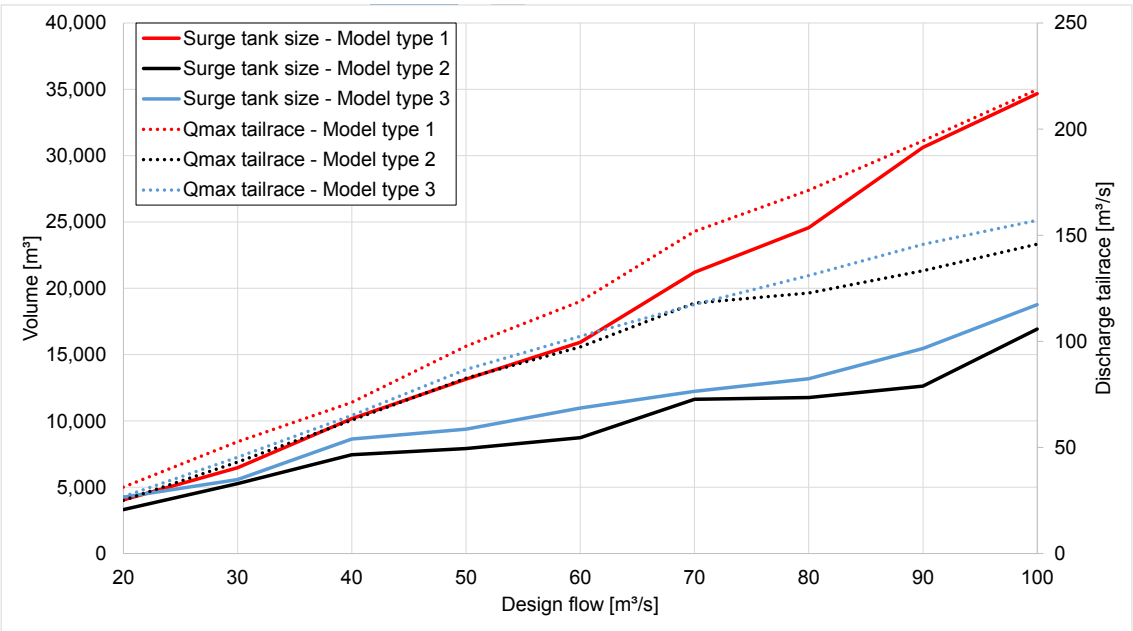

Figure 6.64: *Surge tank variant data (excluding additional 25 % excavation size for surge chambers)*

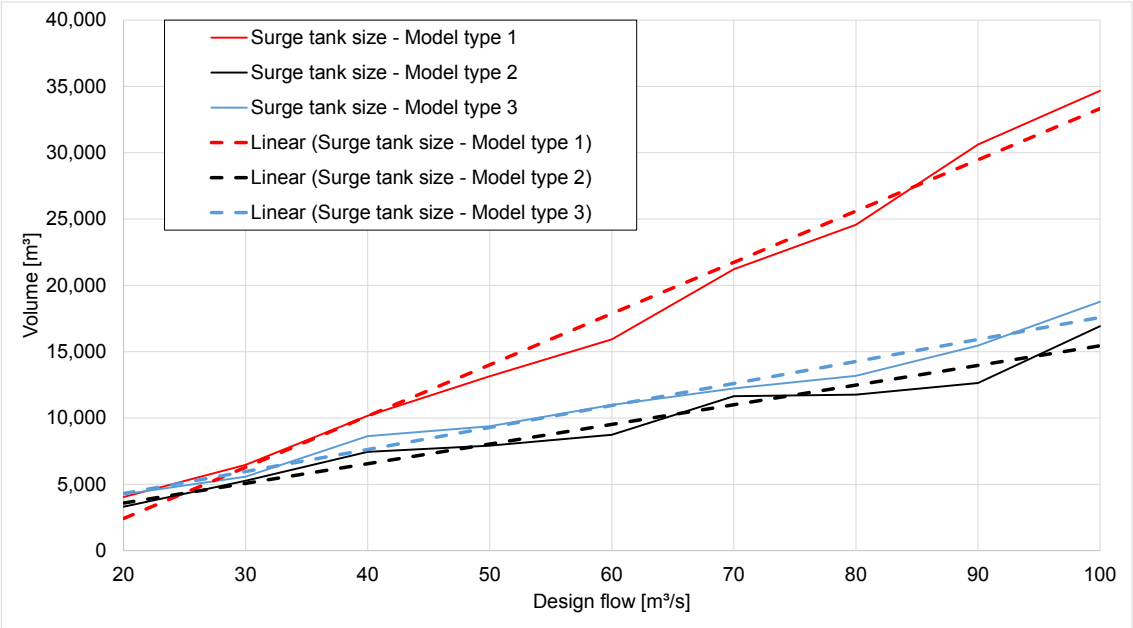

Figure 6.65: *Surge tank size data approximation*

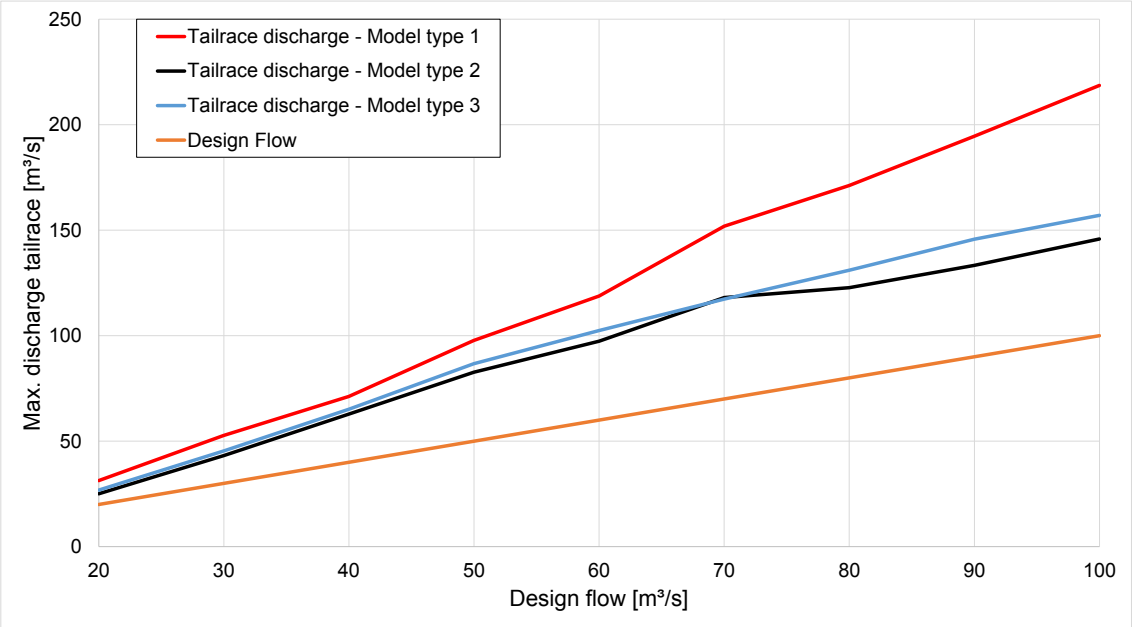

Figure 6.66: *Tailrace discharge comparison*

Table 6.57: *Tailrace discharge amplification*

	Throttled with aeration	Throttled	No throttling
Flow rate $[m^3/s]$	Discharge amplification [-]		
20	1.34	1.26	1.57
30	1.51	1.44	1.76
40	1.63	1.57	1.78
50	1.74	1.65	1.96
60	1.71	1.62	1.98
70	1.68	1.69	2.17
80	1.64	1.53	2.14
90	1.62	1.48	2.16
100	1.57	1.46	2.19

7 The three chamber surge tank

7.1 Basic facts

The three chamber surge tank is a further development of the two chamber surge tank. This type was basically designed for tail water applications. Studies showed that it also has an area of application for headwater areas with long headrace systems and small gross head.
This special surge tank consists of three chambers. The tunnel chamber, which can be integrated in the tailrace, works like a lower chamber of a two chamber surge tank during unsteady conditions. The pump chamber, which may not run empty at any point of the operation, is used to provide enough pressure for the pumps. This is one of the most defining construction parts of this model. If it is designed too small the risk of cavitation increases dramatically.
The third one is the upper chamber, which has the same tasks as in the two chamber surge tank. The two lower chambers are separated by an overflow sill, which allows the hydraulic system to split the water column within the mode of action.
The idea of this surge tank design is to reduce surge tank size, though this is not always the case since every pumped storage hydro power plant has its own characteristics. [12]

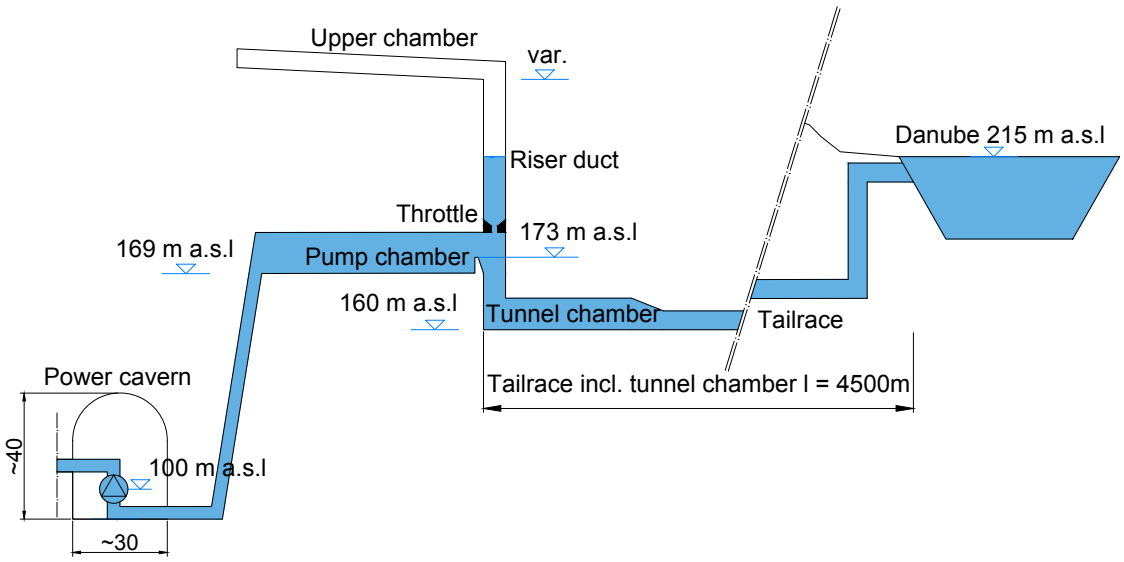

Figure 7.1: *System sketch of a three chamber surge tank layout*

7.2 Modelling and Analysis

7.2.1 The model

This model is based on the previous design of the two chamber surge tank. Deflection losses are not taken into account in this model type since the redirections have been rounded and therefore are very small.
In order to compare the two different hydraulic systems, the height of the pump chamber is determined by the lower surge chamber and the necessary head for the pump, as seen in the previous surge tank design. All defined heights correspond to the findings of Markus Larcher as described in his Doctoral thesis ([12]).
The small shafts in between different construction parts (as seen in figure 7.2) are placed in order to stabilize the simulation. The boundary conditions and the tailrace dimensioning stay the same compared to the two chamber surge tank.
Again models with discharge values reaching from 20 - 100 m³/s are examined individually with the same loading cases. The results are shown subsequently.

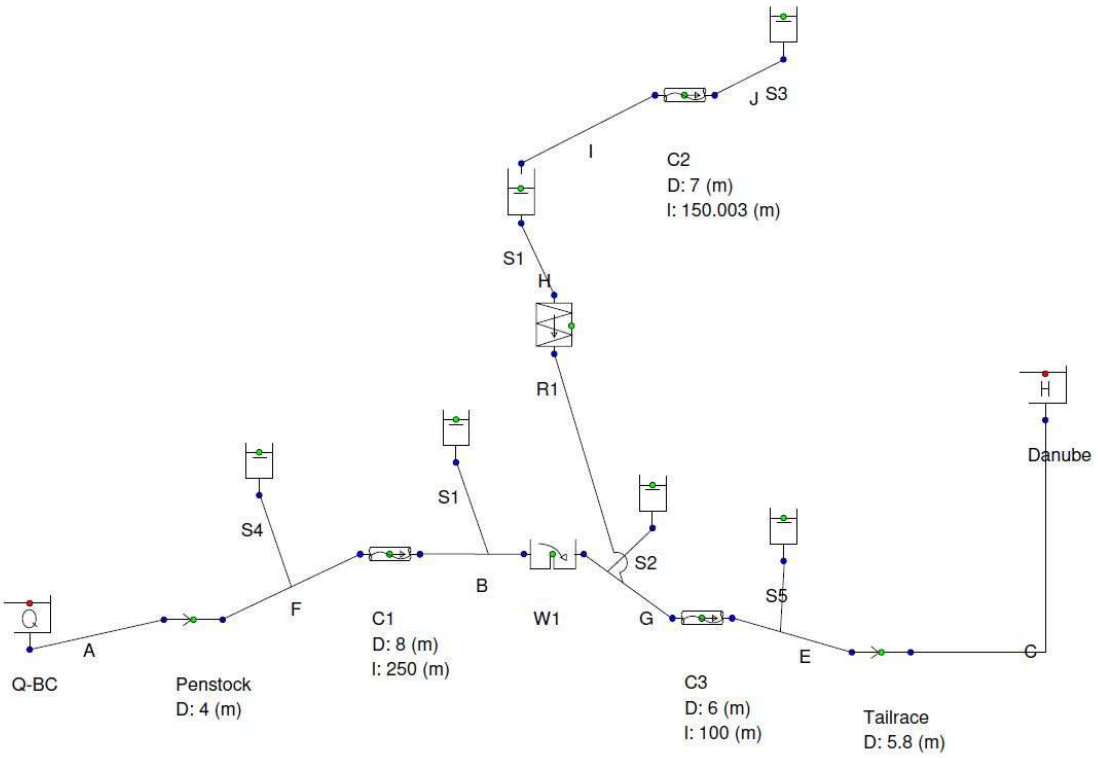

Figure 7.2: *The hydraulic model in WANDA 4.2*

7.2.2 Turbine design flow rates

Turbine design flow rate Q = 20 m³/s

This model shows a very slow reacting change in discharge. The reason for that is the tunnel chamber which has a significantly bigger diameter than the tailrace. This means that the filling process takes time and therefore slows down mass oscillation.
Both loading cases have the same extremes in head within the tailrace (Table 7.1), therefore only one graph is shown. The head never drops below profile height. This means the head is safe from cavitation.

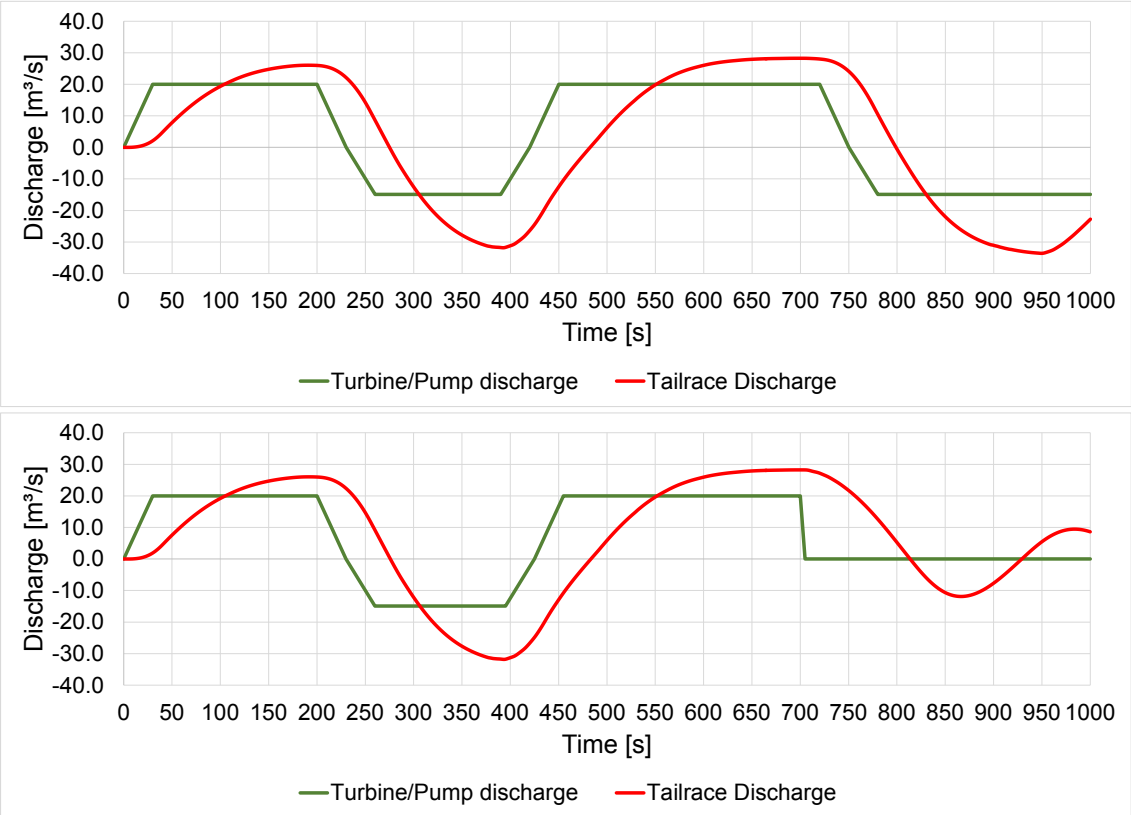

Figure 7.3: *Three chamber surge tank - 20 m³/s - Comparison of the tailrace discharge (load changes top, load shed bottom)*

Table 7.1: *Three chamber surge tank - 20 m³/s - Data comparison of the main loading cases*

Three chamber surge tank - Q = 20 m³/s						
Load case	Qmax	Qmin	Amp+	Amp-	Head min	Head max
	[m³/s]	[m³/s]	[-]	[-]	[m.a.s.l.]	[m.a.s.l.]
Load changes	28.24	-33.60	1.41	2.25	167.83	246.23
Load shed	28.24	-31.82	1.41	2.14	167.83	246.23

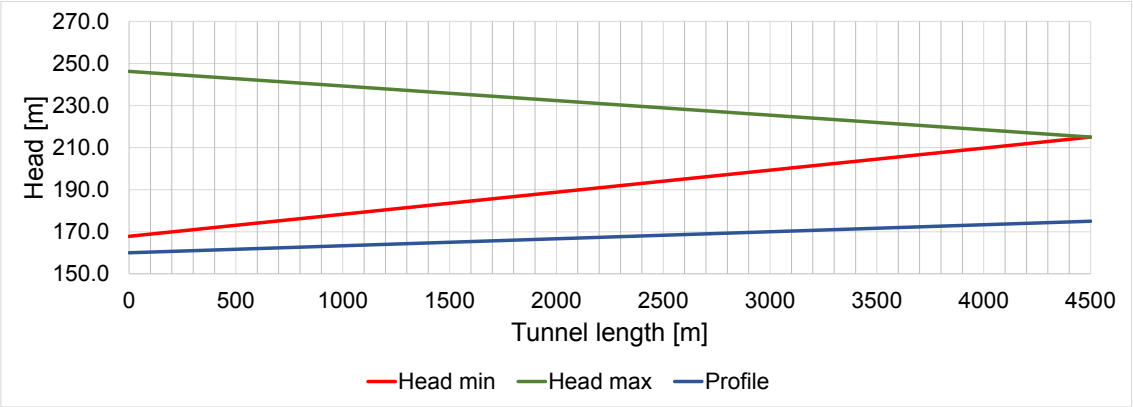

Figure 7.4: *Three chamber surge tank - 20 m³/s - Tailrace head*

Table 7.2: *Three chamber surge tank - 20 m³/s - Surge tank construction parts and their sizes*

Three chamber surge tank - 20 m³/s - Surge tank size	
Construction part	Excavation size
	[m³]
Tunnel chamber	2827
Pump chamber	2748
Riser duct	770
Upper chamber	2160
Sum	8505

Turbine design flow rate Q = 30 m³/s

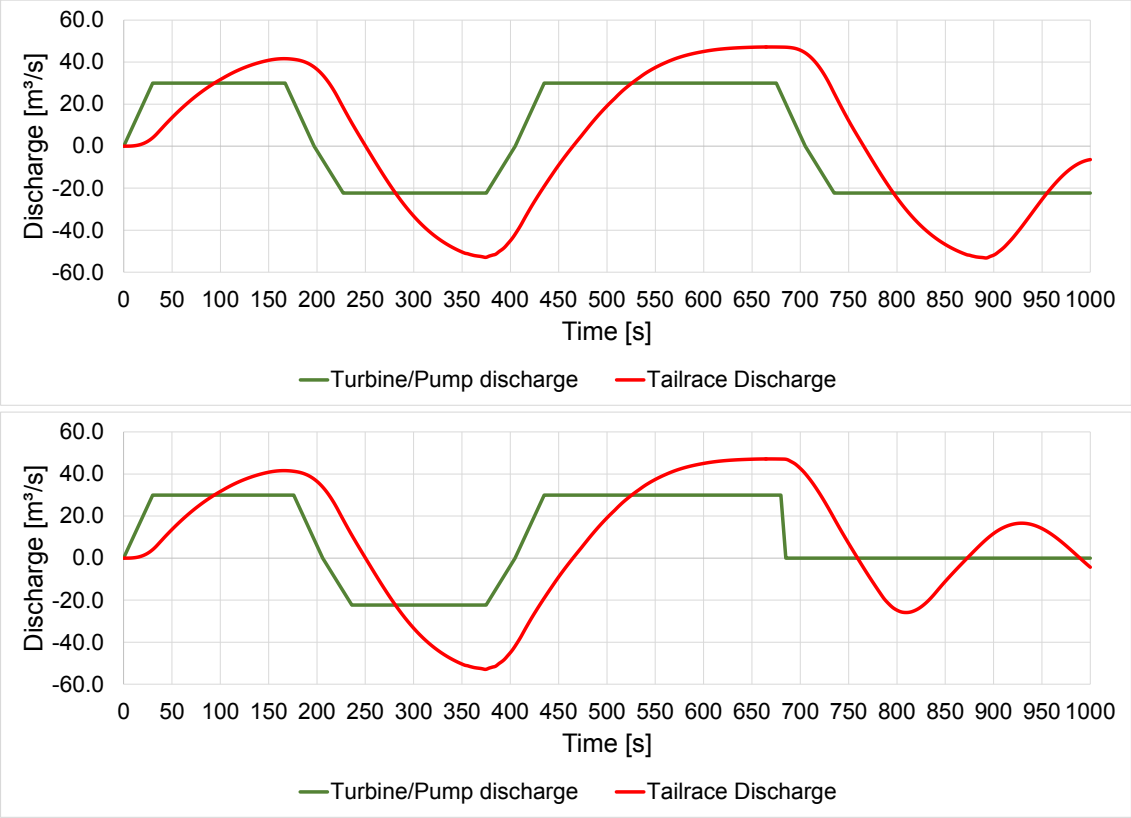

Figure 7.5: *Three chamber surge tank - 30 m³/s - Comparison of the tailrace discharge (load changes top, load shed bottom)*

Table 7.3: *Three chamber surge tank - 30 m³/s - Data comparison of the main loading cases*

Three chamber surge tank - Q = 30 m³/s						
Load case	Qmax	Qmin	Amp+	Amp-	Head min	Head max
	[m³/s]	[m³/s]	[-]	[-]	[m.a.s.l.]	[m.a.s.l.]
Load changes	47.18	-53.21	1.57	2.39	171.34	249.95
Load shed	47.18	-52.92	1.57	2.37	172.37	249.95

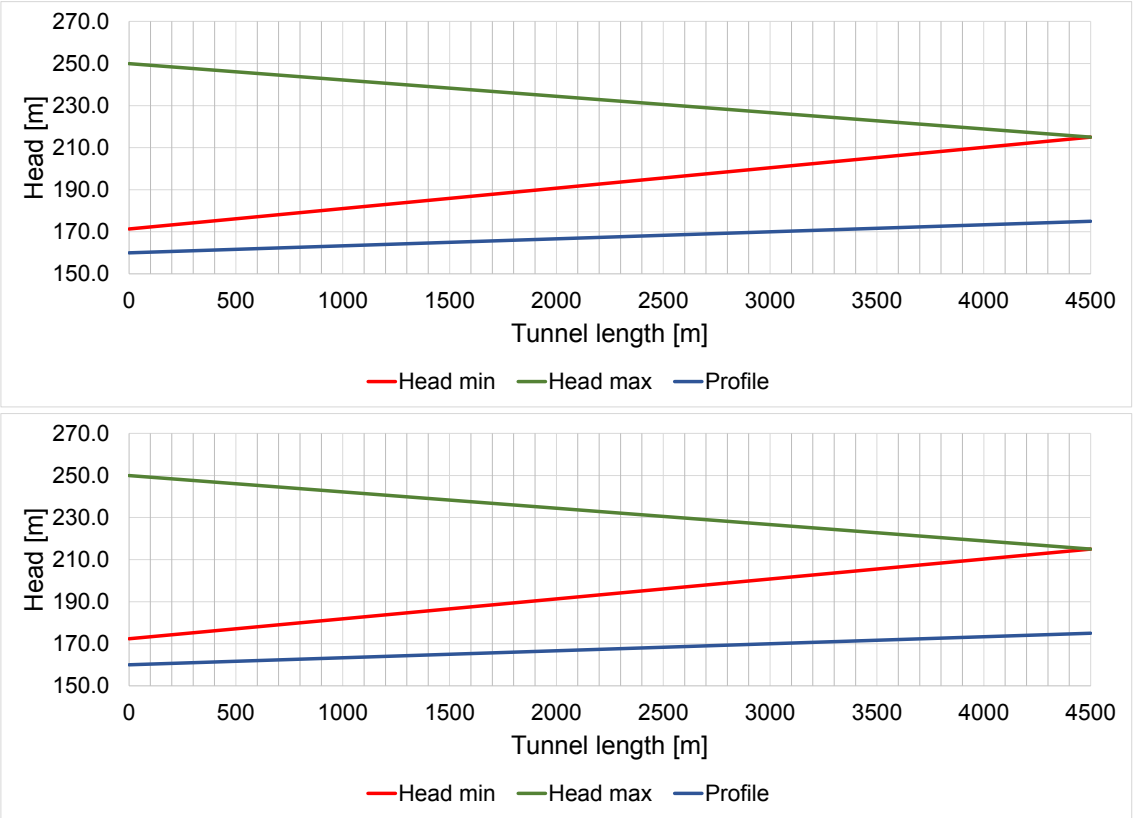

Figure 7.6: *Three chamber surge tank - 30 m³/s - Comparison of the tailrace head (load changes top, load shed bottom)*

Table 7.4: *Three chamber surge tank - 30 m³/s - Surge tank construction parts and their sizes*

Three chamber surge tank - 30 m³/s - Surge tank size	
Construction part	Excavation size
	[m³]
Tunnel chamber	2827
Pump chamber	4162
Riser duct	1005
Upper chamber	2151
Sum	10846

Turbine design flow rate Q = 40 m³/s

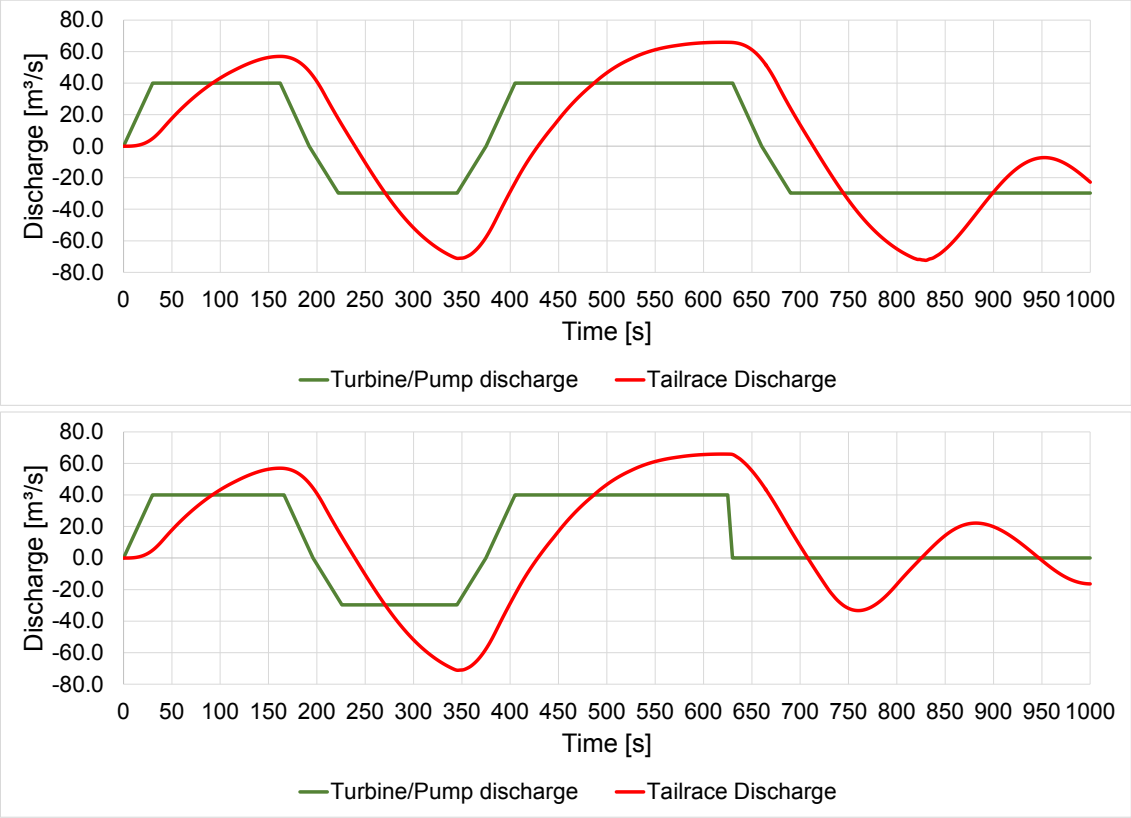

Figure 7.7: *Three chamber surge tank - 40 m³/s - Comparison of the tailrace discharge (load changes top, load shed bottom)*

Table 7.5: *Three chamber surge tank - 40 m³/s - Data comparison of the main loading cases*

Three chamber surge tank - Q = 40 m³/s						
Load case	Qmax	Qmin	Amp+	Amp-	Head min	Head max
	[m³/s]	[m³/s]	[-]	[-]	[m.a.s.l.]	[m.a.s.l.]
Load changes	65.93	-72.42	1.65	2.44	174.14	257.79
Load shed	65.93	-71.18	1.65	2.40	174.14	257.79

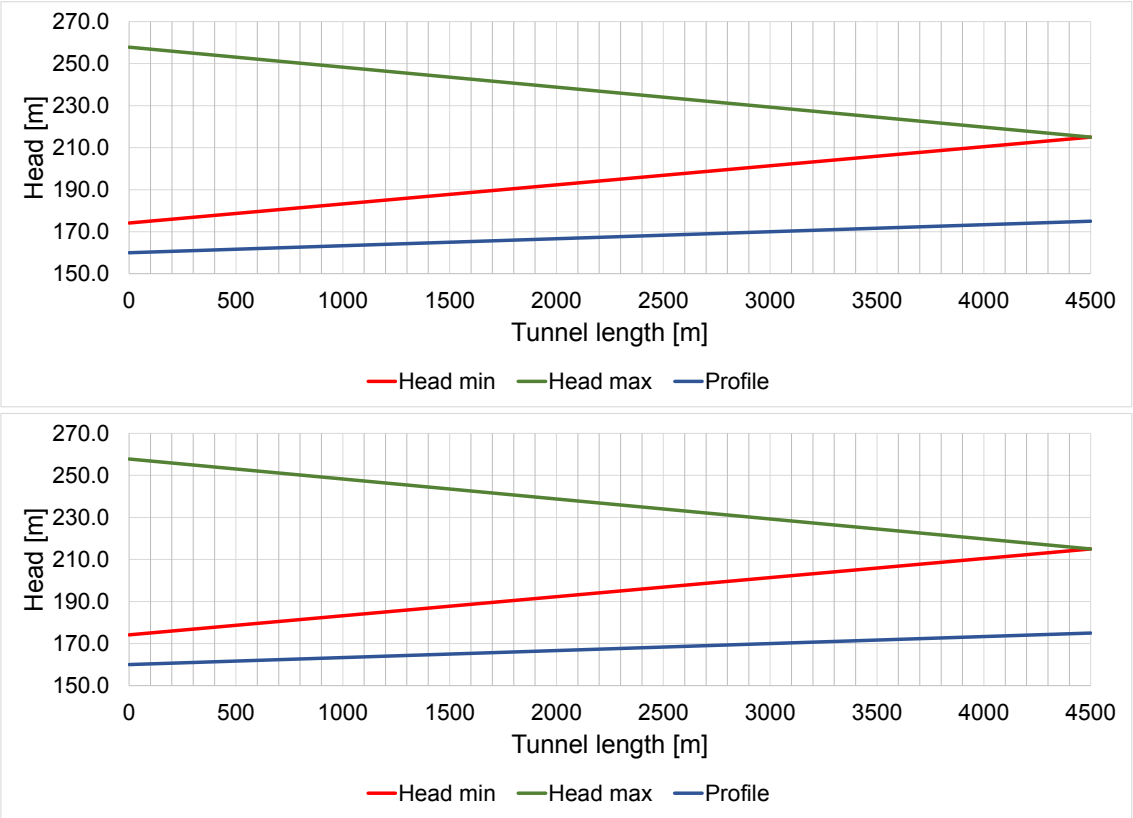

Figure 7.8: *Three chamber surge tank - 40 m³/s - Comparison of the tailrace head (load changes top, load shed bottom)*

Table 7.6: *Three chamber surge tank - 40 m³/s - Surge tank construction parts and their sizes*

Three chamber surge tank - 40 m³/s - Surge tank size	
Construction part	Excavation size
	[m³]
Tunnel chamber	2827
Pump chamber	6503
Riser duct	1901
Upper chamber	3958
Sum	15190

Turbine design flow rate Q = 50 m³/s

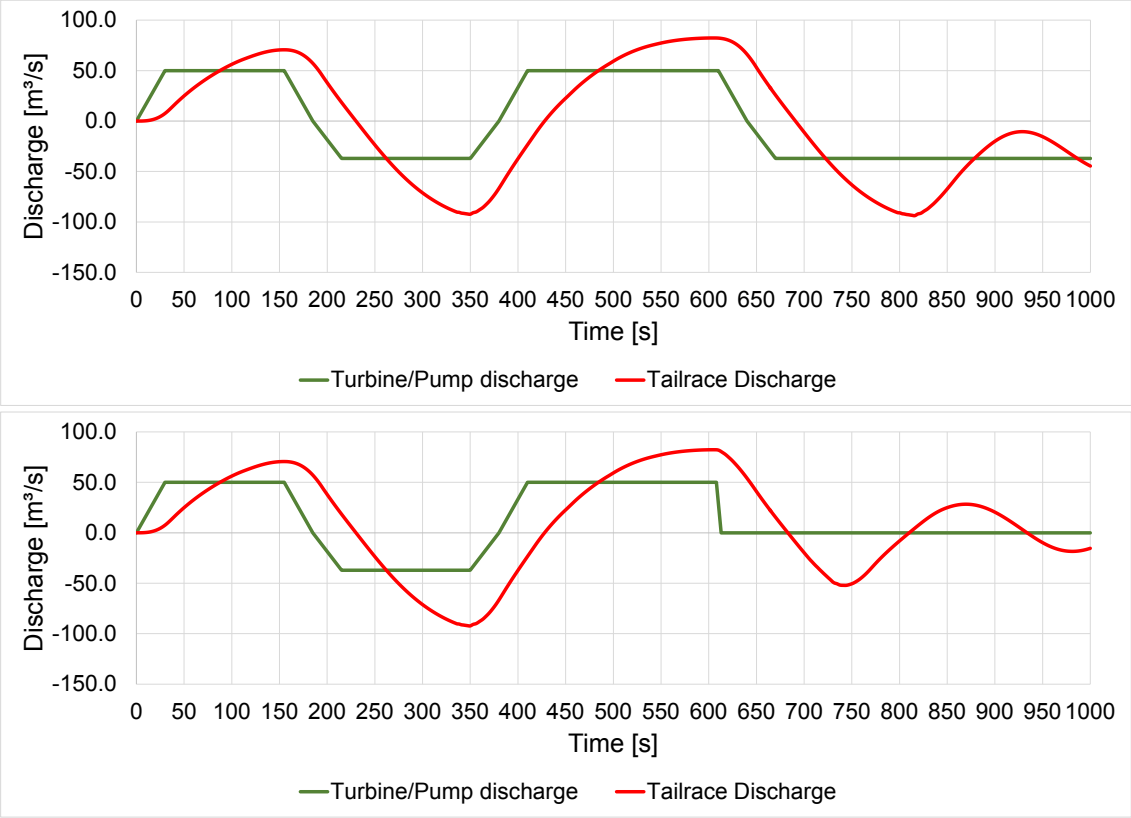

Figure 7.9: *Three chamber surge tank - 50 m³/s - Comparison of the tailrace discharge (load changes top, load shed bottom)*

Table 7.7: *Three chamber surge tank - 50 m³/s - Data comparison of the main loading cases*

Three chamber surge tank - Q = 50 m³/s						
Load case	Qmax	Qmin	Amp+	Amp-	Head min	Head max
	[m³/s]	[m³/s]	[-]	[-]	[m.a.s.l.]	[m.a.s.l.]
Load changes	82.30	-93.75	1.65	2.53	174.46	259.68
Load shed	82.30	-92.35	1.65	2.49	174.49	259.68

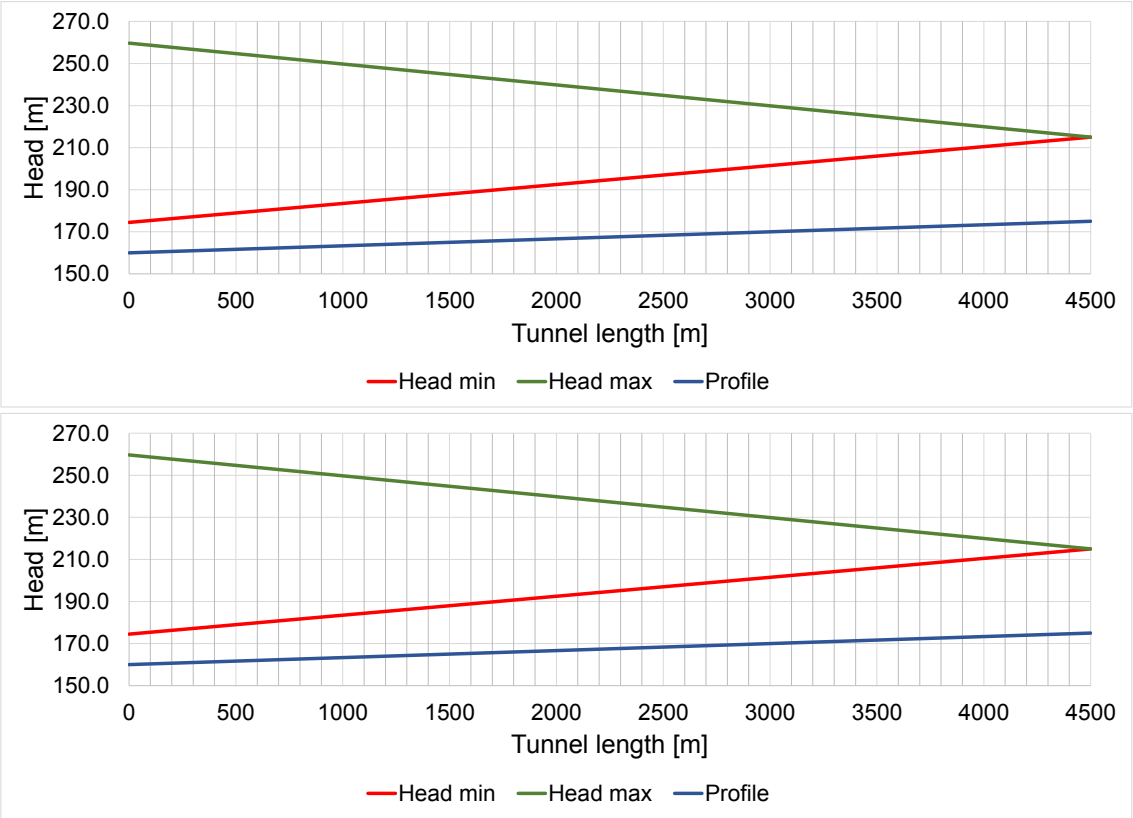

Figure 7.10: *Three chamber surge tank - 50 m³/s - Comparison of the tailrace head (load changes top, load shed bottom)*

Table 7.8: *Three chamber surge tank - 50 m³/s - Surge tank construction parts and their sizes*

Three chamber surge tank - 50 m³/s - Surge tank size	
Construction part	Excavation size
	[m³]
Tunnel chamber	2827
Pump chamber	7170
Riser duct	1901
Upper chamber	4524
Sum	16422

Turbine design flow rate Q = 60 m³/s

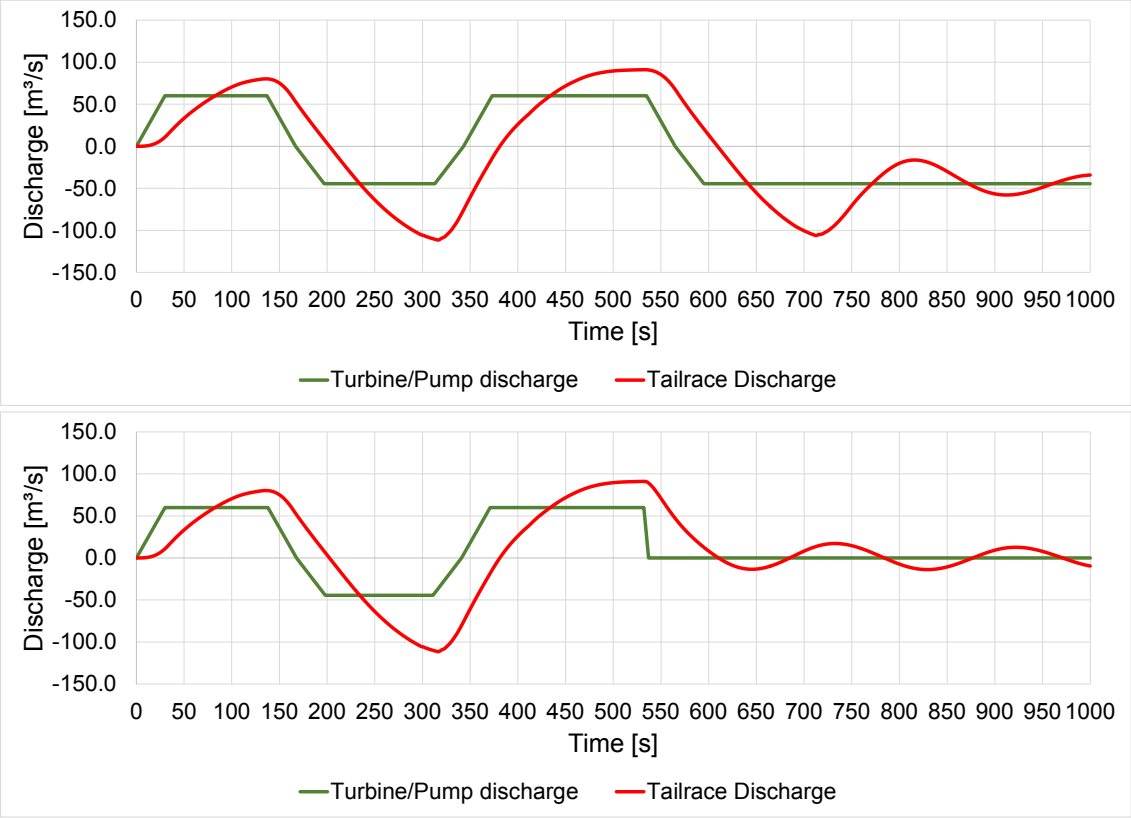

Figure 7.11: *Three chamber surge tank - 60 m³/s - Comparison of the tailrace discharge (load changes top, load shed bottom)*

Table 7.9: *Three chamber surge tank - 60 m³/s - Data comparison of the main loading cases*

Three chamber surge tank - Q = 60 m³/s						
Load case	Qmax	Qmin	Amp+	Amp-	Head min	Head max
	[m³/s]	[m³/s]	[-]	[-]	[m.a.s.l.]	[m.a.s.l.]
Load changes	91.04	-111.43	1.52	2.50	174.86	267.62
Load shed	91.05	-111.43	1.52	2.50	174.86	267.62

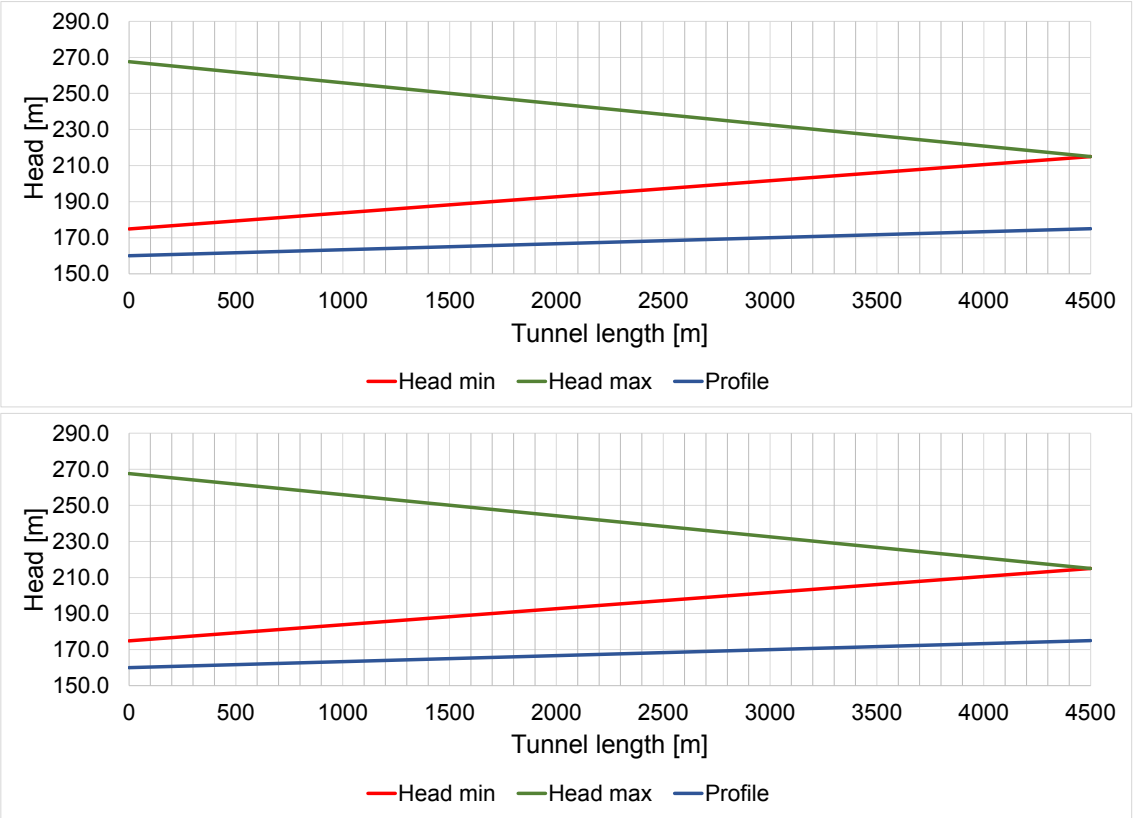

Figure 7.12: *Three chamber surge tank - 60 m³/s - Comparison of the tailrace head (load changes top, load shed bottom)*

Table 7.10: *Three chamber surge tank - 60 m³/s - Surge tank construction parts and their sizes*

Three chamber surge tank - 60 m³/s - Surge tank size	
Construction part	Excavation size
	[m³]
Tunnel chamber	2827
Pump chamber	8109
Riser duct	2138
Upper chamber	5089
Sum	18164

Turbine design flow rate Q = 70 m³/s

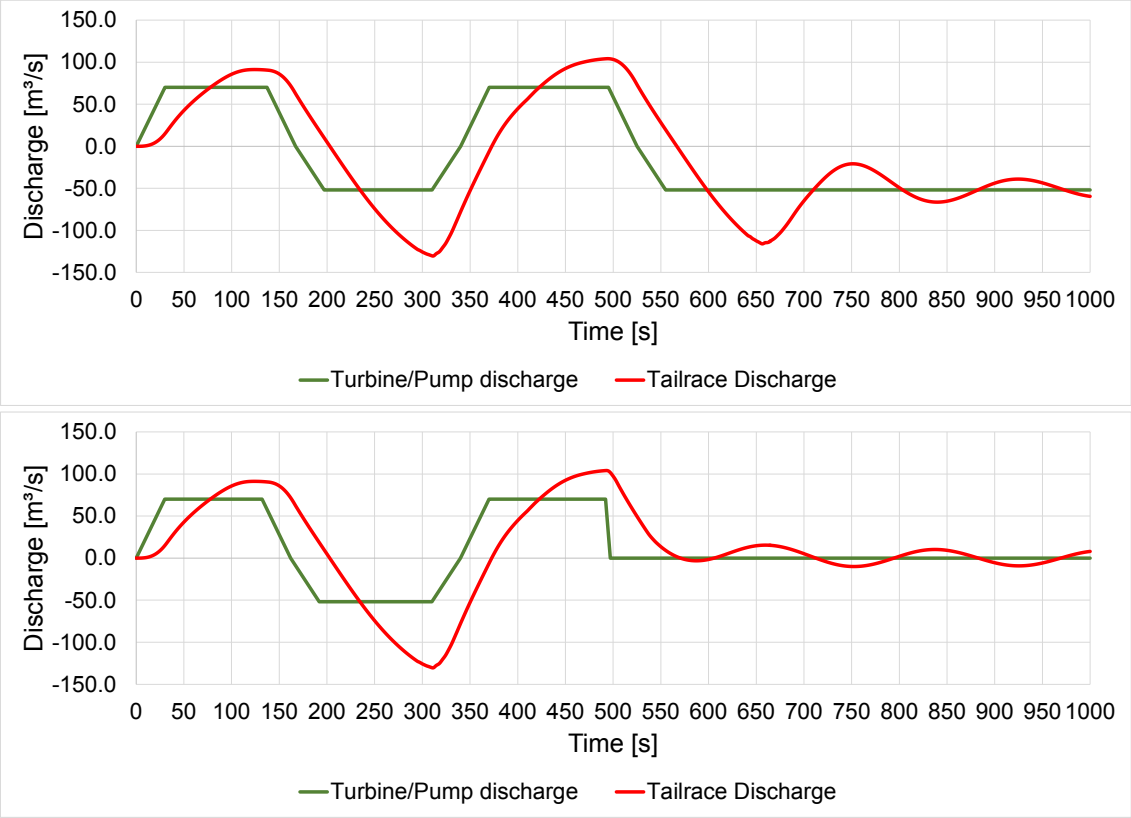

Figure 7.13: *Three chamber surge tank - 70 m³/s - Comparison of the tailrace discharge (load changes top, load shed bottom)*

Table 7.11: *Three chamber surge tank - 70 m³/s - Data comparison of the main loading cases*

Three chamber surge tank - Q = 70 m³/s						
Load case	Qmax	Qmin	Amp+	Amp-	Head min	Head max
	[m³/s]	[m³/s]	[-]	[-]	[m.a.s.l.]	[m.a.s.l.]
Load changes	104.13	-130.45	1.49	2.51	175.27	268.44
Load shed	104.07	-130.45	1.49	2.51	175.27	268.44

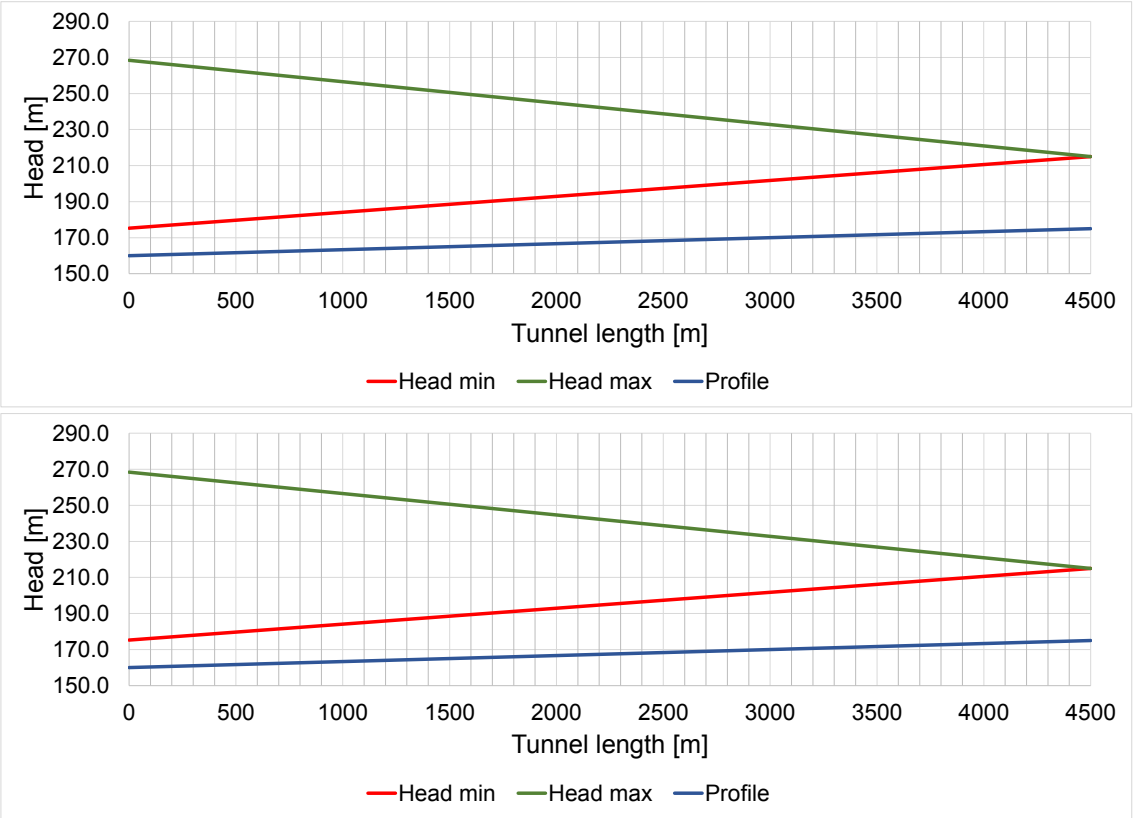

Figure 7.14: *Three chamber surge tank - 70 m³/s - Comparison of the tailrace head (load changes top, load shed bottom)*

Table 7.12: *Three chamber surge tank - 70 m³/s - Surge tank construction parts and their sizes*

Three chamber surge tank - 70 m³/s - Surge tank size	
Construction part	Excavation size
	[m³]
Tunnel chamber	2827
Pump chamber	9621
Riser duct	2138
Upper chamber	5655
Sum	20242

Turbine design flow rate Q = 80 m³/s

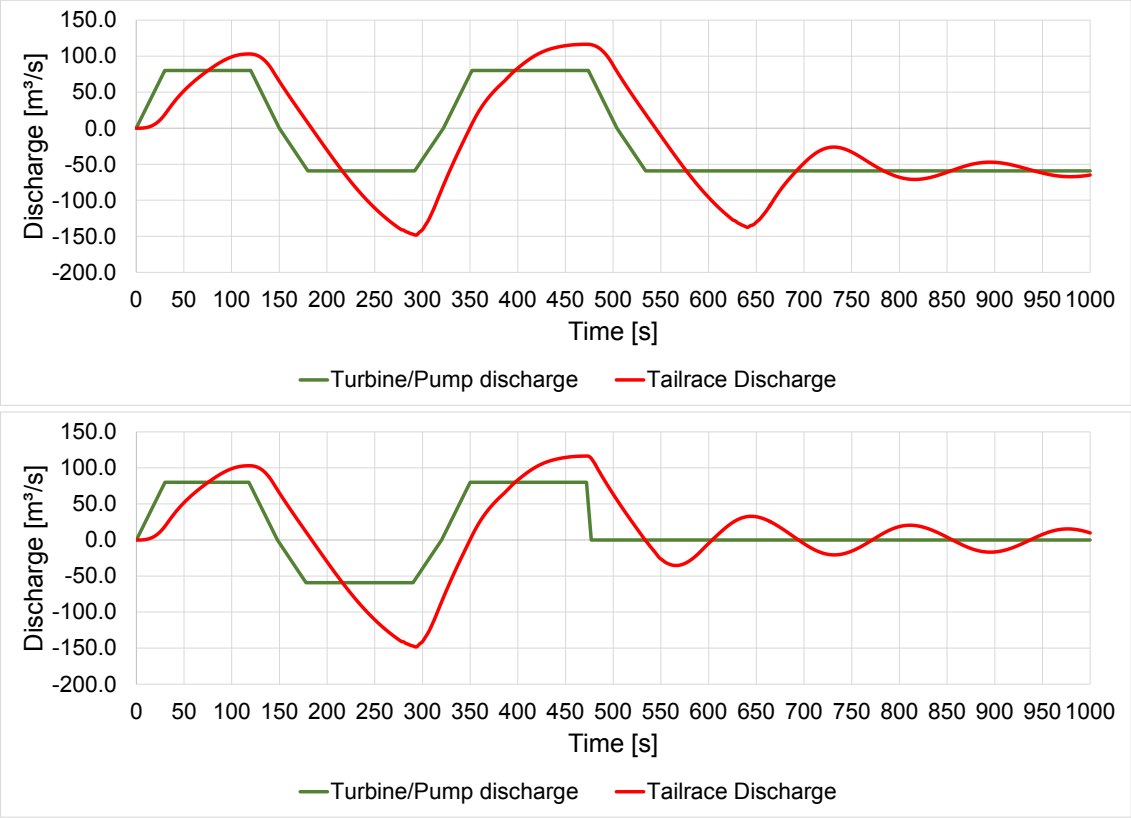

Figure 7.15: *Three chamber surge tank - 80 m³/s - Comparison of the tailrace discharge (load changes top, load shed bottom)*

Table 7.13: *Three chamber surge tank - 80 m³/s - Data comparison of the main loading cases*

Three chamber surge tank - Q = 80 m³/s						
Load case	Qmax	Qmin	Amp+	Amp-	Head min	Head max
	[m³/s]	[m³/s]	[-]	[-]	[m.a.s.l.]	[m.a.s.l.]
Load changes	116.47	-148.36	1.46	2.50	174.57	274.50
Load shed	116.47	-148.36	1.46	2.50	173.30	274.50

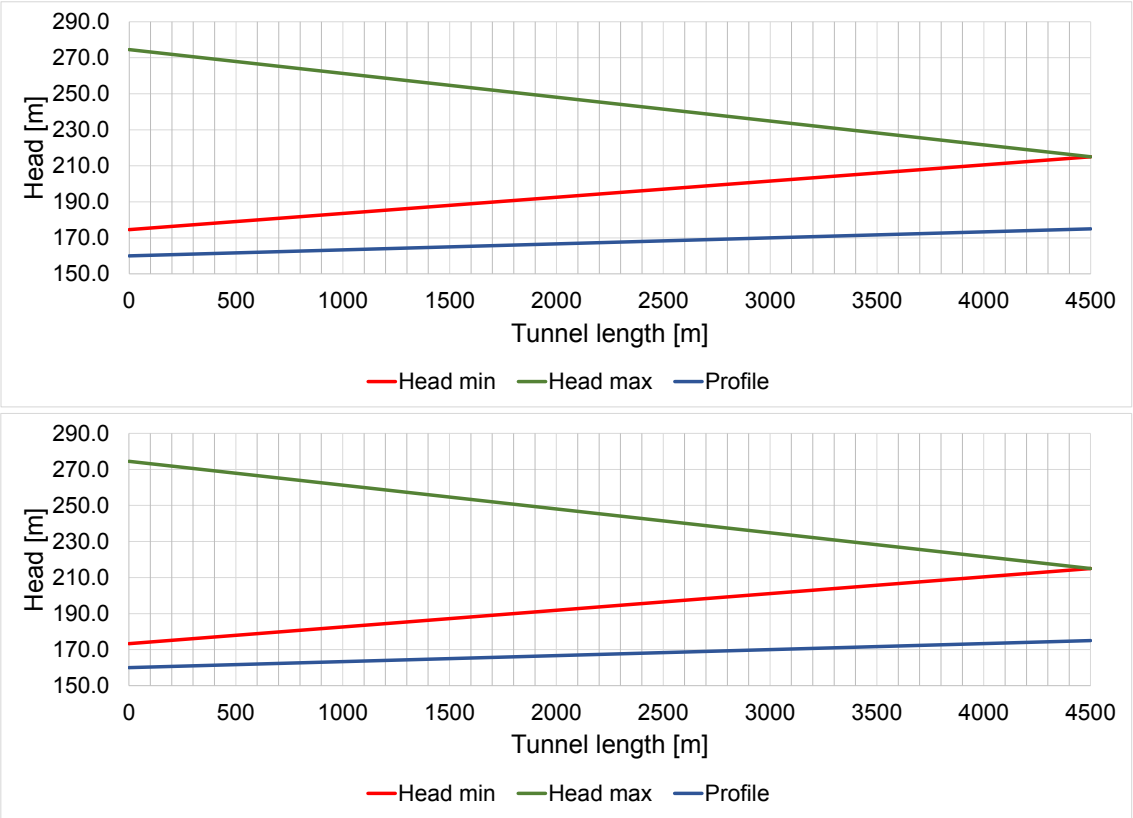

Figure 7.16: *Three chamber surge tank - 80 m³/s - Comparison of the tailrace head (load changes top, load shed bottom)*

Table 7.14: *Three chamber surge tank - 80 m³/s - Surge tank construction parts and their sizes*

Three chamber surge tank - 80 m³/s - Surge tank size	
Construction part	Excavation size
	[m³]
Tunnel chamber	2827
Pump chamber	10464
Riser duct	2138
Upper chamber	5655
Sum	21084

Turbine design flow rate Q = 90 m³/s

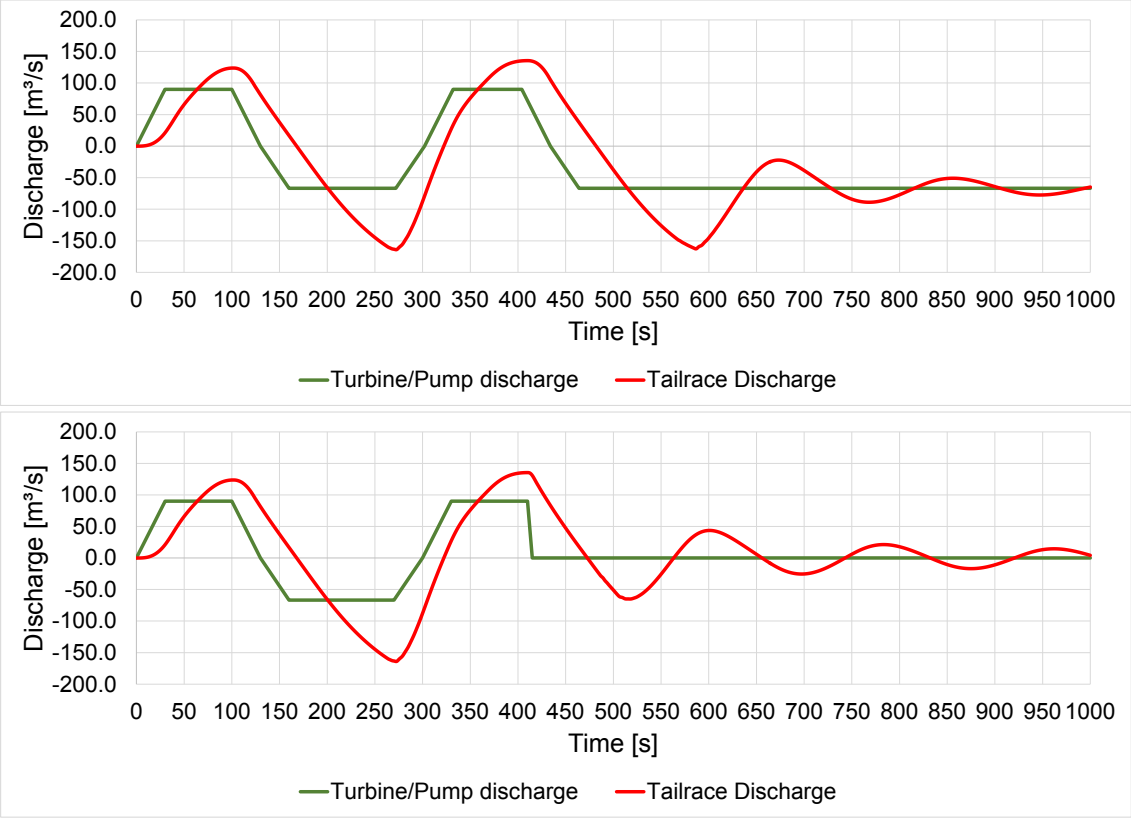

Figure 7.17: *Three chamber surge tank - 90 m³/s - Comparison of the tailrace discharge (load changes top, load shed bottom)*

Table 7.15: *Three chamber surge tank - 90 m³/s - Data comparison of the main loading cases*

Three chamber surge tank - Q = 90 m³/s						
Load case	Qmax	Qmin	Amp+	Amp-	Head min	Head max
	[m³/s]	[m³/s]	[-]	[-]	[m.a.s.l.]	[m.a.s.l.]
Load changes	135.45	-164.07	1.50	2.46	175.15	288.50
Load shed	135.44	-164.07	1.50	2.46	175.42	288.50

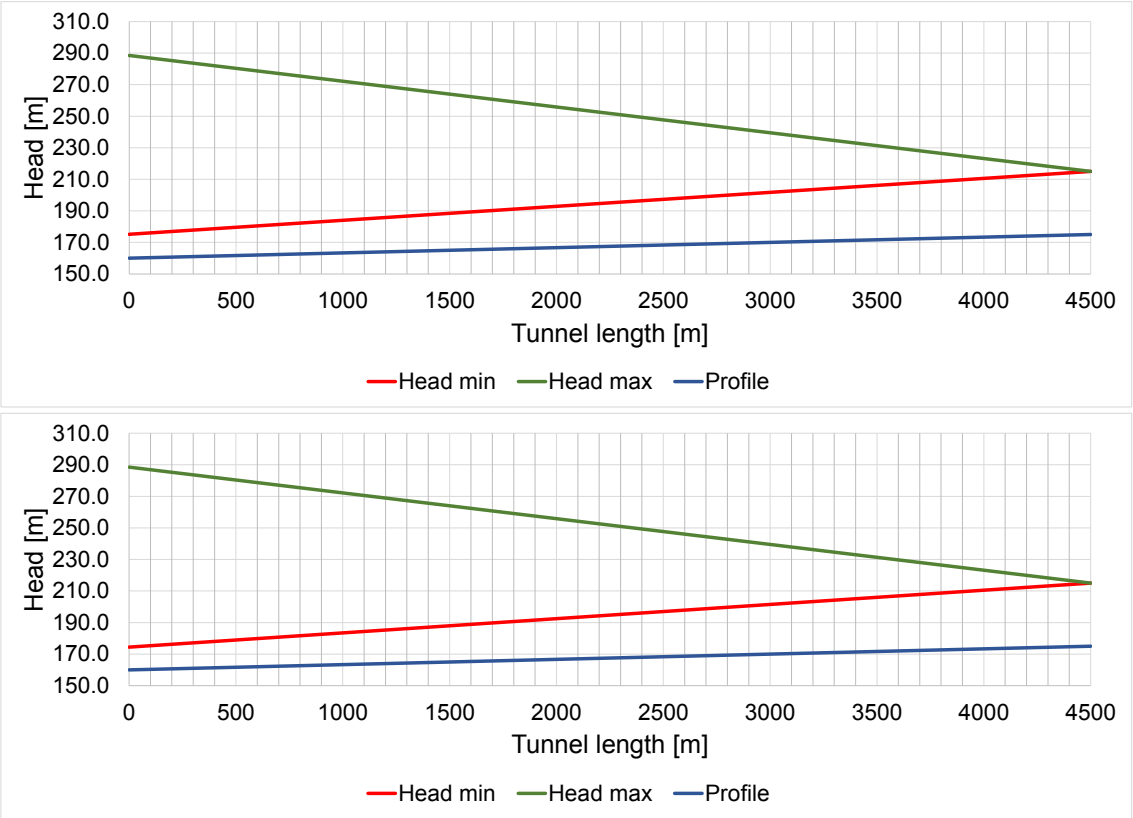

Figure 7.18: *Three chamber surge tank - 90 m³/s - Comparison of the tailrace head (load changes top, load shed bottom)*

Table 7.16: *Three chamber surge tank - 90 m³/s - Surge tank construction parts and their sizes*

Three chamber surge tank - 90 m³/s - Surge tank size	
Construction part	Excavation size
	[m³]
Tunnel chamber	2827
Pump chamber	11642
Riser duct	2987
Upper chamber	5090
Sum	22545

Turbine design flow rate Q = 100 m³/s

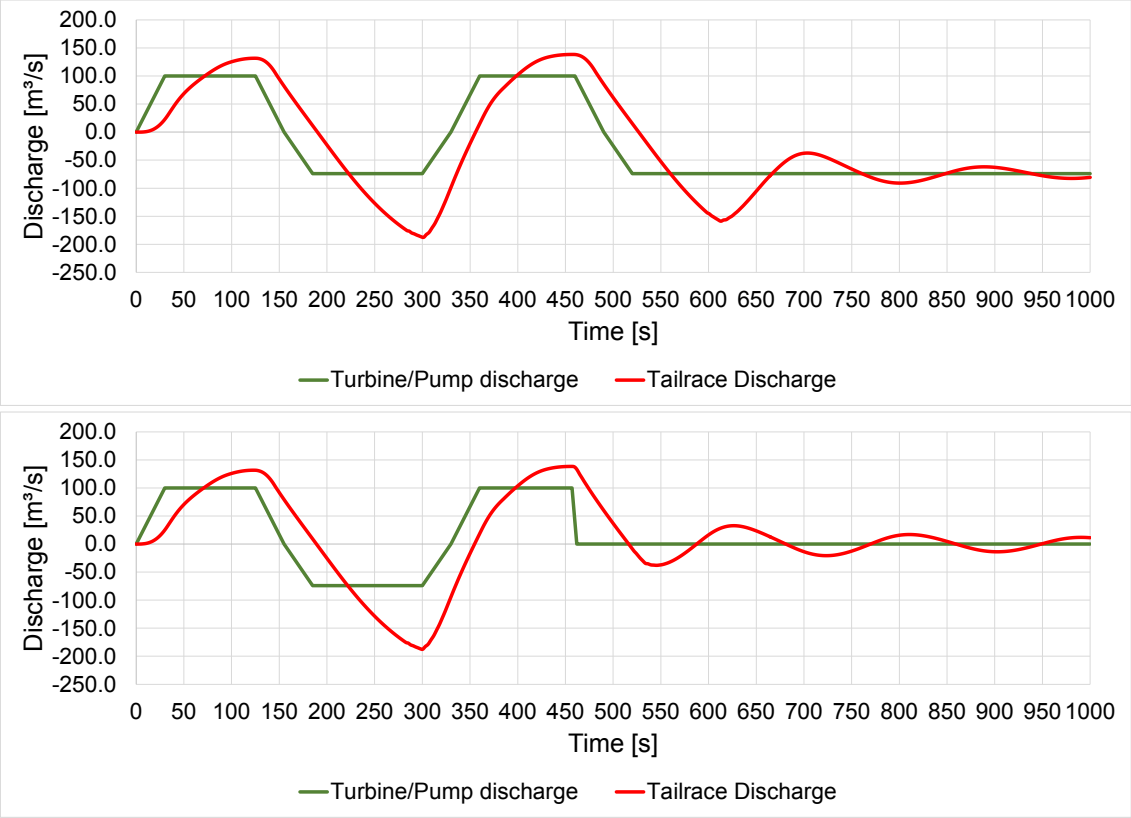

Figure 7.19: *Three chamber surge tank - 100 m³/s - Comparison of the tailrace discharge (load changes top, load shed bottom)*

Table 7.17: *Three chamber surge tank - 100 m³/s - Data comparison of the main loading cases*

Three chamber surge tank - Q = 100 m³/s						
Load case	Qmax	Qmin	Amp+	Amp-	Head min	Head max
	[m³/s]	[m³/s]	[-]	[-]	[m.a.s.l.]	[m.a.s.l.]
Load changes	138.41	-187.69	1.38	2.53	175.48	280.72
Load shed	138.41	-187.69	1.38	2.53	172.92	280.72

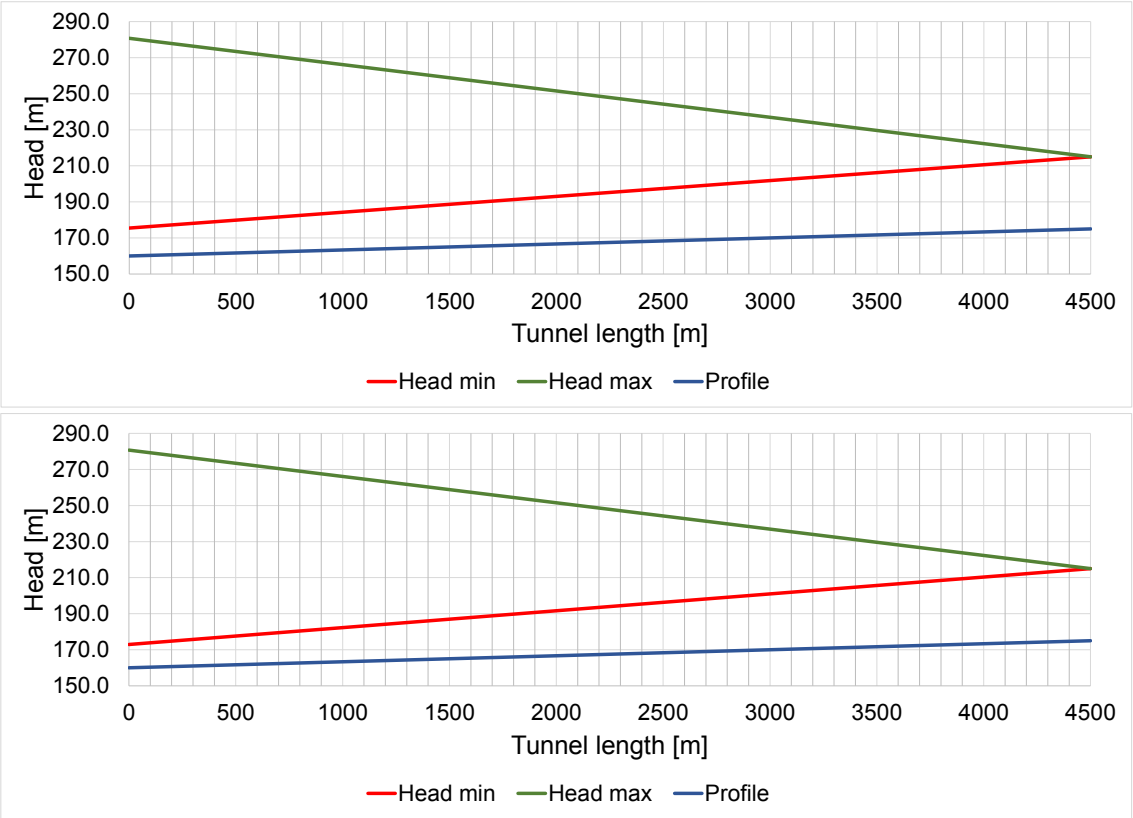

Figure 7.20: *Three chamber surge tank - 100 m³/s - Comparison of the tailrace head (load changes top, load shed bottom)*

Table 7.18: *Three chamber surge tank - 100 m³/s - Surge tank construction parts and their sizes*

Three chamber surge tank - 100 m³/s - Surge tank size	
Construction part	Excavation size
	[m³]
Tunnel chamber	2827
Pump chamber	12566
Riser duct	3079
Upper chamber	5773
Sum	24245

7.2.3 The tunnel chamber

In order to show the influence of the tunnel chamber on the hydraulic behaviour of the system at different design flow rates, a constant value has been chosen for the tunnel chamber size. The size has been chosen to appear big for a design flow of 20 m³/s and small for 100 m³/s.
With a rising gap between the diameters of tunnel chamber and tailrace, it can be observed that oscillation gets stretched out. This means that higher flow rates occur fro a longer time but are less strong, which leads to the conclusion that this effect reduces the consequences on the Danube.

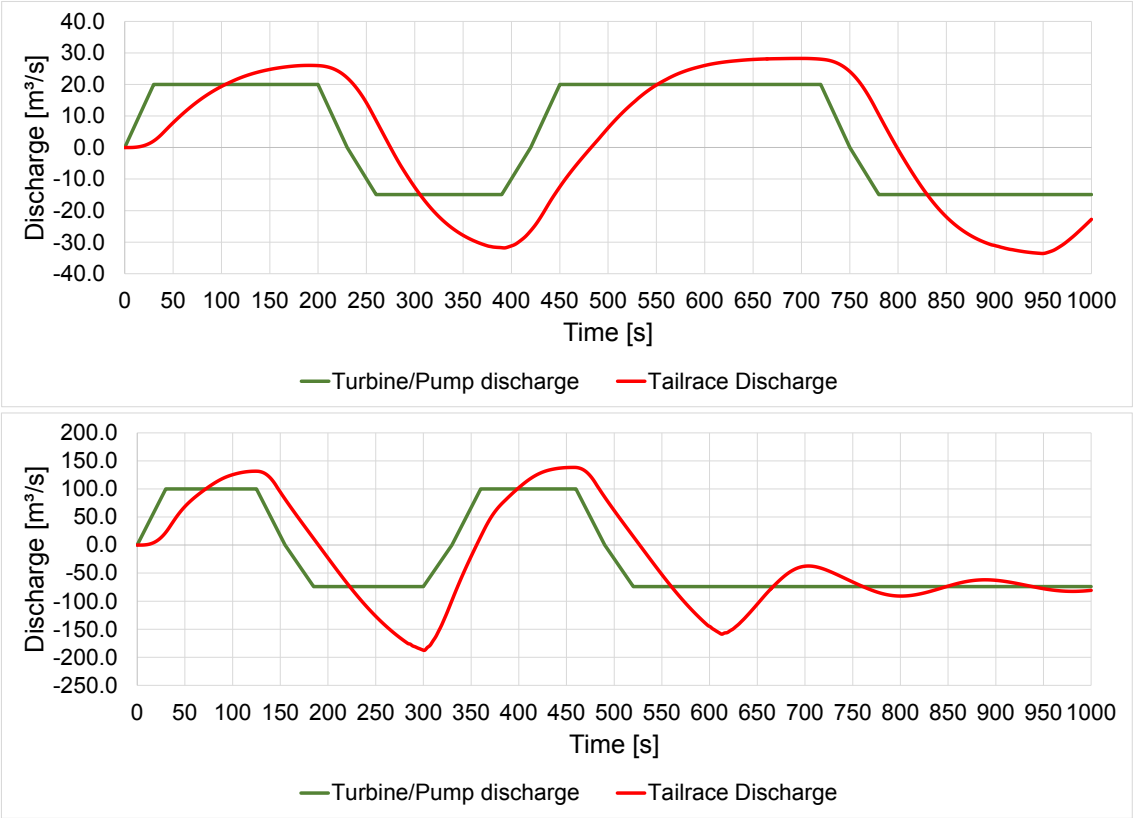

Figure 7.21: *Effect of the tunnel chamber shown by comparison of a 20 m³/s (top) and 100 m³/s (bottom) flow rate*

7.2.4 The pump chamber

The pump chamber has to secure the required head for cavitation free operation of the pump. Therefore a rather big sizing is necessary to compensate for a part of the mass oscillation within the hydraulic system. The basic principle of this surge tank design is the separation of water columns. This means the pump chamber has to contain enough water to bypass the separation time of the water column. Therefore this is the decisive factor for the sizing of this chamber.
Figure 7.22 shows an example of the head development during the simulation (100 m³/s)

within the pump chamber. Once the head drops below the edge level, a fully hydraulic separation has take place.

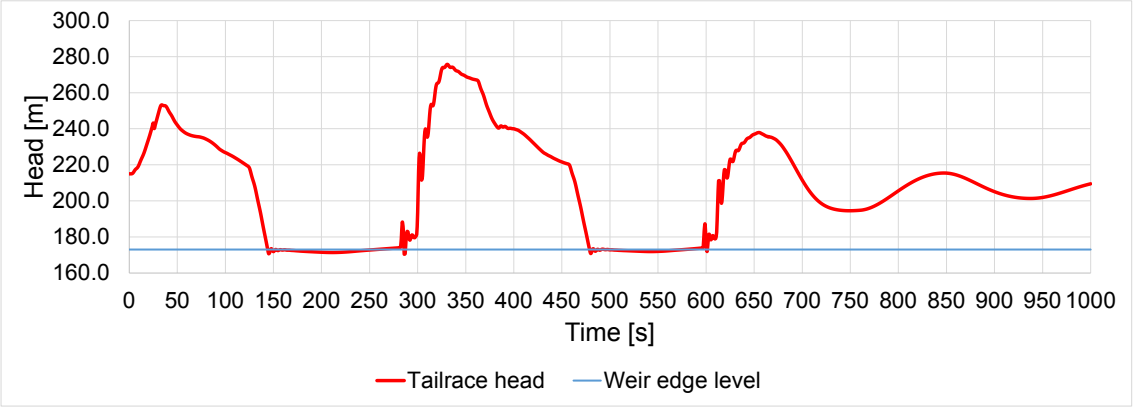

Figure 7.22: *Head within the pump chamber*

7.2.5 The overflow sill

The overflow sill ensures water column separation. The hydraulic shape is of great importance to minimize energy losses and the height of the sill.
Water column separation totally disconnects the pump chamber from the oscillation between surge tank and reservoir. This means the pump can be operated with a more constant head and therefore does not need to be regulated that much. Furthermore the risk of cavitation is lowered by this hydraulic isolation. [12]

7.2.6 Load cases

The load cases for the three chamber surge tank are still the same as described in chapter 5.
The decisive load case for this model is the multiple load change according to figure 7.23. The load shedding showed slightly lower amplification values of the inflow behaviour at lower design flow rates. When flow rates are higher than 50 m³/s the two values start to converge. Surge tank size is also defined by this load case. Outflow amplification stayed the same during both load cases.

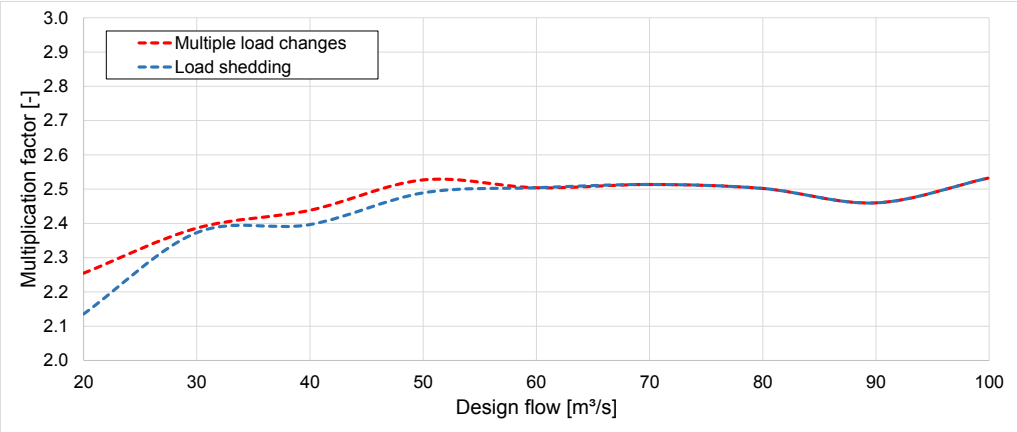

Figure 7.23: *Load case comparison - Inflow amplification*

8 Comparison

In this chapter the two surge tank schemes are compared according to economical, ecological and operational parameters.
By the end of this comparison the data should lead to a conclusion and show which one of the schemes would be the logical choice.

8.1 Surge tank size

A comparison of surge tank size has economical reasons. A bigger excavation size expands construction time and therefore building costs rise.

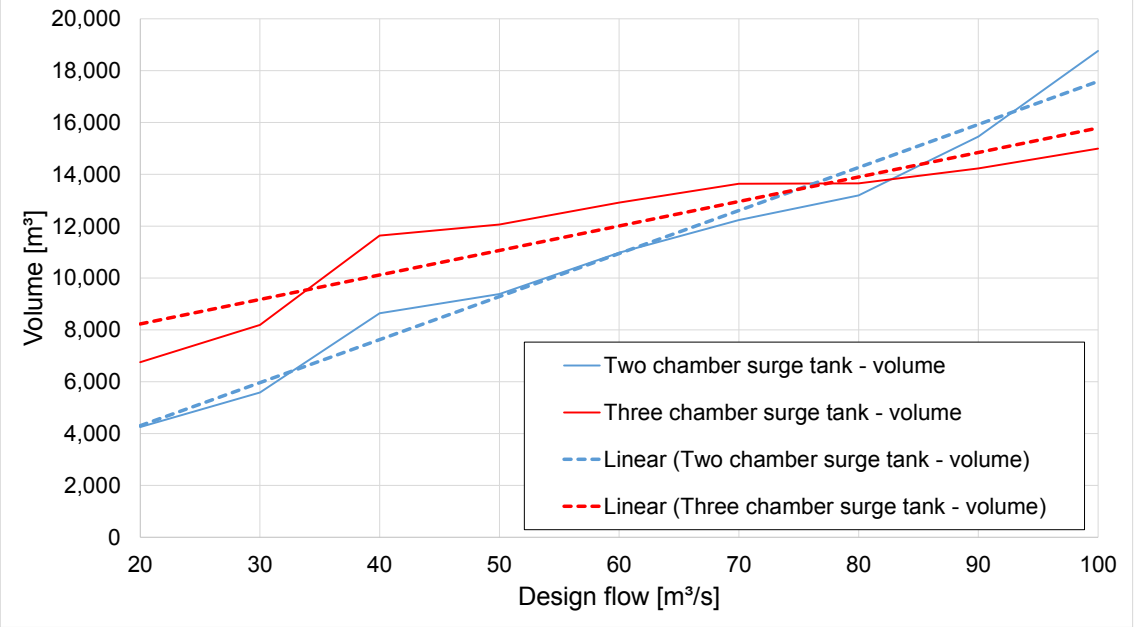

Figure 8.1: *Comparison of the surge tank size*

As can be seen in graph 8.1 the approximation lines intersect between the design flow rates of 70 and 80 m³/s.
The two chamber surge tank shows an increased slope on higher design flow rates (80+ m³/s). This means that this surge tank type would fit a power plant scheme with lower design flow rates quite well, but loses in effectiveness on higher discharge values. The according values are shown in table 8.1.
With regard to surge tank size a three chamber surge tank design is preferable on higher flow rates given the same initial conditions.

Table 8.1: *Surge tank volume comparison of both schemes*

		Two chamber surge tank	**Three chamber surge tank**
Turbine [m³/s]	Pump [m³/s]	Surge tank volume [m³]	Surge tank volume [m³]
20	14.9	4253	6752
30	22.3	5586	8192
40	29.7	8644	11641
50	37.1	9386	12065
60	44.5	10983	12916
70	51.9	12237	13642
80	59.3	13187	13651
90	66.7	15463	14229
100	74.1	18765	14998

8.2 Inflow- and Outflow amplification

Inflow- and outflow amplifications are straight indicators for the effect on the natural behaviour of the lower reservoir. Not only is the ecosystem of the river affected, shipping can also be influenced by strong side drifts. Anyhow, the negative effect of this problem can be reduced by optimizing the outlet structure according to positioning and hydraulic design.

Graph 8.3 shows the inflow/outflow amplification of the power plant. The standard value would be the design flow, but due to mass oscillation higher flow rates occur. Table 8.2 shows the according data as total discharge values.
The optimum would be a low constant value for inflow and outflow. But since the surge tank is throttled asymmetrically this is not possible. With an additional on-site preflooder between outlet structure and the river Danube it would be possible to neglect the negative effects on nature but on the other hand further construction costs would rise.
In order to ensure a suitable discharge velocity the outlet structure has to be 3-D modelled and numerically analysed.

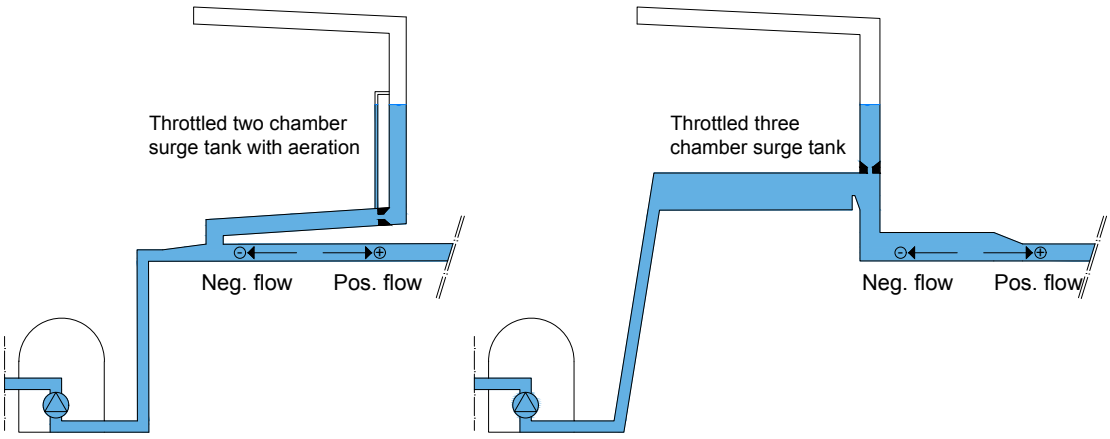

Figure 8.2: *Definition of the flow directions for both hydraulic systems*

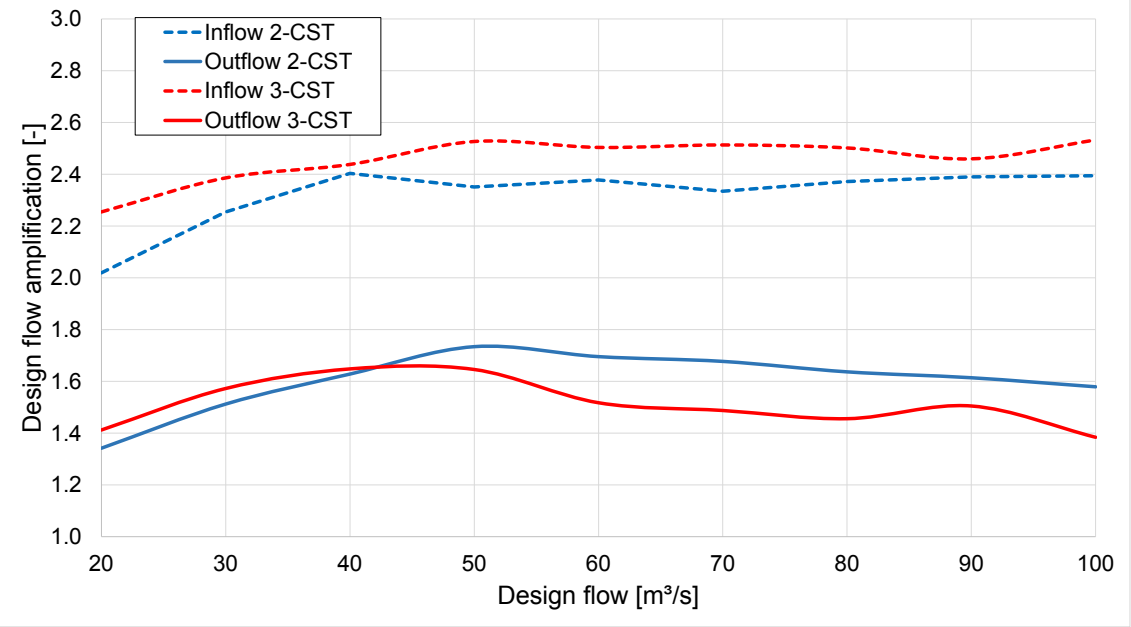

Figure 8.3: *Comparison of the inflow and outflow amplification*

Table 8.2: *Inflow- and Outflow data comparison of the tailrace*

		Two chamber surge tank		**Three chamber surge tank**	
Turbine [m³/s]	Pump [m³/s]	Max. discharge [m³/s]	Min. discharge [m³/s]	Max. discharge [m³/s]	Min. discharge [m³/s]
20	14.9	26.84	-30.09	28.24	-33.60
30	22.3	45.38	-50.27	47.18	-53.21
40	29.7	65.13	-71.40	65.93	-72.42
50	37.1	86.78	-89.42	82.30	-93.75
60	44.5	102.43	-108.53	91.05	-111.43
70	51.9	117.36	-118.84	104.13	-130.45
80	59.3	131.00	-140.62	116.47	-148.36
90	66.7	145.73	-161.00	135.45	-164.07
100	74.1	157.01	-175.60	138.41	-187.69

8.3 Mass oscillation

Not only the minimum and maximum values should be taken into account. The whole system behaviour offers significant information too. The mass oscillation of both surge tank schemes with a design flow rate of 100 m³/s is illustrated in graph 8.4.
The main difference between these two graphs are to be seen in reaction time and in discharge amplification. While the two chamber surge tank aims to have equal in- and outflow values, the three chamber surge tank shows a larger shift between these two. Apart from that both schemes look quite similar, but the most important finding is that neither of these two simulations takes up a natural frequency during mass oscillation.

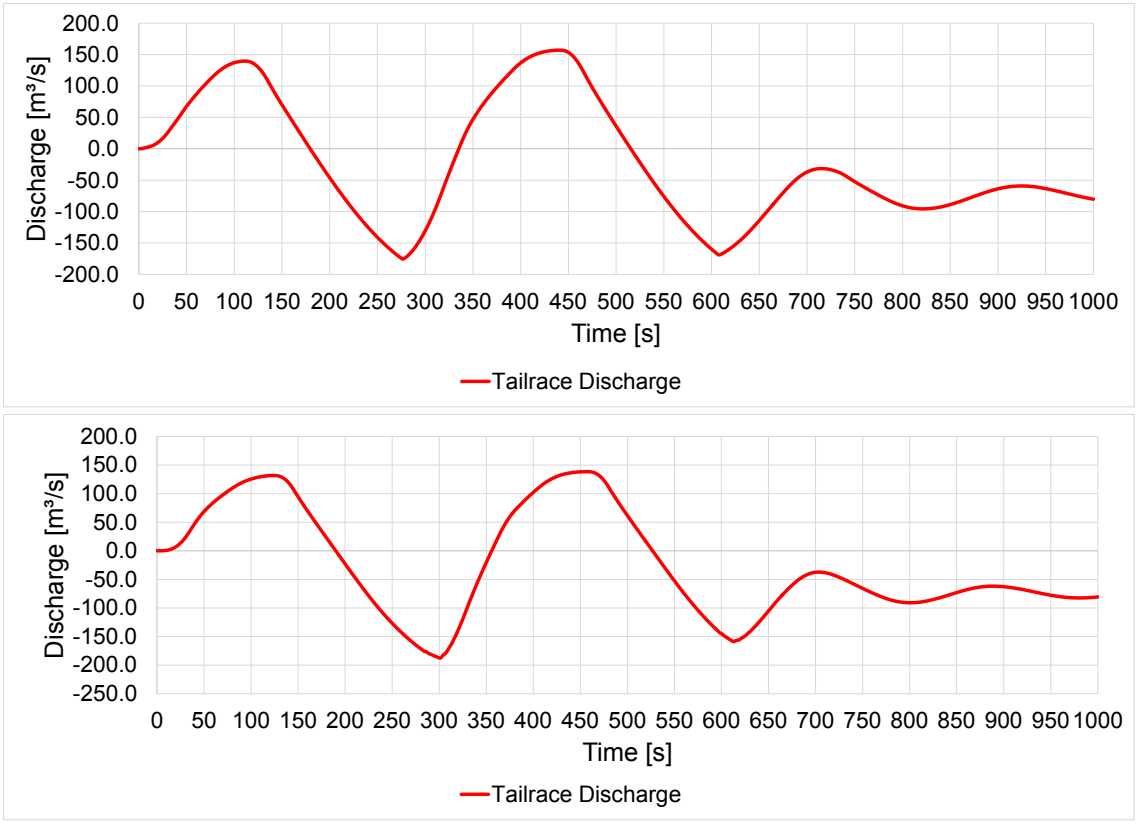

Figure 8.4: *Comparison of the mass oscillation within the hydraulic systems (2-CST top, 3-CST bottom)*

8.4 Conclusion and outlook

Overall it can be said that the two chamber scheme is a more efficient solution at lower flow rates. Having said this, it should be the aim of a pumped storage power plant at a river like the Danube with an approximate flow of 6,500 m³/s to reach the highest possible power generation and storage capacity. Therefore I would recommend to construct a three chamber surge tank scheme with a minimum design flow of 100 m³/s.
Once a design flow is defined, the basic model can be used as a good basis for further optimization of the hydraulic system.
Due to the fact that all surge tank designs have similar geometrical conditions it was possible to do a proper comparison in the first place. For exact performance and optimized design further investigations into chamber positioning, pump/turbine modelling and in general a more detailed model are definitely recommended and necessary.

Bibliography

[1] E-Control Austria. Bestandsstatistik des kraftwerkparks in Österreich zum 31. dezember 2015, Date of access: August, 2017. URL https://www.e-control.at.

[2] Environment Agency Austria, Date of access: June, 2017. URL http://www.umweltbundesamt.at/.

[3] G. Bollrich. *Technische Hydromechanik 1 - Grundlagen*. Beuth, 7. edition, 2013. ISBN 978-3-410-23481-4.

[4] Deltares. WANDA, Version 4.2 User manual, 2013.

[5] Deltares, Date of access: October, 2016. URL https://www.deltares.nl/en/.

[6] Google Earth. Map data: Image landsat / copernicus ©2017 google, Date of access: July, 2017. URL https://www.google.at/maps.

[7] EnArgus, Date of access: March, 2017. URL https://enargus.fit.fraunhofer.de/pub/bscw.cgi/d6312538-2/*/*/Drei-Block-Satz.html?op=Wiki.getwiki.

[8] OneGeology GBA, Date of access: June, 2017. URL http://portal.onegeology.org/OnegeologyGlobal/.

[9] J. Giesecke, S. Heimerl, and E. Mosonyi. *Wasserkraftanlagen - Planung, Bau und Betrieb*. Springer Vieweg, 6. edition, 2014. ISBN 978-3-642-53870-4.

[10] G. Heigerth. *Drossel- und Differential- Wasserschlösser von Regelkraftwerken mit freier Betriebsführung*. PhD thesis, Technische Hochschule, Wien, 1970.

[11] Hydroni, Date of access: March, 2017. URL http://www.hydroni.co.uk/images/Water_Turbine_Chart.png.

[12] M. Larcher. *The Three chamber Surge Tank - A New Way of Construction for the Tail Water Area of Pumped Storage Schemes*. PhD thesis, Technical University, Graz, 2010.

[13] E. Leknes. Comparison of the svee and thoma stability criteria for mass oscillations in surge tanks. Master's thesis, NTNU, 2016.

[14] Land Niederoesterreich. Map data: ©land niederoesterreich, noe atlas, Date of access: July, 2017. URL http://atlas.noe.gv.at.

[15] W. Richter. 3D-numerische Strömungssimulation von hydraulischen Rückstromdrosseln in Wasserschlössern, 2010.

[16] E. Saurer, T. Marcher, and M. John. Decisive design basis and parameters for power plant caverns. pages 1858–1864, 2013.

[17] G. Seeber. *Druckstollen und Druckschächte*. Enke, 1999.

[18] R. Svee. *Untersuchung über die Stabilität bei Wasserkraftanlagen mit idealer Regelung*, volume 15. Institute for Hydraulic Engineering and Water Resources Management, 1970.

List of Figures

Figure 1.1 Renewable and fossil fuel energy production in Austria (2015) [1] 1

Figure 1.2 Detailed energy production of Austria (2015) [1] 1

Figure 1.3 Daily time-variation curve of the electricity demand in Austria (Wednesday, 21st of June 2017) [1] 2

Figure 2.1 Overview of the Lower Austrian Danube - ortho-image [6] 5

Figure 2.2 Project area - ortho-image [6] 5

Figure 2.3 Geological data of the project area [8] 6

Figure 2.4 Nature protection areas within the project region [14] 7

Figure 3.1 System sketch of a power plant with Scandinavian design 9

Figure 3.2 Scaled image of the tailwater area 10

Figure 3.3 Diameter determination scheme 11

Figure 3.4 Basin- and Shaft surge tanks 13

Figure 3.5 Chamber surge tanks 14

Figure 3.6 Throttled surge tanks 15

Figure 3.7 Return-flow throttle pumped storage hydro-power Kaunertal . . . 16

Figure 3.8 Impact loss 16

Figure 3.9 Turbine application chart [11] 19

Figure 4.1 Critical flow over weir 26

Figure 4.2 Flush flow over weir 26

Figure 5.1 Pump and Tailrace discharge for a load change scenario 28

Figure 5.2 Pump and Tailrace discharge for a load shedding scenario 28

Figure 5.3 Scheme sections of a Francis turbine [9] 30

Figure 6.1 Trifurcation model 34

Figure 6.2 Differential effect of the upper surge chamber 36

Figure 6.3 Cross-section of the upper surge chamber at top end 36

Figure 6.4 Physical (top) and 1-D numerical model (bottom): Type 1 (turbine design flow = 100 m³/s) 37

Figure 6.5 Model type 1 - 20 m³/s - Comparison of the tailrace discharge (load changes top, load shed bottom) 38

Figure 6.6 Physical model for the tailrace 39

Figure 6.7 Model type 1 - 20 m³/s - Comparison of the tailrace head (load changes top, load shed bottom) 39

Figure 6.8 Model type 1 - 30 m³/s - Comparison of the tailrace discharge (load changes top, load shed bottom) 41

Figure 6.9 Model type 1 - 30 m³/s - Comparison of the tailrace head (load changes top, load shed bottom) 42

Figure 6.10 Model type 1 - 40 m³/s - Comparison of the tailrace discharge (load changes top, load shed bottom) 43

Figure 6.11 Model type 1 - 40 m³/s - Comparison of the tailrace head (load changes top, load shed bottom) 44

Figure 6.12 Model type 1 - 50 m³/s - Comparison of the tailrace discharge (load changes top, load shed bottom) 45

Figure 6.13 Model type 1 - 50 m³/s - Comparison of the tailrace head (load changes top, load shed bottom) 46

Figure 6.14 Model type 1 - 60 m³/s - Comparison of the tailrace discharge (load changes top, load shed bottom) 47

Figure 6.15 Model type 1 - 60 m³/s - Comparison of the tailrace head (load changes top, load shed bottom) 48

Figure 6.16 Model type 1 - 70 m³/s - Comparison of the tailrace discharge (load changes top, load shed bottom) 49

Figure 6.17 Model type 1 - 70 m³/s - Comparison of the tailrace head (load changes top, load shed bottom) 50

Figure 6.18 Model type 1 - 80 m³/s - Comparison of the tailrace discharge (load changes top, load shed bottom) 51

Figure 6.19 Model type 1 - 80 m³/s - Comparison of the tailrace head (load changes top, load shed bottom) 52

Figure 6.20 Model type 1 - 90 m³/s - Comparison of the tailrace discharge (load changes top, load shed bottom) 53

Figure 6.21 Model type 1 - 90 m³/s - Comparison of the tailrace head (load changes top, load shed bottom) 54

Figure 6.22 Model type 1 - 100 m³/s - Comparison of the tailrace discharge (load changes top, load shed bottom) 55

Figure 6.23 Model type 1 - 100 m³/s - Comparison of the tailrace head (load changes top, load shed bottom) 56

Figure 6.24 Physical (top) and 1-D numerical model (bottom): Type 2 57

Figure 6.25 Model type 2 - 20 m³/s - Comparison of the tailrace discharge (load changes top, load shed bottom) 58

Figure 6.26 Model type 2 - 20 m³/s - Tailrace head 59

Figure 6.27 Flow comparison of the surge tank and tailrace 59

Figure 6.28 Model type 2 - 30 m³/s - Comparison of the tailrace discharge (load changes top, load shed bottom) 60

Figure 6.29 Model type 2 - 30 m³/s - Tailrace head 61

Figure 6.30 Model type 2 - 40 m³/s - Comparison of the tailrace discharge (load changes top, load shed bottom) 62

Figure 6.31 Model type 2 - 40 m³/s - Tailrace head 63

Figure 6.32 Model type 2 - 50 m³/s - Comparison of the tailrace discharge (load changes top, load shed bottom) 64

Figure 6.33 Model type 2 - 50 m³/s - Tailrace head 65

Figure 6.34 Model type 2 - 60 m³/s - Comparison of the tailrace discharge (load changes top, load shed bottom) 66

Figure 6.35 Model type 2 - 60 m³/s - Comparison of the tailrace head (load changes top, load shed bottom) 67

Figure 6.36 Model type 2 - 70 m³/s - Comparison of the tailrace discharge (load changes top, load shed bottom) 68

Figure 6.37 Model type 2 - 70 m³/s - Comparison of the tailrace head (load changes top, load shed bottom) 69

Figure 6.38 Model type 2 - 80 m³/s - Comparison of the tailrace discharge (load changes top, load shed bottom) 70

Figure 6.39 Model type 2 - 80 m³/s - Comparison of the tailrace head (load changes top, load shed bottom) 71

Figure 6.40 Model type 2 - 90 m³/s - Comparison of the tailrace discharge (load changes top, load shed bottom) 72

Figure 6.41 Model type 2 - 90 m³/s - Comparison of the tailrace head (load changes top, load shed bottom) 73

Figure 6.42 Model type 2 - 100 m³/s - Comparison of the tailrace discharge (load changes top, load shed bottom) 74

Figure 6.43 Model type 2 - 100 m³/s - Comparison of the tailrace head (load changes top, load shed bottom) 75

Figure 6.44 Physical (top) and 1-D numerical model (bottom): Type 3 76

Figure 6.45 Model type 3 - 20 m³/s - Comparison of the tailrace discharge (load changes top, load shed bottom) 77

Figure 6.46 Model type 3 - 20 m³/s - Tailrace head 78

Figure 6.47 Model type 3 - 30 m³/s - Comparison of the tailrace discharge (load changes top, load shed bottom) 79

Figure 6.48 Model type 3 - 30 m³/s - Comparison of the tailrace head (load changes top, load shed bottom) 80

Figure 6.49 Model type 3 - 40 m³/s - Comparison of the tailrace discharge (load changes top, load shed bottom) 81

Figure 6.50 Model type 3 - 40 m³/s - Tailrace head 82

Figure 6.51 Model type 3 - 50 m³/s - Comparison of the tailrace discharge (load changes top, load shed bottom) 83

Figure 6.52 Model type 3 - 50 m³/s - Comparison of the tailrace head (load changes top, load shed bottom) 84

Figure 6.53 Model type 3 - 60 m³/s - Comparison of the tailrace discharge (load changes top, load shed bottom) 85

Figure 6.54 Model type 3 - 60 m³/s - Comparison of the tailrace head (load changes top, load shed bottom) 86

Figure 6.55 Model type 3 - 70 m³/s - Comparison of the tailrace discharge (load changes top, load shed bottom) 87

Figure 6.56 Model type 3 - 70 m³/s - Comparison of the tailrace head (load changes top, load shed bottom) 88

Figure 6.57 Model type 3 - 80 m³/s - Comparison of the tailrace discharge (load changes top, load shed bottom) 89

Figure 6.58 Model type 3 - 80 m³/s - Comparison of the tailrace head (load changes top, load shed bottom) 90

Figure 6.59 Model type 3 - 90 m³/s - Comparison of the tailrace discharge (load changes top, load shed bottom) 91

Figure 6.60 Model type 3 - 90 m³/s - Comparison of the tailrace head (load changes top, load shed bottom) 92

Figure 6.61 Model type 3 - 100 m³/s - Comparison of the tailrace discharge (load changes top, load shed bottom) 93

Figure 6.62 Model type 3 - 100 m³/s - Comparison of the tailrace head (load changes top, load shed bottom) 94

Figure 6.63 The three different observed surge tank model types 95

Figure 6.64 Surge tank variant data (excluding additional 25 % excavation size for surge chambers) 96

Figure 6.65 Surge tank size data approximation 96

Figure 6.66 Tailrace discharge comparison 97

Figure 7.1 System sketch of a three chamber surge tank layout 99

Figure 7.2 The hydraulic model in WANDA 4.2 100

Figure 7.3 Three chamber surge tank - 20 m³/s - Comparison of the tailrace discharge (load changes top, load shed bottom) 101

Figure 7.4 Three chamber surge tank - 20 m³/s - Tailrace head 102

Figure 7.5 Three chamber surge tank - 30 m³/s - Comparison of the tailrace discharge (load changes top, load shed bottom) 103

Figure 7.6 Three chamber surge tank - 30 m³/s - Comparison of the tailrace head (load changes top, load shed bottom) 104

Figure 7.7 Three chamber surge tank - 40 m³/s - Comparison of the tailrace discharge (load changes top, load shed bottom) 105

Figure 7.8 Three chamber surge tank - 40 m³/s - Comparison of the tailrace head (load changes top, load shed bottom) 106

Figure 7.9 Three chamber surge tank - 50 m³/s - Comparison of the tailrace discharge (load changes top, load shed bottom) 107

Figure 7.10 Three chamber surge tank - 50 m³/s - Comparison of the tailrace head (load changes top, load shed bottom) 108

Figure 7.11 Three chamber surge tank - 60 m³/s - Comparison of the tailrace discharge (load changes top, load shed bottom) 109

Figure 7.12 Three chamber surge tank - 60 m³/s - Comparison of the tailrace head (load changes top, load shed bottom) 110

Figure 7.13 Three chamber surge tank - 70 m³/s - Comparison of the tailrace discharge (load changes top, load shed bottom) 111

Figure 7.14 Three chamber surge tank - 70 m³/s - Comparison of the tailrace head (load changes top, load shed bottom) 112

Figure 7.15 Three chamber surge tank - 80 m³/s - Comparison of the tailrace discharge (load changes top, load shed bottom) 113

Figure 7.16 Three chamber surge tank - 80 m³/s - Comparison of the tailrace head (load changes top, load shed bottom) 114

Figure 7.17 Three chamber surge tank - 90 m³/s - Comparison of the tailrace discharge (load changes top, load shed bottom) 115

Figure 7.18 Three chamber surge tank - 90 m³/s - Comparison of the tailrace head (load changes top, load shed bottom) 116

Figure 7.19 Three chamber surge tank - 100 m³/s - Comparison of the tailrace discharge (load changes top, load shed bottom) 117

Figure 7.20 Three chamber surge tank - 100 m³/s - Comparison of the tailrace head (load changes top, load shed bottom) 118

Figure 7.21 Effect of the tunnel chamber shown by comparison of a 20 m³/s (top) and 100 m³/s (bottom) flow rate 119

Figure 7.22 Head within the pump chamber 120

Figure 7.23 Load case comparison - Inflow amplification 121

Figure 8.1 Comparison of the surge tank size 123

Figure 8.2 Definition of the flow directions for both hydraulic systems 125

Figure 8.3 Comparison of the inflow and outflow amplification 126

Figure 8.4 Comparison of the mass oscillation within the hydraulic systems (2-CST top, 3-CST bottom) 127

List of Tables

Table 2.1 Performance and energy storage capability of the project 4

Table 5.1 Load case scenarios 27

Table 5.2 Synchronous speed n_{syn} with the according number of poles and pole pairs [9] 29

Table 5.3 Calculated turbine parameters 30

Table 5.4 Calculated turbine dimensions 31

Table 6.1 Tailrace diameter and head loss 34

Table 6.2 Surge shaft diameter 35

Table 6.3 Model type 1 - 20 m³/s - Data comparison of the main loading cases 39

Table 6.4 Model type 1 - 20 m³/s - Surge tank construction parts and their sizes 40

Table 6.5 Model type 1 - 30 m³/s - Data comparison of the main loading cases 41

Table 6.6 Model type 1 - 30 m³/s - Surge tank construction parts and their sizes 42

Table 6.7 Model type 1 - 40 m³/s - Data comparison of the main loading cases 43

Table 6.8 Model type 1 - 40 m³/s - Surge tank construction parts and their sizes 44

Table 6.9 Model type 1 - 50 m³/s - Data comparison of the main loading cases 45

Table 6.10 Model type 1 - 50 m³/s - Surge tank construction parts and their sizes 46

Table 6.11 Model type 1 - 60 m³/s - Data comparison of the main loading cases 47

Table 6.12 Model type 1 - 60 m³/s - Surge tank construction parts and their sizes 48

Table 6.13 Model type 1 - 70 m³/s - Data comparison of the main loading cases 49

Table 6.14 Model type 1 - 70 m³/s - Surge tank construction parts and their sizes 50

Table 6.15 Model type 1 - 80 m³/s - Data comparison of the main loading cases 51

Table 6.16 Model type 1 - 80 m³/s - Surge tank construction parts and their sizes 52

Table 6.17 Model type 1 - 90 m³/s - Data comparison of the main loading cases 53

Table 6.18 Model type 1 - 90 m³/s - Surge tank construction parts and their sizes 54

Table 6.19 Model type 1 - 100 m³/s - Data comparison of the main loading cases 55

Table 6.20 Model type 1 - 100 m³/s - Surge tank construction parts and their sizes 56

Table 6.21 Model type 2 - 20 m³/s - Data comparison of the main loading cases 59
Table 6.22 Model type 2 - 20 m³/s - Surge tank construction parts and their sizes 60
Table 6.23 Model type 2 - 30 m³/s - Data comparison of the main loading case 61
Table 6.24 Model type 2 - 30 m³/s - Surge tank construction parts and their sizes 61
Table 6.25 Model type 2 - 40 m³/s - Data comparison of the main loading cases 62
Table 6.26 Model type 2 - 40 m³/s - Surge tank construction parts and their sizes 63
Table 6.27 Model type 2 - 50 m³/s - Data comparison of the main loading cases 64
Table 6.28 Model type 2 - 50 m³/s - Surge tank construction parts and their sizes 65
Table 6.29 Model type 2 - 60 m³/s - Data comparison of the main loading cases 66
Table 6.30 Model type 2 - 60 m³/s - Surge tank construction parts and their sizes 67
Table 6.31 Model type 2 - 70 m³/s - Data comparison of the main loading cases 68
Table 6.32 Model type 2 - 70 m³/s - Surge tank construction parts and their sizes 69
Table 6.33 Model type 2 - 80 m³/s - Data comparison of the main loading cases 70
Table 6.34 Model type 2 - 80 m³/s - Surge tank construction parts and their sizes 71
Table 6.35 Model type 2 - 90 m³/s - Data comparison of the main loading cases 72
Table 6.36 Model type 2 - 90 m³/s - Surge tank construction parts and their sizes 73
Table 6.37 Model type 2 - 100 m³/s - Data comparison of the main loading cases 74
Table 6.38 Model type 2 - 100 m³/s - Surge tank construction parts and their sizes 75
Table 6.39 Model type 3 - 20 m³/s - Data comparison of the main loading cases 77
Table 6.40 Model type 3 - 20 m³/s - Surge tank construction parts and their sizes 78
Table 6.41 Model type 3 - 30 m³/s - Data comparison of the main loading cases 79
Table 6.42 Model type 3 - 30 m³/s - Surge tank construction parts and their sizes 80
Table 6.43 Model type 3 - 40 m³/s - Data comparison of the main loading cases 81
Table 6.44 Model type 3 - 40 m³/s - Surge tank construction parts and their sizes 82
Table 6.45 Model type 3 - 50 m³/s - Data comparison of the main loading cases 83
Table 6.46 Model type 3 - 50 m³/s - Surge tank construction parts and their sizes 84
Table 6.47 Model type 3 - 60 m³/s - Data comparison of the main loading cases 85
Table 6.48 Model type 3 - 60 m³/s - Surge tank construction parts and their sizes 86
Table 6.49 Model type 3 - 70 m³/s - Data comparison of the main loading cases 87
Table 6.50 Model type 3 - 70 m³/s - Surge tank construction parts and their sizes 88

Table 6.51 Model type 3 - 80 m³/s - Data comparison of the main loading cases 89

Table 6.52 Model type 3 - 80 m³/s - Surge tank construction parts and their sizes 90

Table 6.53 Model type 3 - 90 m³/s - Data comparison of the main loading cases 91

Table 6.54 Model type 3 - 90 m³/s - Surge tank construction parts and their sizes 92

Table 6.55 Model type 3 - 100 m³/s - Data comparison of the main loading cases 93

Table 6.56 Model type 3 - 100 m³/s - Surge tank construction parts and their sizes 94

Table 6.57 Tailrace discharge amplification 97

Table 7.1 Three chamber surge tank - 20 m³/s - Data comparison of the main loading cases 101

Table 7.2 Three chamber surge tank - 20 m³/s - Surge tank construction parts and their sizes 102

Table 7.3 Three chamber surge tank - 30 m³/s - Data comparison of the main loading cases 103

Table 7.4 Three chamber surge tank - 30 m³/s - Surge tank construction parts and their sizes 104

Table 7.5 Three chamber surge tank - 40 m³/s - Data comparison of the main loading cases 105

Table 7.6 Three chamber surge tank - 40 m³/s - Surge tank construction parts and their sizes 106

Table 7.7 Three chamber surge tank - 50 m³/s - Data comparison of the main loading cases 107

Table 7.8 Three chamber surge tank - 50 m³/s - Surge tank construction parts and their sizes 108

Table 7.9 Three chamber surge tank - 60 m³/s - Data comparison of the main loading cases 109

Table 7.10 Three chamber surge tank - 60 m³/s - Surge tank construction parts and their sizes 110

Table 7.11 Three chamber surge tank - 70 m³/s - Data comparison of the main loading cases 111

Table 7.12 Three chamber surge tank - 70 m³/s - Surge tank construction parts and their sizes 112

Table 7.13 Three chamber surge tank - 80 m³/s - Data comparison of the main loading cases 113

Table 7.14 Three chamber surge tank - 80 m³/s - Surge tank construction parts and their sizes 114

Table 7.15 Three chamber surge tank - 90 m³/s - Data comparison of the main loading cases 115

Table 7.16 Three chamber surge tank - 90 m³/s - Surge tank construction parts and their sizes 116

Table 7.17 Three chamber surge tank - 100 m³/s - Data comparison of the main loading cases 117

Table 7.18 Three chamber surge tank - 100 m³/s - Surge tank construction parts and their sizes 118

Table 8.1 Surge tank volume comparison of both schemes 124

Table 8.2 Inflow- and Outflow data comparison of the tailrace 126